EXTRACTION AND CHARACTERIZATION OF XYLOGLUCAN-RHAMNOGALACTURONAN CROSSLINKED COMPLEX IN COTTON SUSPENSION CELL WALLS

By

JUN FU

Bachelor of Science

Fudan University

Shanghai, China

1992

Submitted to the Faculty of the
Graduate College of the
Oklahoma State University
in partial fulfillment of
the requirements for
the Degree of
DOCTOR OF PHILOSOPHY
December, 1999

EXTRACTION AND CHARACTERIZATION OF XYLOGLUCAN-RHAMNOGALACTURONAN CROSSLINKED COMPLEX IN COTTON SUSPENSION CELL WALLS

Thesis Approved:

Andrew Mort

Thesis Adviser

Robert L Matts

H. Chris Spivey

Nils Nossaman

Margaret L. Pierce

Wayne B. Powell

Dean of the Graduate College

ACKNOWLEDGMENTS

I would like to thank Dr. Andrew Mort, my major adviser for his advice, time, encouragement and friendship during my study. Appreciation is also extended to Dr. Marlee Pierce, Dr. Robert Matts, Dr. Olin Spivey and Dr. Niels Maness for serving on my committee and giving me advice.

In addition, I would like to express my appreciation to Dr. Rolf Prade for his help and advice on the enzyme cloning and expression, to Dr. Dongfeng Zhan for his helpful suggestions, to Mr. Bruce Baggenstoss for obtaining MALDI-MS spectra (University of Oklahoma Health sciences Center Laser Mass Facility) and to all my colleagues and friends for their help and friendship.

I would also like to give my special thanks to my husband, Yang Huang and my parents for their precious support, love, patience and understanding which was necessary for me to achieve this accomplishment.

Finally, I would like to thank the Department of Biochemistry and Molecular Biology for giving me this wonderful opportunity and support during all these years.

TABLE OF CONTENTS

LIST OF TABLES

LIST OF FIGURES

LIST OF ABBREVIATIONS

ANTS	8-Aminonaphthalene-1,3,6-trisulphonate
APTS	9-Aminopyrene-1,4,6-trosulfonate
AGP	arabinogalactan protein
ara	arabinose
CZE	capillary gel electrophoresis
EG	endoglucanase
EPG	endopolygalacturonase
fuc	fucose
gal	galactose
galA	galacturonic acid
glc	glucose
glcA	glucuronic acid
GRP	glycine-rich protein
HG	homogalacturonan
HF	hydrogen fluoride
HyPro	hydroxyproline
kDa	kilodalton
MALDI-MS	matrix assisted laser desorption/ionization mass spectrometry
man	mannose
NMR	nuclear magnetic resonance
PRP	proline-rich protein
rha	rhanmose
RGase	rhamnogalacturonase
RG	rhamnogalacturonan
RG I	rhamnogalacturonan I
RG II	rhamnogalacturonan II

Ser	serine
SCB	sodium cyanoborohydride
SDS-PAGE	sodium dodecyl sulfate polyacrylamide gel electrophoresis
XET	xyloglucan endotransglycosylase
XG	xyloglucan
XGA	xylogalacturonan
xyl	xylose

CHAPTER 1 GENERAL INTRODUCTION

The plant cell wall is a dynamic extracellular matrix which maintains the rigidity of the cell, controls cell growth and also acts as a pre-existing structural barrier to many invasive microorganisms (1). Plant cell walls are divided into primary cell walls and secondary cell walls. Primary cell walls are synthesized during the early stage of cell differentiation and expansion. Secondary cell walls are deposited on the inner surface of the primary walls after growth has ceased with the characteristic of enrichment in cellulose microfibrils and lignification.

Primary cell walls contain mostly polysaccharides and a small amount of proteins. The polysaccharides are mainly cellulose, hemicellulose and pectin in varying amounts depending on the source. Cellulose is the best known polysaccharide of cell walls. It is a linear polymer of β-1-4-D-glucan and aggregates together to form cellulose microfibrils. Hemicellulose includes xyloglucan, arabinoxylan and minor types of glucomannan or galactoglucomannan. Xyloglucan is the major type of hemicellulose in dicots. Xyloglucan is characterized by a cellulose-like β-1-4-D-glucan backbone with sidechains of xylose, galactosyl-xylose or fucosyl-galactosyl-xylose (structure illustrated in Fig. 1-1).

Pectin is the most abundant and complex component in the primary walls. Four distinguishable pectic regions have been identified: homogalacturonan (HG), rhamnogalacturonan I (RG I), rhamnogalacturonan II (RG II) and xylogalacturonan (XGA). Homogalacturonan is a homopolymer of α-1-4-D-galactosyluronic acid residues (2). The most common modification of HG is methylesterification of the carboxyl group of galA residues. Acetylation at the O-2 and O-3 hydroxyl groups is also observed. RG I

is composed of repeating disaccharide (1-2)-α-L-rhamnosyl-(1-4)-α-D-galactosyluronic acid (3). Many of the rha residues are glycosylated at the O-4 position with arabinose and galactose rich sidechains. Galactose is present predominantly as a single galactose or β-1-4-galactan. Arabinose is present mostly as α-1-5-arabinan with some α-1-3 arabinose branches. Arabinogalactan is another type of sidechain, type I arabinogalactan has β-1-4-galactan and α-1-3 arabinose branches and type II has β-1-3 galactan and β-1-6 galactose branches and/or α-1-3 arabinose branches. The galA residues of RG I are reported to have acetylation at the O-2 and O-3 hydroxyl positions (4). RG II is a low molecular weight (~4.8 kDa) complex region (5). It is composed of a homogalacturonan backbone of about nine α-1-4-D-galA residues. Four different complex sidechains are attached to the O-2 or O-3 position of galA residues including the unusual glycosyl residues 2-O-methylfucose, 2-O-methylxylose, apiose, 3-C-carboxy-5-deoxy-L-xylose (aceric acid) and 2-keto-3-deoxy-D-manno-octulosonic acid (KDO). XGA is the fourth identified pectic region. It contains a homogalacturonan backbone with a non-reducing terminal xyl attached at the O-3 position of galA residues. XGA has been considered as a minor type and is found concentrated near RG I (6). The structures of the four pectic regions are illustrated in Fig. 1-2 and Fig. 1-3.

Cell wall proteins include wall structural proteins and wall enzymes. Extensins are the most abundant and well-studied structural proteins. Extensins are a member of the hydroxyproline rich glycoproteins with the characteristic of a repeating sequence of $Ser(HyPro)_4$. They are accumulated in cell walls in response to wounding, infection, oligosaccharide elicitors or ethylene (7). Other cell wall structural proteins include glycine-rich proteins (GRPs), arabinogalactan proteins (AGPs) and proline-rich proteins (PRPs). The arabinogalactan protein is primarily localized in the extracellular matrix and is thought to be involved in cell-cell recognition rather than have a structural role (7). Cell wall enzymes include polysaccharide degrading enzymes e.g. endoglucanase and

pectinase, wall modification enzymes e.g. esterase, xyloglucan endotransglycosylase (XET), peroxidase and phosphatase.

All cell wall polymers are held together through many crosslinks, both non-covalent and covalent, to form a strong dynamic wall. Non-covalent bonds consist of hydrogen bonds and ionic bonds, e.g. multiple hydrogen bonds between cellulose and hemicellulose and calcium bridges between homogalacturonan polymers. Covalent bonds consist of glycosidic bonds, phenolic coupling e.g. intramolecular isodityrosine bridges in extensin and diferulate bridges between feruloylated sugars, and ester bonds e.g. the condensation between COOH group of a uronic acid residue and OH group of a neutral sugar residue (8).

The first cell wall model was proposed by Peter Albersheim's group in 1973 which was based on carbohydrate analysis of sycamore suspension cell walls. This model describes the whole cell wall as one macromolecule, in which xyloglucan non-covalently binds to cellulose and covalently crosslinks to pectin while pectin covalently crosslinks to wall proteins (9). Recently, a two network cell wall model for the primary wall of most flowering plants was proposed by Carpita and Gibeaut, in which a stretch resistant load bearing cellulose-xyloglucan network is embedded in a compression resistant pectin network (10, 11).

The cellulose/xyloglucan network

Cellulose and xyloglucan are important structural components of primary wall of plants. Xyloglucan is believed not only to bind to cellulose microfibrils but also to span between different microfibrils. Electron micrographs of the putative xyloglucan crosslinks were observed in a pectin depleted onion cell wall using the fast-freeze, deep-etched and rotary-shadow replica technique. The crosslinks between microfibrils are about 20-40 nm while the extracted xyloglucan chains are up to 400 nm. The xyloglucan chains are predicted to be long enough to interlink several microfibrils. Extraction of

pectin did not affect the integrity of the wall, but removal of xyloglucan by 1 M KOH caused aggregation of microfibrils (12). This indicates that xyloglucan prevents lateral association of cellulose and interlocks the microfibrils into the space.

Xyloglucan is thought to bind to cellulose through its glucan backbone, sidechains of xyloglucan have been studied for the regulation of the binding. Conformational dynamic simulation studies predicted that the fucosylated trisaccharide sidechains straighten the XG backbone and thus facilitate steric accessibility of XG to microfibrils (13). *In vitro* binding assays revealed results consistent with this that the fucosylated xyloglucan derived from pea cell walls showed a higher absorption constant for cellulose than the nonfucosylated xyloglucan extracted from tamarind and nasturtium (14).

Since xyloglucan is proposed to be a major tension bearing wall compound, hydrolysis, dissociation and replacement of XG crosslinks between microfibrils are thought to be requisite events in cell expansion (10). Endo-β-1,4-glucanase has long been implicated in auxin induced cell expansion. However, simple hydrolytic cleavage of xyloglucan crosslinks can not reorganize a cellulose-XG network in response to cell expansion. Xyloglucan endotransglycosylase (XET) has been found not only to hydrolyze the XG backbone but also to transfer the newly formed XG reducing end to a non-reducing end of an acceptor XG. Such transglycosylation between two potential load bearing xyloglucan chains could allow the movement of adjacent microfibril during wall loosening and expansion (15, 16, 17). In expanding tomato hypocotyls, auxin induced accumulation of both Cel7 and LeXET mRNAs which encode for endoglucanase and XET, respectively (18). In arabidopsis seedlings, TCH4 genes which encode for XET are found to be upregulated by the growth-promoting hormones. The TCH4-encoded XET is proposed to integrate newly synthesized XGs into walls during cell expansion and reinforcement (19). A newly discovered protein called expansin was found to be involved in the acid induced cucumber hypocotyl cell expansion and relaxation. Expansins have an estimated size of 25-27 kDa without any detectable

activities of XG hydrolase or transglycosylase. This protein is thought to cause wall creep by loosening non-covalent association between cellulose and XG. Pretreatment by endoglucanase or pectinase enhanced the subsequent extension in response to expansins. This indicates that co-operations between hydrolase and expansins would act synergistically in the regulation of wall expansion (20, 21, 22).

The pectin network

Pectins are considered to form an integrated network by all pectic polymers (23). Degradation of sycamore suspension cell walls by endopolygalacturonase (EPG), which degrades non-methylesterified HG, solubilized a portion of RG I and RG II (24). Digestion of apple cell walls by rhamnogalacturonase (RGase), which specifically degrades RG I region, released a portion of HG along with RG I fragments rich in arabinan (25). Similarly, cleavage of rha linkages in RG I by liquid hydrogen fluoride (HF) at -23 °C released most of galA as polymeric HG from cotton cell walls. The highly methylesterified HG can be extracted with water and the sparsely methylesterified HG can be extracted with chelators or imidazole (26). Furthermore, a polymeric XGA segment was released from the modified hairy region (RG rich) of apples by RGase (6). All the results support that HG, RG I, RG II and XGA are interconnected, even though the content of each pectic polymer varies depending on the cell wall source. The chemical nature of the linkages and the sequence of the interconnections among them remain unclear.

The pectin network is thought to function as a physical barrier to wall proteins by controlling the wall porosity (10). HG is the most abundant pectic polymer and it can form Ca^{2+} bridges between carboxyl group of galA residues of different HGs. However, in nature many of the galA residues are methylesterified. The degree of methylesterification can be controlled by a pectin methylesterase (PME), which removes the methyl groups from galAs. The deesterified HGs can form an expanded junction

zone and thus prevent diffusion of wall proteins. Furthermore, the acidic blocks will decrease the local pH, which may influence the activities of enzymes. Recently, borate ester crosslinks were found between apioses of two RG II polymers (27, 28) and oxidative diferulate crosslinks were found between RG I polymers in sugar beet pulp (29). In addition to crosslinks between polymers, the wall porosity might be limited by galactan sidechains on RG I forming short flexible rods and protruding into the pores of the network, as suggested by an NMR study of the onion cell walls (30).

Interactions between the two networks

The pectin network is proposed to be independent of and coexist with the cellulose-XG network (11). During regeneration of the cell wall by carrot protoplasts, a pectin rich shell was laid down first, through which the cellulose-XG network was intercalated later (31). Tomato suspension culture cells were reported to be able to grow on 2,6-dichlorobenzonitrile (DCB), a cellulose synthesis inhibitor. The DCB-adapted cells formed a pectin rich cell wall while most of the xyloglucan remained soluble in the culture medium in the absence of cellulose to bind (32).

In contrast, covalent crosslinks between XG and pectin were hypothesized from structural studies of the wall polymers extracted by enzymes and chemical methods. Cell walls are water-insoluble materials. Chelating reagents and sodium bicarbonate are conventional ways to extract calcium bound pectin and ester-linked pectin, respectively. Strong alkali (24% KOH) is used to extract XG from cellulose by breaking the hydrogen bonds between them. However, none of these methods could completely solubilize all of the pectin or XG separately. Sequential extraction of rose suspension cell walls by chelating reagents and strong alkali only solubilized a limited amount of pectin and XG (33). Alkali extraction of EPG pre-treated sycamore suspension cell walls extracted a putative pectin-XG complex whose components were co-eluted on an anion exchange column (34). Furthermore, endoglucanase digestion of EPG-pretreated sycamore walls

solubilized pectin, which only digests XG, but not RG (34). Similarly, enzymatic extraction of pectin from apple walls also revealed that the apple pectin could be extracted mostly by a combination of pectin lyase and endoglucanase (35). These results indicated that a covalent crosslink could exist between XG and pectin and thus prevent either of them from being solubilized completely. Recently, the occurrence of pectin-xylan-xyloglucan complexes was reported in the cell walls of cauliflower stem tissues (36). The formation of these complexes was suggested to be involved in the wall secondary thickening. To understand the function of the crosslink between XG and pectin, e.g. how it is formed or developed, why it is formed, we need to know the structure of the crosslink.

AIM AND OUTLINE OF THESIS

Preliminary results showed that over 90% of the RG and XG could be solubilized by 24% KOH-0.1%$NaBH_4$ from EPG pre-treated cotton suspension cell walls. Strong evidence was found that about half of the extracted XG was covalently crosslinked to half of the RG. Sequential enzymatic and chemical extraction and various chromatographic methods were applied to isolate the XG-RG crosslinked complex (Chapter 3). *In vitro* cellulose binding of the XG-RG complex further confirmed that RG and XG are covalently crosslinked (Chapter 4). Due to contamination of commercial cell wall degrading enzymes with extraneous activities, cloned endoarabinase and RGase were expressed in *pichia* to obtain specific enzymes (Chapter 5). Chapter 6 describes the structural studies of the XG-RG complex with application of RGase, endoarabinase and endoglucanase. Chapter 7 introduces a lithium/ethylenediamine reaction for characterization of the XG-RG complex, which selectively cleaves the galA residues of the RG polymer.

The aim of this thesis project was to characterize the crosslink structure between XG and RG. Crosslinking of wall polymers between the cellulose/xyloglucan network

and the pectin network could have profound effects on the physical properties of the cell wall and thus affect the cell growth or defense. By knowing the nature of the XG-RG crosslink, we hope to understand the role of such a crosslink in the architecture of the whole cell wall, why it is formed and how it is formed.

REFERENCES

1. **McNeil, M., Darvill, A. G., Fry, S. C. and Albersheim, P.** 1984. Structure and function of the primary cell walls of plants. *Ann. Rev. Biochem.* 53: 625-663
2. **Thibault, J. F., Renard, C. M. G. C., Axelos, M. A. V., Roger, P. and Crepeay, M. J.** 1993. Studies of the length of homogalacturonic regions in pectins by acid hydrolysis. *Carbohydr. Res.* 283: 271-286
3. **Lau, J. M., McNeil, M., Darvill, A. G. and Albersheim, P.** 1985. Structure of the backbone of rhamnogalacturonan I, a pectic polysaccharide in the primary cell walls of plants. *Carbohydr. Res.* 137: 111-125
4. **Komalavilas, P. and Mort, A. J.** 1989. The acetylation at O-3 of galacturonic acid in the rhamnose-rich region of pectins. *Carbohydr. Res.* 189: 261-272
5. **Darvill, A. G., McNeil, M. and Albersheim, P.** 1978. Structure of plant cell walls. VIII. A new pectic polysaccharide. *Plant Physiol.* 62: 418-422
6. **Schols, H. A., Bakx, E. J., Schipper, D. and Voragen, A. G., J.** 1995. A xylogalacturonan subunit present in the modified hairy regions of apple pectin. *Carbohydr. Res.* 279: 265-279
7. **Varner, J.E., Lin, L.S.** 1989. Plant cell wall architecture. *Cell.* 56: 231-239
8. **Fry, S. C.** 1986. Cross-linking of matrix polymers in the growing cell walls of angiosperms. *Annu. Rev. Plant Physiol.* 37: 165-186
9. **Keegstra, K., Talmadge, K. W., Bauer, W. D., and Albershem, P.** 1973. The structure of plant cell walls. III. A model of the walls of suspension-cultured sycamore cells based on the interconnections of the macromolecular components. *Plant Physiol.* 51: 188-196
10. **Carpita, N. C., Gibeaut, D. M.** 1993. Structural models of primary cell walls in flowering plants: consistency of molrcular structure with the physical properties of the walls during growth. *The Plant Journal.* 3(1): 1-30
11. **McCann, W. C., Roberts, K.** 1994. Changes in cell wall architecture during cell elongation. *J. Exp. Bot.* 45: 1683-1691
12. **McCann, M. C., Wells, B., Roberts, K.** 1992. Complexity in the spatial localization and length distribution of plant cell-wall matrix polysaccharides. *Journal of Microscopy.* 166(1): 123-136
13. **Levy, S., Maclachlan, G., Staehelin, L.A.** 1997. Xyloglucan sidechains modulate binding to cellulose during in vitro binding assays as predicted by conformational dynamics simulations. *The Plant Journal.* 11(3): 373-386

14. **Hayashi, T., Takeda, T., Ogawa, K., Mitsuishi, Y.** 1994. Effects of the degree of polymerization on the binding of xyloglucans to cellulose. *Plant Cell Physiol.* 35: 893-899

15. **De Silva, J., Arrowsmith, D., Hellyer, A., Whiteman, S., and Robinson, S.** 1994. Xyloglucan endotransglycosylase and plant growth. *J. Exp. Bot.* 45: 1693-1701

16. **Fry. S. C., Smith, R. C., Renwick, K. F., Martin, D. J., and Hodge, S. K., Matthews, K. J.** 1992. Xyloglucan endotransglycosylase, a new wall-loosening enzyme activity from plants. *Biochem. J.* 282: 821-828

17. **Potter, I., and Fry. S. C.** 1994. Changes in xyloglucan endotransglycosylase (XET) activity during hormone-induced growth in lettuce and cucumber hypocotyls and spinach cell suspension cultures. *J. Exp. Bot.* 45: 1703-1710

18. **Catala, C., Rose, J.K.C., Bennett, A.B.** 1997. Auxin regulation and spatial localization of an endo-1,4-β-D-glucanase and a xyloglucan endotransglycosylase in expanding tomato hypocotyls. *The Plant Journal.* 12(2): 417-426

19. **Braam, J., Sistruck, M. L., Polisensky, D. H., Xu, W., Purugganan, M. M., Antosiewicz, D. A., Campbell, P., Johson, K. A.** 1997. Plant responses to environmental stress: regulation and functions of the Arabidopsis TCH genes. *Planta.* 203: S35-S41

20. **McQueen-Mason, S., Durachko, D. M., and Cosgrove, D. J.** 1992. Two endogenous proteins that induce cell wall expansion in plants. *Plant Cell.* 4: 1425-1433

21. **Cosgrove, D. J.** 1997. Relaxation in high-stress environment: the moleculart bases of extensible cell walls and cell enlargement. *The Plant Cell.* 9: 1031-1041

22. **Cosgrove, D. J.** 1997. Assembly and enlargement of the primary cell wall in plants. *Annu. Rev. Cell Dev. Biol.* 13: 171-201

23. **Albersheim, P., Darvill, A. G., O'Neill, M. A., Schols, H. A., Voragen, A. G. J.** 1996. An hypothesis: the same six polysaccharides are components of the primary cell walls of all higher plants. *Pectins and Pectinases.* Elsevier Science B.V. 47-55

24. **O'Neill, M., Albersheim, P. and Darvill, A.** 1990. The pectic polysaccharide of primary cell walls. *Methods Plant Biochem.* 2: 415-441

25. **Renard, C. M. G. C., Thilbault, J. F., Voragen, A. G. J., Van den broek L. A. M., Pilnik, W.** 1993. Studies on apple protopectin VI: extraction of pectins from apple cell walls with rhamnogalacturonase. *Carbohydr. polym.* 22: 203-210

26. **Mort, A. J., Moerschbacher, B. M., Pierce, M. L., Maness, N. O.** 1991. Problems one may encounter during the extraction, purification, and chromatography of pectin fragments and some solutions to them. *Carbohydr. Res.* 215:219-227

27. **Kobayashi, M., Matoh, T., Azuma, J.** 1996. Two chains of rhamnogalacturonan II are crosslinked by borate-diol ester bonds in higher plant cell walls. *Plant Physiol.* 110: 1017-1020

28. **O'Neill, M. A., Warrenfeltz, D., Kates, K., Pellerin, P., Doco, T., Darvill, A.G., and Albersheim, P.** 1996. Rhamnogalacturonan-II, a pectic polysaccharide in the walls of growing plant cells, forms a dimer that is covalently cross-linked by a borate ester: In vitro conditions for the formation and hydrolysis of the dimer. *J. Biol. Chem.* 271: 22923-22930

29. **Oosterveld, A., Grabber, J. H., Beldman, G., Ralph, J., Voragen, A. G. J.** 1997. Formation of ferulic acid dehydrodimers through oxidative cross-linking of sugar beet pectin. *Carbohydr. Res.* 300: 143-153

30. **Foster, T. J., Ablett, S., McCann, M. C., Gidley, M. J.** 1996. Mobility-resolved 13C-NMR spectroscopy of primary plant cell walls. *Biopolymers.* 39(1): 51-66

31. **Shea, E. M., Gilbeaut, D. M., Carpita, N. C.** 1989. Structural analysis of the cell walls regenerated by carrot protoplasts. *Planta.* 179 (3): 293-308

32. **Shedletzky, E., Shmuel, M., Delmer, D. P., Lamport, D. T. A.** 1990. Adaptation and growth of tomato cells on the herbicide 2,6-dichlorobenzonitrile leads to production of unique cell walls virtually lacking a cellulose-xyloglucan network. *Plant Physiol.* 94: 980-987

33. **Chambat, G., Barnound, F., Joseleau, J. P.** 1984. Structure of the primary cell walls of suspension-cultured rose glauca cells. *Plant Physiol.* 74: 687-693

34. **Bauer, W. D., Talmadge, K. W., Keegstra, K., Albersheim, P.** 1973. The structure of plant cell walls. II. The hemicellulose of the walls of suspension-cultured sycamore cells. *Plant Physiol.* 51: 174-187

35. **Renard, C. M. G. C., Voragen, A. G. J., Thibault, J. F., Pilnik.** 1991. Studies on apple protopectin V: structure studies on enzymatically extracted pectins. *Carbohydr. polym.* 16: 137-154

36. **Femenia, A., Rigby, N. M., Selvendran, R. R. and Waldron, K. W.** 1999. Investigation of the occurrence of pectic-xylan-xyloglucan complexes in the cell walls of cauliflower stem tissues. *Carbohydr. polym.* 39: 151-164

37. **Fry, S. C., York, W. S., Albersheim, P., Darvill, A., Hayashi, T., Joseleau,J P., Kato, Y., Lorences, E. P., Maclachlan, G. A., McNeil, M., Mort, A. J., Reid, G., Seitz, H.U., Selvendran, R. R., Voragen, A. G. J., White, A. R.** 1993. An unambiguous nomenclature for xyloglucan-derived oligosaccharides. *Physiologia Plantarum* 89: 1-3

38. **Penhoat, C. H., Gey, C., Pellerin, P. and Perez. S.** 1999. An NMR solution study of the mega-oligosaccharide, rhamnogalacturonan II. *Journal of Biomolecular NMR* 14: 253-271

Figure 1-1 Structure of xyloglucan subunits

The nomenclature proposed by Fry et al. (37) is used to designate xyloglucan structure. The letter G refers to an unbranched glc, the letter X refers to a xyl substitution, the letter L refers to a gal-xyl substitution and the letter F refers to a fuc-gal-xyl substitution.

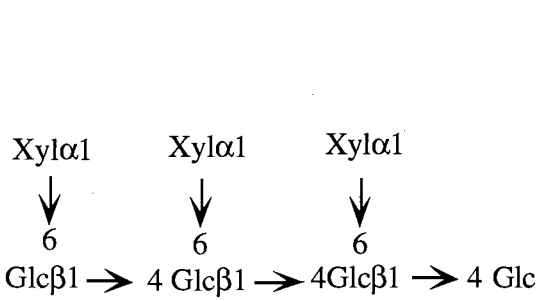

XXXG

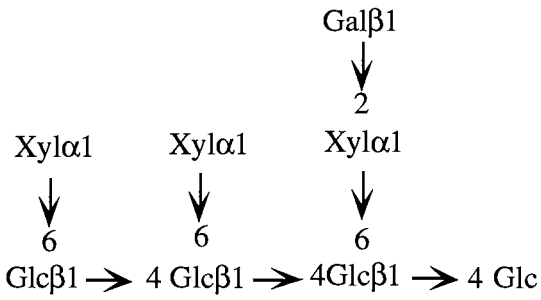

XXLG

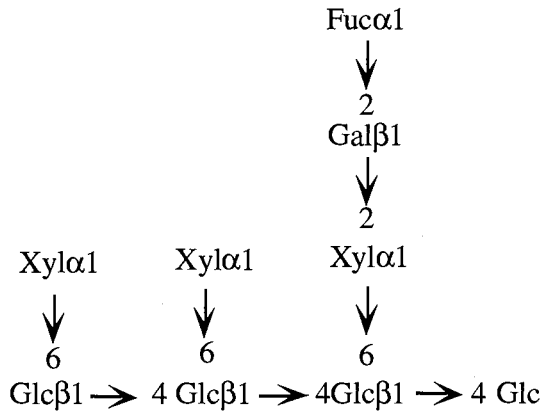

XXFG

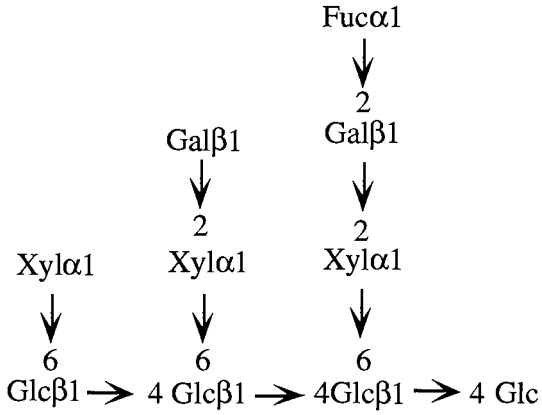

XLFG

Figure 1-2 Structures of HG, XGA and RG I

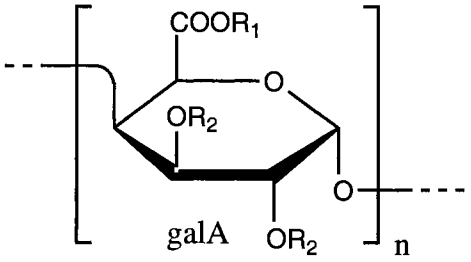

Homogalacturonan

R_1=H, Methyl or non-methyl esters
R_2=H or acetyl

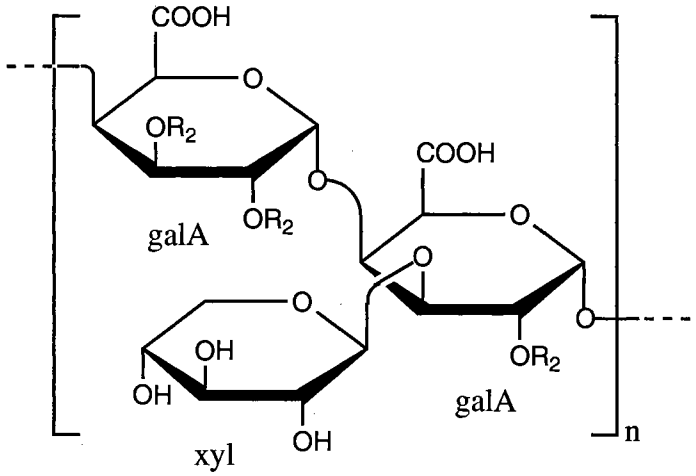

Xylogalacturonan

R_1=H, Methyl or non-methyl esters
R_2=H or acetyl

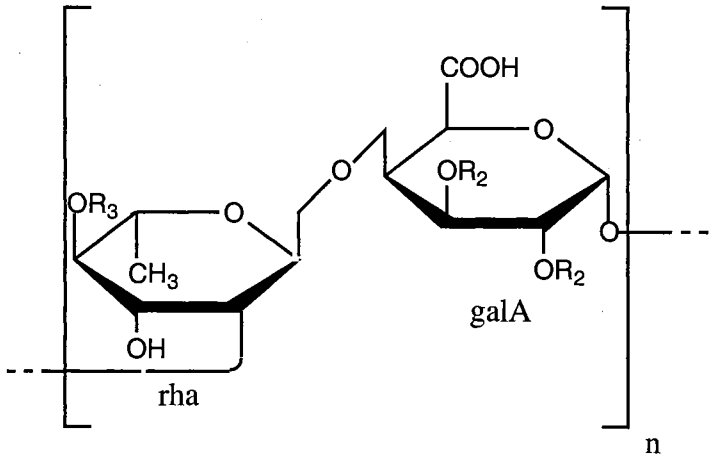

Rhamnogalacturonan I

R_2=H or acetyl
R_3 =H, gal, ara, galactan,arabinan or arabinogalactan

Figure 1-3 Schematic drawing of RG II (Penhoat et al. (38))

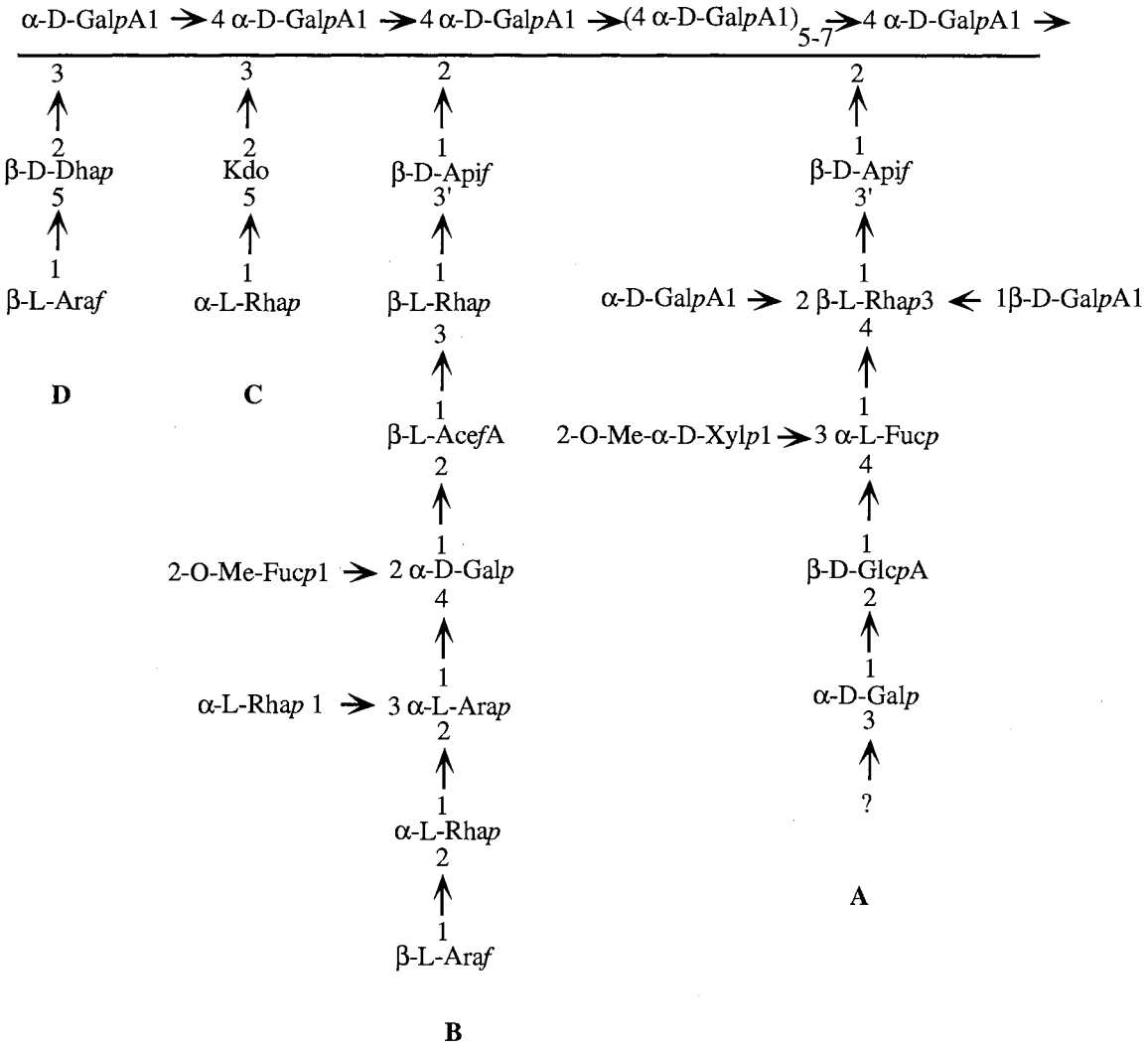

CHAPTER 2 SEQUENTIAL EXTRACTION AND ISOLATION OF XG AND RG CROSSLINKED COMPLEX FROM COTTON SUSPENSION CELL WALLS

INTRODUCTION

In the early 70's, Peter Albershem's group proposed a cell wall model in which xyloglucan (the major hemicellulose of primary cell walls of dicots) was covalently crosslinked to pectin and non-covalently adsorbed to the surface of cellulose as a monolayer (1). Now it is generally accepted that xyloglucan not only binds to the surface of cellulose microfibrils, but also spans between different microfibrils to form a XG-cellulose network. Pectin, which is found to be composed of four distinguishable regions: HG, RG I, RG II and XGA, is proposed to form an independent network. The potential crosslinking of XG to pectin has been questioned or practically disregarded (2). However, during experiments designed to solubilize rhamnogalacturonan from cell walls of cotton suspension cultures, we found that the cotton rhamnogalacturonan was only solubilized to a small extent by the homogalacturonan degrading enzyme endopolygalacturonase (EPG). But, it could be totally solubilized by a combination of EPG digestion followed by a strong alkali extraction or partially solubilized by EPG digestion followed by endoglucanase (EG) digestion, suggesting a covalent crosslink between xyloglucan and rhamnogalacturonan. Interestingly, there also appears to be a covalent crosslink between the hydroxylproline rich cell wall protein (extensin) and rhamnogalacturonan in the cotton walls (3).

Here we provide evidence that there truly is a covalent crosslink between half of the cotton xyloglucan and rhamnogalacturonan.

MATERIALS AND METHODS

Preparation of cell walls

Cotton suspension cell walls were prepared from suspension cultured cotton cells (*Gossypium hirsutum* L. cv Acala 44) (4). Suspension cultures were started by adding 3 to 4 g of callus in the late logarithmic phase from agar medium to 125 ml culture flasks containing 50 ml of Schenk and Hildebrandt liquid medium. After about two weeks (late logrithmic phase) the cells were harvested by filtration. Cell walls were prepared using the method described by Komalavilas and Mort (5). Cells were harvested by filtering the culture fluid using a very fine nylon cloth. Cells were washed with 10 volumes of 100 mM potassium phosphate buffer (pH 7) and 6 volumes of 500 mM potassium phosphate buffer (pH 7). After washing, the cells were resuspended in 1 volume of 500 mM potassium phosphate buffer (pH 7) and broken using a Polytron homogenizer on ice for 12 minutes at high speed (stopped for cooling every 3 minutes). Breakage of the cells was monitored under the microscope for a complete disruption. The walls were washed by 5 volumes of 500 mM potassium phosphate buffer (pH 7), 10 volumes of distilled water and 5 volumes of 1:1 chloroform-methanol. The washed cell walls were rinsed with acetone to remove the remaining water and air dried.

EPG digestion of cell walls

Dry cell walls (1.0 gram) were suspended in 50 mM ammonium acetate buffer (pH 4.0), to a concentration of approximately 10 mg/ml. Eight units of EPG (Megazyme, Ireland) were applied and the mixture was gently stirred overnight at 37 °C. A few drops of tolulene were added to prevent fungi from growing. The reaction mixture was centrifuged at 13,200 g for 10 min. The pellets were rinsed with distilled water twice and centrifuged at 13,200 g for 10 min. The supernatants were pooled, pellets were combined, and both were freeze dried.

KOH (24%) extraction

Dry cell walls or EPG pre-digested cell walls were suspended in 24% KOH-0.1% $NaBH_4$, to a concentration of approximately 10 mg/ml, and gently stirred overnight at room temperature. The suspension was centrifuged at 13,200 g for 10 min and rinsed with distilled water twice and centrifuged again. The supernatants were combined and neutralized with concentrated acetic acid to pH 5.5 and dialyzed in membrane of Mr=12,000-14,000 cut off against distilled water. After dialysis the supernatant was freeze dried.

Endoglucanase digestion of EPG-predigested walls

Two hundred mg of EPG pre-digested cell walls were suspended in 50 mM ammonium acetate buffer (pH 4.5), to a concentration of approximately 10 mg/ml. Five units of endoglucanase (Megazyme, Ireland) were applied and the mixture was gently stirred overnight at 37 °C. The reaction mixture was centrifuged at 13,200 g for 10 min. The pellets were rinsed with distilled water twice and centrifuged at 13,200 g for 10 min. The supernatants were pooled, pellets were combined and both were freeze dried.

Gel filtration chromatography

Polysaccharides were fractionated on Toyopearl HW65 (S), HW55 (S), HW50 (S), HW40 (S) gel filtration mediums from Supelco Inc. (Bellefonte, PA), packed in a stainless steel column (50 x 1 cm or 50 x 1.5 cm) from Alltech Associates, Inc. The column was equilibrated with 50 mM ammonium acetate, pH 5.2 with a flow rate of 1.0 or 2.0 ml/min. The sugars were monitored by a refractive index detector (SHODEX R1-71). The fractions were collected every minute on a Gilson Fraction collector. Pullulan fractions were used as molecular weight standards (Polymer Laboraories Technical Center, Amherst, MA).

Anion exchange chromatography

Neutral polysaccharides and acidic polysaccharides were separated on anion exchange columns: PA1 (Carbo Pac, Dionex), HQ (Poros 50 HQ, Perseptive Biosystems) or DEAE (Poros 50 DEAE, Perseptive Biosystems). The column was eluted with an ammonium acetate gradient with a flow rate of 2 ml/min using a Dionex Bio-LC carbohydrate system. A permanganate bleaching based detector (6) was used to monitor sugars in the eluate.

GLC sugar composition analysis

Sugar compositions were determined by GLC analysis of the trimethylsilyl methyl glycosides. Methanolysis and derivatization were performed using the protocol of Chaplin as modified by Komalavilas and Mort (5).

About 100 μg of sample was weighed on a Cahn 29 electrobalance and the exact amount was recorded. The sample was placed in a 4 ml glass vial with a teflon-lined screw lid. One hundred nmoles of inositol was added as an internal standard and dried in a speed vacuum. Two hundred μl of 1.5 M methanolic HCl and 50 μl of methyl acetate were added to each vial. The vial was sealed tightly and placed in a heating block at 80 °C for at least 3 hours. After cooling to room temperature, a few drops of t-butanol were added to each vial and the sample was dried under a stream of N_2. Fifty μl of a 3:1 Trisyl (Pierce): Pyridine mixture was added to the sample and allowed to react for 15 min at room temperature. The derivatized sample was then evaporated just to dryness under a stream of N_2 and redissolved in 100 μl of isooctane. The trimethylsilyl sugar derivatives were separated on a fused silica capillary column (30 m x 0.25 mm i.d., Durabond-1 liquid phase; J & W Scientific Inc., Rancho Cordova, CA) installed in a Varian (Sunnyvale, CA) 3300 gas chromatograph equipped with an on column injector.

One μl of sample was injected at 105 °C. After injection, the oven was held at 105 °C for 1 min. Then the temperature was raised to 160 °C at a rate of 10 °C/min and

held for 4 min, then raised to 220 °C at a rate of 2 °C/min, finally raised to 240 °C at a rate of 10 °C/min and held for 10 min. Peaks were integrated on a Varian 4290 integrator.

Capillary zone electrophoresis

Approximately 100 μg of sample was heated at 90 °C for at least 1 h in a mixture of 50 μl of 23 mM ANTS (in 3:17 v/v of acetic acid: water) and 5 μl of 1 M sodium cyanoborohydride (in dimethylsulfoxide) (7).

Sample was run on a custom-built instrument with a laser-induced fluorescence detector which used a helium-cadmium laser for excitation and an intensified charge-coupled device camera for detection (8). A fused-silica capillary (Polymicro Technologies, Phoenix, AZ, USA) of 50 μm ID (355 μm OD) was used as the separation column for oligosaccharides. The capillary was 50 cm in length, with 26 cm to the detection window. 0.1 M NaH_2PO_4, pH 2.5, was used as a running buffer. The capillary was rinsed with running buffer after each run and sample was introduced by gravity-driven flow for several seconds. Electrophoresis was conducted at 18 kV with the negative electrode on the injection side.

RESULTS

EPG-KOH Extraction

The scheme of sequential extraction of intact cell walls by EPG and KOH is illustrated in Fig. 2-1. One gram of dried acala 44 cotton suspension cell walls were digested by 8 units of EPG (Megazyme). After an exhaustive digestion around 30% of the weight of the walls became water soluble including around 70% of the initial GalA content. Analysis of what was solubilized showed it to be predominantly the monomer, dimer, and trimer of galA (the limit digest of pectic acid by EPG), along with the

complex fragments of pectin which have been designated as rhamnogalacturonan II (RG II) by Darvill et al (9), and a very small amount of the rhamnose rich region of pectin called rhamnogalacturonan I (RG I). Since only a very small proportion of the Glc or Xyl was solubilized (Table 2-1), it was clear that the xyloglucan, as expected, remained insoluble. Treatment of the residue from the EPG digestion with 24% KOH containing 0.1% $NaBH_4$ solubilized around 50% of its weight, accounting for around 35% of the starting cell walls. Essentially 90% of the xyloglucan and RG I were solubilized. The residue after KOH extraction was mainly cellulose.

Keegstra et al. (1) hypothesized that much of the xyloglucan of sycamore cell suspension culture cell walls was crosslinked to pectin. We have investigated the possibility that this is the case in cotton culture cell walls. When the alkali extract was chromatographed on either a PA 1 or Poros HQ anion exchange column using an ammonium acetate gradient and a permanganate bleaching based detector we obtained chromatograms as illustrated in Fig. 2-2. The sugar composition of each fraction is given in Table 2-2. The non-adsorbed material (B-1), from its sugar composition, appears to be a mixture of xyloglucan, xylan, and an arabinose containing polymer (possibly extensin with its arabinosylated hydroxyproline residues). The main adsorbed material (B-5), from its sugar composition, could be a combination of RG I, xyloglucan and a xylogalacturonan. The presence of xyloglucan is indicated by the high content of xylose and glucose, and the presence of galactose and fucose. RG I is indicated by the presence of galacturonic acid and rhamnose in a relatively low molar ratio. One expects a GalA to Rha ratio of 1:1 for RG I and a ratio of at least 25:1 for homogalacturonan. As will be discussed in later chapters, xylogalacturonan (10) (an EPG resistant homogalacturonan with single terminal xylose linked at 3-position of galacturonic acid residue) is also present in this fraction (B-5). Another polymer with a high xylose content is xylan, but this is not considered to be abundant in primary cell walls of dicots. The sugar composition of fraction B-2 indicates that this fraction could be arabinoxylan, but it only

accounts for about 2% of the total extract. Fractions B-3 and B-4 are also minor fractions; their sugar compositions are similar to fraction B-5, but with a relative lower galA content. Re-chromatography of the main adsorbed material (B-5) on a PA 1 column did not yield any non-adsorbed material (data not shown). Thus it appears that there is a considerable proportion of the xyloglucan that adsorbs strongly to an anion exchange column. Since xyloglucans are composed of neutral sugars, there must be an association with an acidic polymer causing the chromatographic behavior. If one takes the sugar weight recovery of glc or fuc to represent the xyloglucan recovery (gal and xyl are also present in other polymers), around 50% by weight, is in the adsorbed fraction (B-5).

To verify that at least a high proportion of the xylose is in xyloglucan each fraction was subjected to endoglucanase digestion followed by analysis of the products by capillary electrophoresis. Endoglucanase digests xyloglucan of cotton (11) to characteristic fragments which can be readily separated and identified. Fig. 2-3 shows the electropherograms obtained from the unadsorbed and adsorbed fractions along with the digestion products of tamarind xyloglucan. We have previously shown (11) that total cotton xyloglucan consists of predominantly XXXG, XXLG, XXFG, and XLFG (using the nomenclature proposed by Fry et al (12)). Both the unadsorbed and adsorbed material gave rise to oligosaccharides co-migrating with these previously characterized oligomers.

KOH-EPG-KOH Extraction

One gram of intact cell walls were directly extracted by 24% KOH containing 0.1% $NaBH_4$ (scheme illustrated in Fig. 2-4). About 20% weight of the walls was solubilized by direct KOH extraction (Table 2-3). The extracted material was chromatographed on an HQ anion exchange column. The chromatographic profile was similar to Fig. 2-2. Two major fractions were obtained as a non-adsorbed fraction and an adsorbed fraction. The sugar composition of each fraction is given in Table 2-4. If one

takes the sugar weight recovery of glc or fuc to represent the xyloglucan recovery, over 80% of the extracted XG is in the non-adsorbed fraction and only a small proportion of XG appears to be co-eluted with RG in the adsorbed fraction. Although most of the free XG was solubilized directly by KOH, most of the RG linked XG remained insoluble. A subsequent EPG digestion of the insoluble material allowed a second KOH extraction to solubilize most of the remaining RG linked XG. The sugar composition of each fraction is given in Table 2-3. The second KOH extract was separated on an HQ anion exchange column. The sugar composition of the non-adsorbed and adsorbed fractions is listed in Table 2-4. In the second KOH extraction, the majority of the extracted XG co-eluted with RG on the HQ anion exchange column.

EPG-Endoglucanase Extraction

In the EPG pre-digested wall residue, most of the XG and RG stayed intact. To investigate if RG is held by XG or not, endoglucanase (EG) was applied to digest the residue. Interestingly, in the endoglucanase solubilized fraction, the sugar composition showed (in mole%) 8% rha, 21% galA, in addition to the XG sugars. If one takes the sugar weight recovery of rha and fuc to represent the recovery of RG I and XG, respectively, about 50% by weight of the XG and 50% by weight of the RG I, were solubilized by endoglucanase (Table 2-5). Further separation of the soluble material on a DEAE anion exchange column resulted in five fractions (Fig. 2-6). The sugar composition of each separated fraction is listed in Table 2-6. The unadsorbed fraction (F-1) is rich in XG sugars. The ANTS labeled electropherogram showed it is mainly endoglucanase digested XG subunits (data not shown). Fractions F-2 and F-3 are mainly galA dimer and trimer, respectively. A small proportion of galA dimer and trimer could be left from the previous EPG digestion products. Fractions F-4 and F-5 are eluted under 1 M ammonium acetate and 2 M ammonium acetate, respectively. The sugar compositions showed that these two fractions are mainly composed of RG with a trace of

XG. Releasing of RG by endoglucanase indicates that part of the RG is interconnected to the XG.

However, there was still about 50% that could not be solubilized by endoglucanase. The remaining XG could be tightly associated with cellulose microfibrils where they could not be accessed by endoglucanase. The remaining RG could be linked to XG tightly associated with cellulose or other insoluble material e.g. extensin. A subsequent 24% KOH-0.1% $NaBH_4$ was applied to extract the residue after endoglucanase. More XG and RG material were solubilized. The chromatographic profile of separation of the KOH extracts on an anion exchange column is illustrated in Fig. 2-7. The unbound fraction was mainly XG and the bound fraction, from its sugar composition, was a combination of RG and a trace of XG.

Gel Filtration Chromatography of Extracted Cell Wall Fractions

The extracted co-eluted XG-RG complex (B-5), unadsorbed XG (B-1) and endoglucanase released RG (F-4 or F-5) were chromatographed on an HW 65 (S) gel filtration column (Fig. 2-8). The fractionation range of HW 65 (S) is from 10 kDa to 1000 kDa with comparison to pullulan standards. The co-eluted XG-RG complex fraction gave a single broad peak with an apparent average molecular mass of 400 kDa. The unadsorbed XG showed a single broad peak with an apparent average molecular mass of 110 kDa. The endoglucanase released RG fraction showed a peak with an apparent average molecular mass of 250 kDa and a small molecular mass peak around the included volume. This small molecular mass fraction might be galA oligomers left from the previous EPG digestion products.

DISCUSSION

Comparison of EPG-KOH extraction and KOH-EPG-KOH extraction

24% KOH is the conventional solvent used to extract XG from cell walls by breaking the strong hydrogen bonds between XG and cellulose and causing swelling of the cellulose microfibrils (13). Lower concentrations of KOH (4%, 10%) were reported to be inefficient for extraction of XG from intact walls (14). Chelating reagents like CDTA, EDTA have been used to extract calcium bound HGs. Sodium bicarbonate was reported to extract ester linked RG I. However, none of them alone or in a combination can extract most of the XG or pectin. Chelating reagents followed by strong alkali only extracted 25% of the original pectic acids and 50% of the original XG from rose suspension cell walls (15).

In cotton suspension cell walls, 24% KOH extraction of the intact cell walls only solubilized about 40% of the total XG and 20% of the total pectin (mostly RG I). However, the combination of EPG and 24% KOH solubilized about 90% of the total XG and 90% of the total pectin which includes HG, RG I, RG II and XGA. The presence of HG seems to prevent the co-extraction of the XG-RG complex by strong alkali. It could be that, the HG polymers form calcium bridges and cause physical entanglement preventing other wall polymers from being solubilized; or, if HG and RG I are interconnected, that the HG polymer does not dissolve well in alkali solution and thus keeps the whole complex insoluble. The KOH solubilized RG I from the intact walls could be some base labile linked RG I or cleaved off by β-elimination.

Non-crosslinked XG

In cotton suspension cell walls, two types of XG are present: non-crosslinked XG and RG crosslinked XG. EPG-KOH extracted XGs are half non-crosslinked XG and half RG crosslinked XG. KOH extracted XGs are over 80% non-crosslinked XG. However,

the non-crosslinked XG extracted using either method (B-1 or C-1) shows a similar sugar composition, a total sugar weight (which accounts for about 45% of the original XG in the intact walls) and a similar molecular mass (110 kDa). Since 24% KOH is a very alkaline solution, 0.1% $NaBH_4$ was added to prevent β-elimination of the polymer. Incubation of the taramind XG with 24% KOH-0.1% $NaBH_4$ was done as a control experiment. However, it did not show a significant size shift of XG on an HW 65 (S) gel filtration column (data not shown).

Crosslinked XG-RG complex

The co-eluted XG-RG complex showed an apparent molecular mass of 400 kDa. It appeared to be mainly contributed from the RG I which showed about 250 kDa apparent molecular mass after degradation of the XG-RG complex with endoglucanase. The basic components of the XG in non-crosslinked XG and RG crosslinked XG are almost identical. Both XGs shows similar subunits with the major types being XXXG (25-29%), XXFG (40-42%) and minor types being XXLG (13-14%) and XLFG (16-21%) (Fig. 2-3).

The extraction of the crosslinked XG-RG complex is much harder than the non-crosslinked XG. It can be extracted extensively only after the removal of HG. In the residue after KOH extraction of the intact walls, further EPG digestion followed by a KOH extraction solubilized more XG-RG complex. The sum of the extracted XG-RG complex amount (C-2 plus E-2) is close to the complex amount from EPG-KOH extraction (B-5). Approximately 100 mg of the XG-RG complex can be extracted from 1.0 gram of intact walls.

In the adsorbed fraction of KOH extract (C-2), the co-extraction of HG and RG I was expected if HG and RG I are interconnected, since there is no EPG pre-digestion of the walls. However, in comparison to the sugar composition of the adsorbed fraction of EPG-KOH extraction (B-5), there is only a slightly higher content of galA and rha

present in the C-2 fraction. The lack of co-extraction of HG with the RG-XG complex from the intact walls by strong alkali could have several explanations. First, if HG is linked to RG I, during strong alkali extraction β-elimination of methyl-esterified galA might occur and result in breaking of the HG backbone and release of the RG I from the HG. Second, in comparison to RG I, the HG polymer does not solubilize well in alkali solution no matter whether it is linked to RG I or not. Third, most of HG might not be linked to RG I, so alkali extraction only released RG-linked XG. If this is true, then the presence of HG could just act as a physical entanglement between XG and RG.

XG-RG complex is covalently crosslinked

Much of the XG extracted by the combination of EPG and 24% KOH co-eluted with RG on an anion exchange column. Are these two polymers linked by covalent linkage? Since 24% KOH is a very harsh extractant, most linkages such as ester bonds would be destroyed. So the linkage between XG and RG must be alkali resistant as are glycosidic bonds. Endoglucanase digestion of the EPG pre-treated walls released 50% of the total RG and 50% of the XG oligomers. The remaining RG which could be extracted by 24% KOH was co-eluted with part of the XG on an anion exchange column. If RG is not linked to XG covalently, but only physically stuck to the insoluble residue, then endoglucanase which does not digest RG (except it contains a trace of EPG) would not liberate RG from the residue. The reasonable explanation would be the cleavage of the XG backbone freed the RG which was held in the wall by connection to the XG. The remaining XG or RG which are tightly associated with cellulose or other insoluble polymers can be extracted by strong alkali. All these results provide evidence that XG and RG are covalently crosslinked.

CONCLUSION

During the sequential extraction of intact cotton walls by enzymes and strong alkali, we found that removal of the HG by EPG enabled 24% KOH to extract most of the XG and RG from the cellulose residue. Half of the extracted XG was present as non-crosslinked XG while the other half was RG crosslinked to XG. A hypothesized covalent linkage between XG and RG is under investigation and will be discussed more in the later chapters.

REFERENCES

1. **Keegstra, K., Talmadge, K. W., Bauer, W. D., and Albershem, P.** 1973. The structure of plant cell walls. III. A model of the walls of suspension-cultured sycamore cells based on the interconnections of the macromolecular components. *Plant Physiol.* 51: 188-196
2. **Carpita, N. C., Gibeaut, D. M.** 1993. Structural models of primary cell walls in flowering plants: consistency of molrcular structure with the physical properties of the walls during growth. *The Plant Journal.* 3(1): 1-30
3. **Qi, X., Behrens, B. X., West, P. R. and Mort, A. J.** 1995. Solubilization and partial characterization of extensin fragments from cell walls of cotton suspension cultures. Evidence for a covalent crosslink between extensin and pectin. *Plant Physiol.* 108(4): 1691-1701
4. **Ruyack, J., Downing, M. R., Chang, J. S. and Mitchell, E. D.** 1979. Growthof callus and suspension culture cells from cotton varirties (*Gossypium hursutum* L.) resistant and susceptible to *Xanthomonas malvacearum* (E. F. SM) Dows. *In Vitro* 15: 368-373
5. **Komalavilas, P. and Mort, A. J.** 1989. The acetylation at O-3 of galacturonic acid in the rhamnose-rich region of pectins. *Carbohydr. Res.* 189: 261-272
6. **Thomas, J. and Mort, A. J.** 1994. Continous postcolumn detection of underivatized polysaccharides in high-performance liquid chromatography by reaction with permanganate. *Anal. Biochem.* 223(1): 99-104
7. **Zhang, Z., Pierce, M. L. and Mort, A. J.** 1996. Detection and differentiation of pectic enzyme activity in vitro and in vivo by capillary electrophoresis of products from fluorescent-labeled substrate. *Electrophoresis* 17(2): 372-378
8. **Merz, J. M. and Mort, A. J.** 1998. A computer-controlled variable light attenuator for protection and autoranging of a laser-induced fluorescence detector for capillary zone electrophoresis. *Electrophoresis* 19(12): 2239-2242
9. **Darvill, A. G., McNeil, M. and Albersheim, P.** 1978. Structure of plant cell walls. VIII. A new pectic polysaccharide. *Plant Physiol.* 62: 418-422
10. **Schols, H. A., Bakx, E. J., Schipper, D. and Voragen, A. G., J.** 1995. A xylogalacturonan subunit present in the modified hairy regions of apple pectin. *Carbohydr. Res.* 279: 265-279

11. **El Rassi, Z., Tedford, D., An, J. and Mort, A. J.** 1991. High performance reversed-phase chromatographic mapping of 2-pyridylamino derivatives of xyloglucan oligosaccharides. *Carbohydr. Res.* 215(1): 25-38

12. **Fry, S.C., York, W.S., Albersheim, P., Darvill, A., Hayashi, T., Joseleau,JP., Kato, Y., Lorences, E.P., Maclachlan, G. A., McNeil, M., Mort, A. J., Reid, G., Seitz, H.U., Selvendran, R. R., Voragen, A. G. J., White, A. R.** 1993. An unambiguous nomenclature for xyloglucan-derived oligosaccharides. *Physiologia Plantarum* 89: 1-3

13. **Hayashi T. and Maclachlan, G.** 1984. Pea xyloglucan and cellulose, I Macromolecular organization. *Plant physiol.* 75: 596-604

14. **Hayashi T. Marsden, M. P. and Delmer, D. P.** 1987. Pea xyloglucan and cellulose, V Xyloglucan-cellulose interactions *in vitro* and *in vivo*. *Plant physiol.* 83: 384-389

15. **Chambat, G., Barnound, F., Joseleau, J. P.** 1984. Structure of the primary cell walls of suspension-cultured rose glauca cells. *Plant Physiol.* 74: 687-693

Figure 2-1 Flow chart of EPG-KOH extraction and isolation of the XG-RG complex

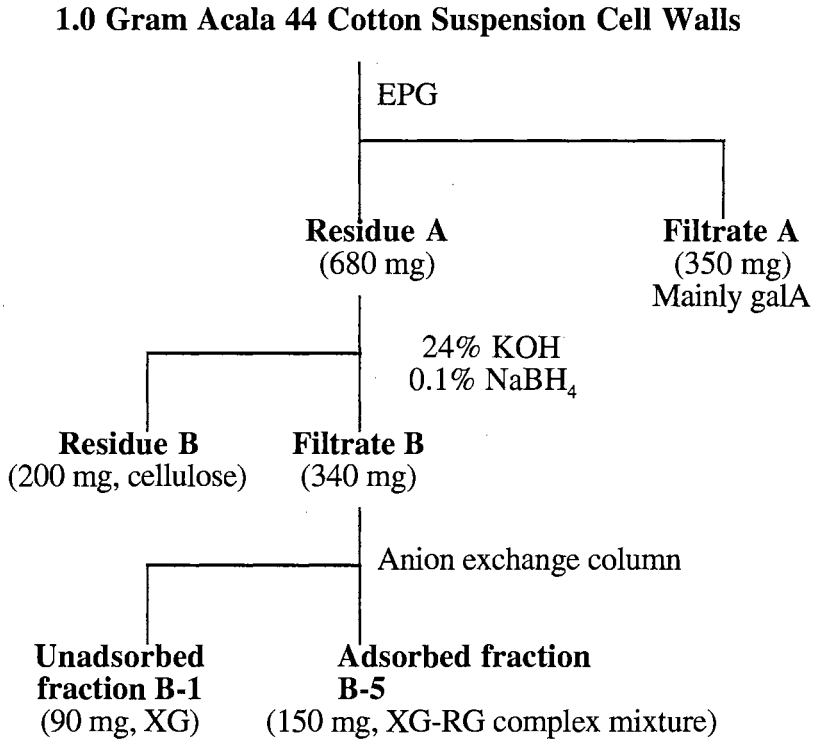

Table 2-1. Sugar composition of fractions from EPG-KOH sequential extraction of 1.0 gram of intact walls

Sugar	Intact Wall		EPG (S)		EPG (R)		KOH (S)		KOH (R)	
	Mole%	wt(mg)	Mole%	wt(mg)	Mole%	wt(mg)	Mole%	wt(mg)	Mole%	wt(mg)
Ara	23	(84)	8	(14)	30	(85)	26	(50)	12	(6)
Rha	8	(35)	4	(7)	9	(27)	9	(19)	6	(3)
Fuc	2	(10)	0.4	(0.7)	2	(7)	3	(6)	2	(1)
Xyl	14	(52)	1	(2)	17	(49)	22	(44)	13	(6)
GalA	37	(180)*	81	(175)	22	(85)	13	(35)	24	(15)
Gal	10	(46)	4	(8)	13	(44)	14	(35)	11	(7)
Glc	5	(21)*	0.2	(0.5)	6	(20)*	13	(30)	31	(18)*
Total sugar wt		(430)		(215)		(340)		(221)		(56)
Fraction wt		(1000)		(350)		(680)		(340)		(200)

Mole%: molar percentage of sugars accounted for in the GLC analysis
wt (mg): sugar weight in mg calculated from GLC analysis
Total sugar wt: total sugar weight of each fraction calculated from GLC analysis
Fraction wt: total weight of each fraction
S: soluble fraction
R: residue fraction
The number marked with an * was underestimated due to the sugar polymer's resistance to hydrolysis under the condition used.

Figure 2-2 Separation of EPG-KOH extracts on an HQ anion exchange column

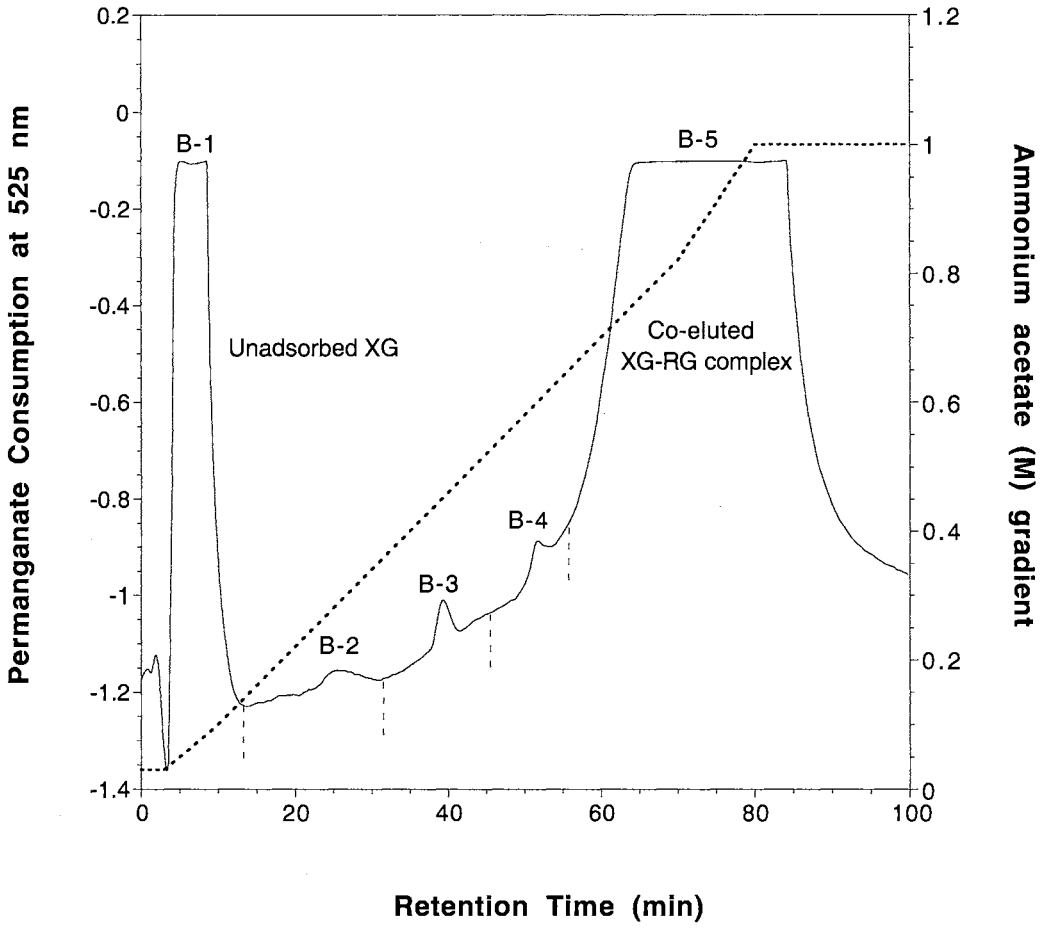

Table 2-2. Sugar composition of HQ column separated fractions of EPG-KOH extracts

Sugar	B-1		B-2		B-3		B-4		B-5	
	Mole%	wt(mg)	Mole%	wt(mg)	Mole%	wt(mg)	Mole%	wt(mg)	Mole%	wt(mg)
Ara	23	(8)	15	(0.4)	39	(1)	30	(1.4)	26	(24)
Rha	n.d.		2	(tr.)	7	(0.2)	10	(0.5)	12	(13)
Fuc	6	(2)	1	(tr.)	2	(tr.)	1	(0.1)	3	(3)
Xyl	34	(12)	55	(1.7)	21	(0.5)	17	(0.8)	17	(16)
GalA	n.d.		9	(0.4)	8	(0.2)	15	(0.9)	18	(22)
Gal	13	(6)	9	(0.3)	12	(0.4)	13	(0.7)	13	(15)
Glc	25	(11)	6	(0.2)	10	(0.3)	10	(0.6)	10	(12)
Total sugar wt		(39)		(3)		(2.6)		(5)		(105)
Fraction wt		(90)		(8)		(6)		(10)		(150)

Mole%: molar percentage of sugars accounted for in the GLC analysis
wt (mg): sugar weight in mg calculated from GLC analysis
Total sugar wt: total sugar weight of each fraction calculated from GLC analysis
Fraction wt: total weight of each fraction
n.d.: not detected
tr.: trace

Figure 2-3 Electropherograms of ANTS labeled XG subunits generated from endoglucanase digestion of tamarind XG (A), unadsorbed XG (B) and co-eluted XG-RG complex mixture (C)

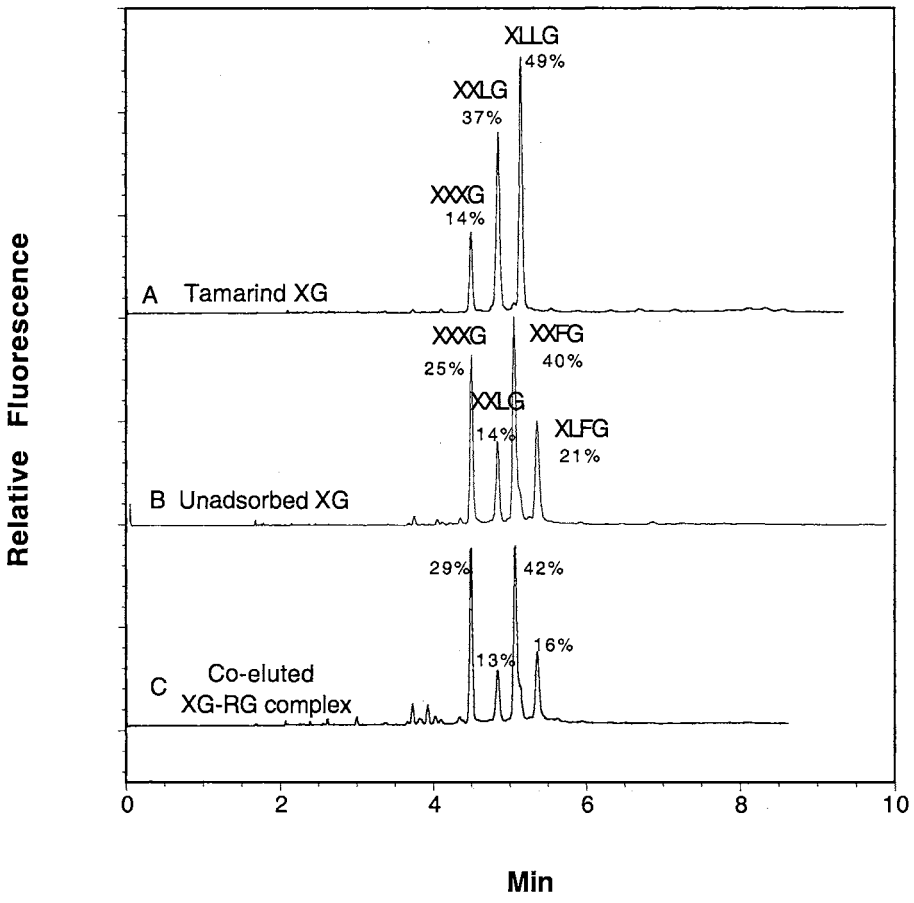

Figure 2-4 Flow chart of KOH-EPG-KOH sequential extraction and isolation of the XG-RG complex

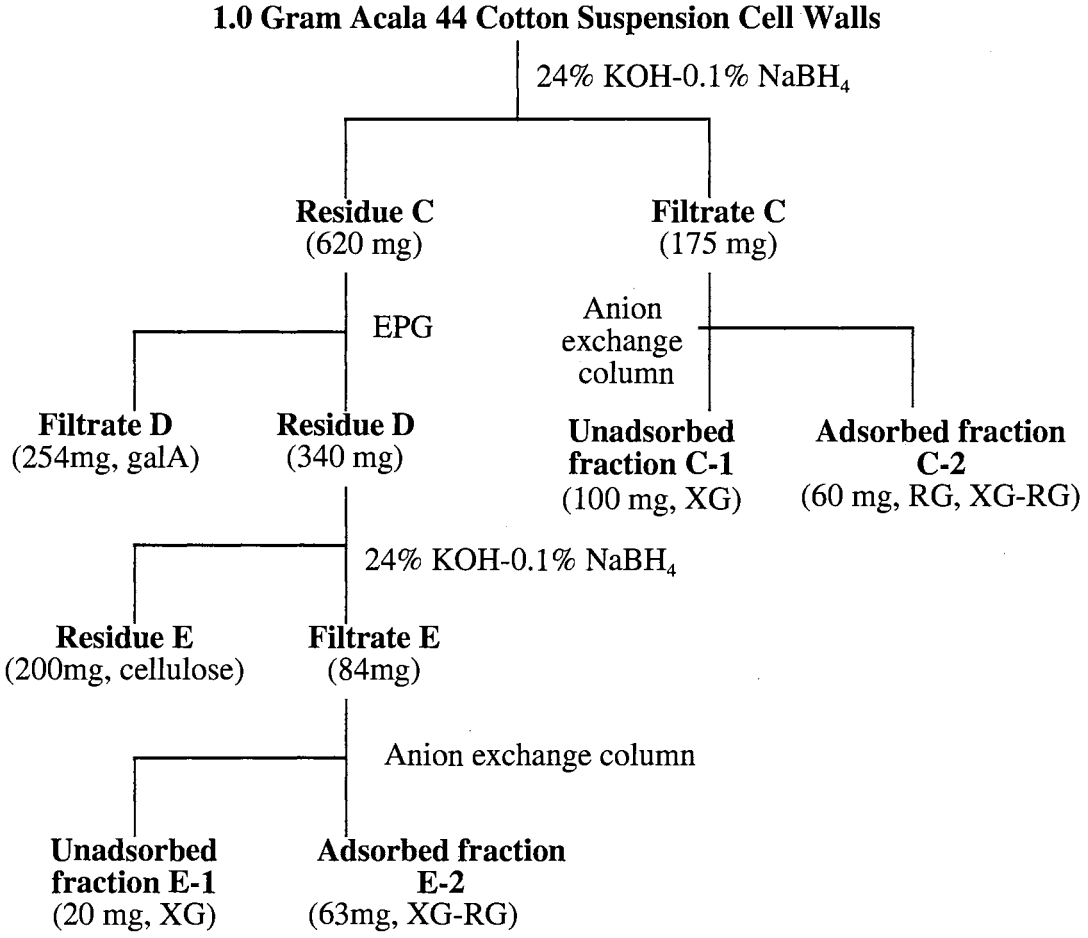

Table 2-3. Sugar composition of fractions from KOH-EPG-KOH sequential extraction of 1.0 gram of intact walls

Sugar	Intact Wall		KOH (S)		KOH (R)		EPG (S)		KOH (S)		KOH (R)	
	Mole%	wt(mg)	Mole%	wt(mg)	Mole%	wt(mg)	Mole%	wt(mg)	Mole%	wt(mg)	Mole%	wt(mg)
Ara	23	(84)	28	(28)	14	(36)	13	(17)	21	(11)	5	(1)
Rha	8	(35)	7	(7)	8	(22)	7	(10)	10	(6)	3	(0.8)
Fuc	2	(10)	3	(3)	2	(5)	0.5	(0.7)	3	(2)	2	(0.6)
Xyl	14	(52)	21	(21)	10	(24)	3	(4)	26	(14)	19	(5)
GalA	37	(180)*	12	(16)	54	(186)	69	(120)	14	(10)	7	(2)
Gal	10	(46)	14	(17)	8	(23)	6	(9)	14	(10)	10	(3)
Glc	5	(21)*	15	(18)	5	(16)*	1	(1)	12	(8)	54	(17)*
Total sugar wt		(430)		(110)		(310)		(160)		(60)		(30)
Fraction wt		(1000)		(175)		(620)		(254)		(84)		(200)

Mole%: molar percentage of sugars accounted for in the GLC analysis
wt (mg): sugar weight in mg calculated from GLC analysis
Total sugar wt: total sugar weight of each fraction calculated from GLC analysis
Fraction wt: total weight of each fraction
S: soluble fraction
R: residue fraction
The number marked with an * was underestimated due to the sugar polymer's resistance to hydrolysis under the condition used.

Table 2-4. Sugar composition of HQ anion exchange column unbound and bound fractions of the first KOH extracts and the second KOH extracts

Sugar	First KOH extraction				Second KOH extraction			
	C-1 (UB)		C-2 (B)		E-1 (UB)		E-2 (B)	
	Mole%	wt(mg)	Mole%	wt(mg)	Mole%	wt(mg)	Mole%	wt(mg)
Ara	25	(10)	30	(12)	4	(0.2)	20	(8)
Rha	n.d.		15	(6)	n.d.		11	(5)
Fuc	5	(2)	1	(0.4)	6	(0.4)	3	(1)
Xyl	32	(12)	10	(4)	46	(3)	23	(9)
GalA	n.d.		25	(10)	n.d.		15	(8)
Gal	11	(5)	15	(7)	14	(1)	14	(7)
Glc	26	(12)	4	(2)	29	(2)	12	(6)
Total sugar wt		(40)		(42)		(7)		(45)
Fraction wt		(100)		(60)		(20)		(63)

Mole%: molar percentage of sugars accounted for in the GLC analysis
wt (mg): sugar weight in mg calculated from GLC analysis
Total sugar wt: total sugar weight of each fraction calculated from GLC analysis
Fraction wt: total weight of each fraction
UB: HQ anion exchange column unbound fraction
B: HQ anion exchange column bound fraction
n.d.: not detected

Figure 2-5 Flow chart of EPG-EG-KOH sequential extraction of cotton intact walls

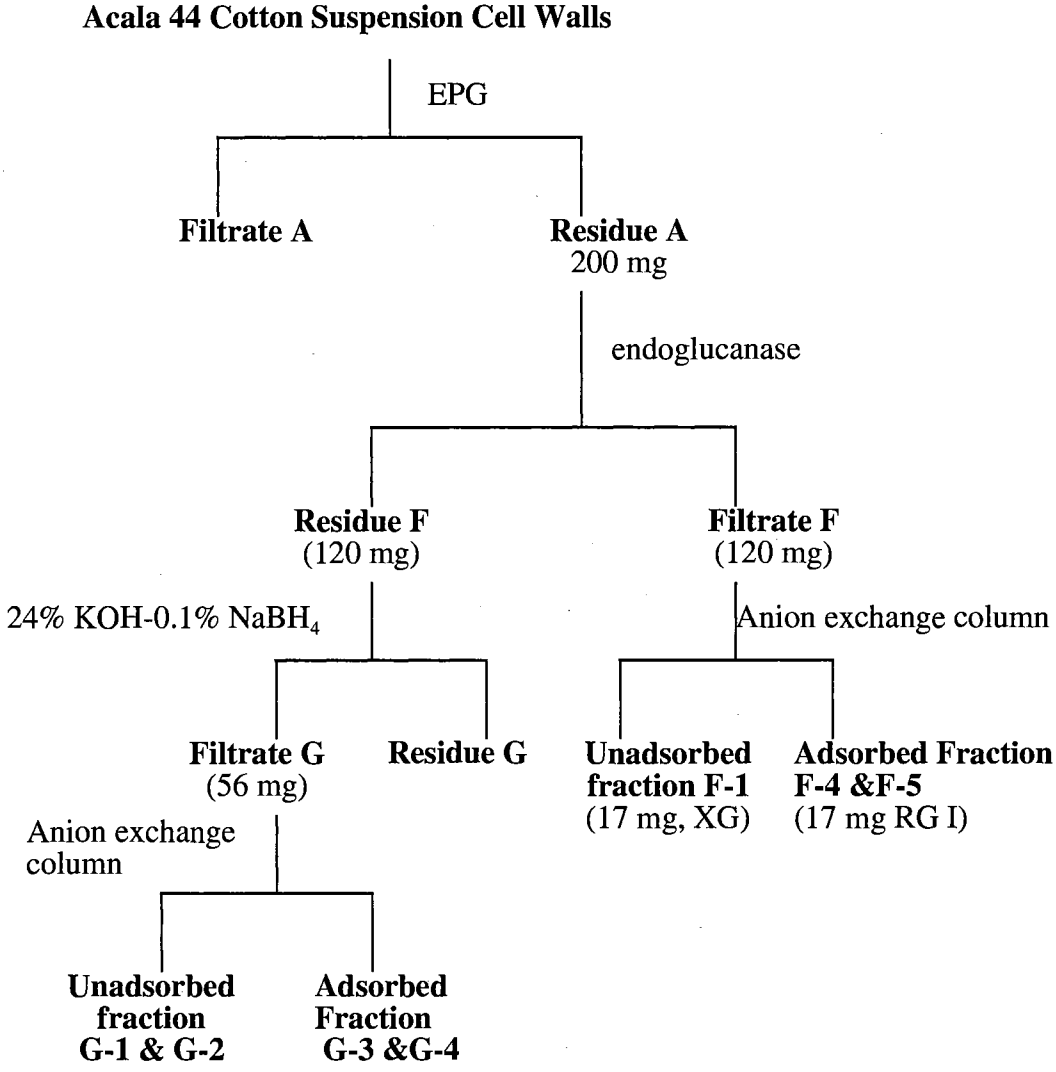

Table 2-5. Sugar composition of fractions from EG-KOH extraction of 200 mg of EPG pre-treated walls

Sugar	EPG (R)		EG (S)		EG (R)		KOH(S)	
	Mole%	wt(mg)	Mole%	wt(mg)	Mole%	wt(mg)	Mole%	wt(mg)
Ara	30	(25)	20	(10)	35	(14)	37	(11)
Rha	9	(8)	8	(5)	8	(4)	12	(4)
Fuc	2	(2)	2	(1)	2	(1)	1	(0.3)
Xyl	17	(15)	16	(8)	15	(6)	12	(4)
GalA	22	(25)	21	(14)	19	(10)	21	(8)
Gal	13	(13)	14	(9)	14	(7)	12	(5)
Glc	6	(6)*	19	(12)	6	(3)*	5	(2)
Total sugar wt		(100)		(60)		(50)		(34)
Fraction wt		(200)		(120)		(120)		(56)

Mole%: molar percentage of sugars accounted for in the GLC analysis
wt (mg): sugar weight in mg calculated from GLC analysis
Total sugar wt: total sugar weight of each fraction calculated from GLC analysis
Fraction wt: total weight of each fraction
S: soluble fraction
R: residue fraction
The number marked with an * was underestimated due to the sugar polymer's resistance to hydrolysis under the condition used.

Figure 2-6 DEAE anion exchange column profile of the endoglucanase solubilized material from the EPG pre-treated walls

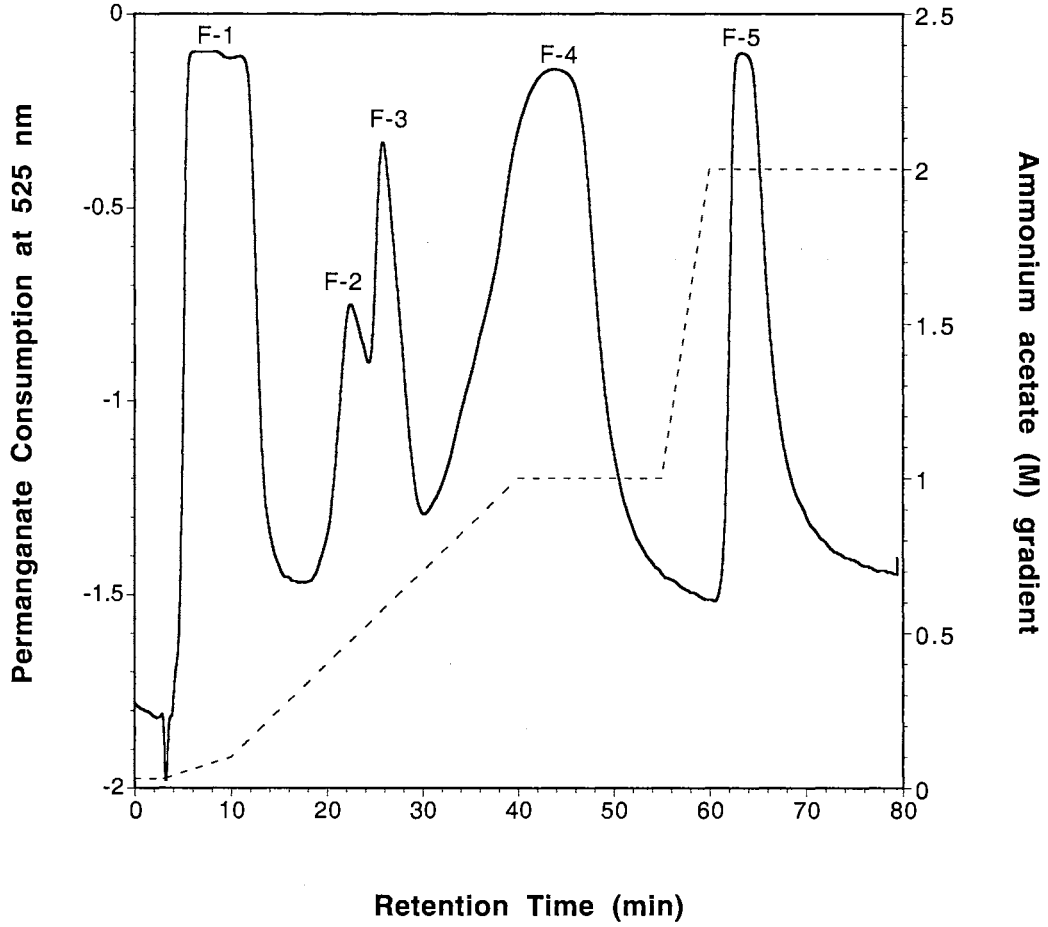

Table 2-6 Sugar composition of DEAE separated fractions of endoglucanase solubilized EPG pre-treated wall residue

Fraction	Sugar composition in mole%							Sugar twt (mg)
	Ara	Rha	Fuc	Xyl	GalA	Gal	Glc	
F-1	1	n.d.	6	37	2	11	43	17
F-2	2	n.d.	0.4	4	84	4	4	2.3
F-3	1	n.d.	2	13	68	4	12	0.6
F-4	36	13	0.4	4	30	14	1	12
F-5	29	20	0.7	5	30	15	2	5

Mole%: molar percentage of sugars accounted for in the GLC analysis
Sugar twt (mg): total sugar weight of each fraction calculated from GLC analysis
n.d.: not detected

Figure 2-7 DEAE anion exchange column profile of the KOH solubilized material from the EPG-EG treated residue

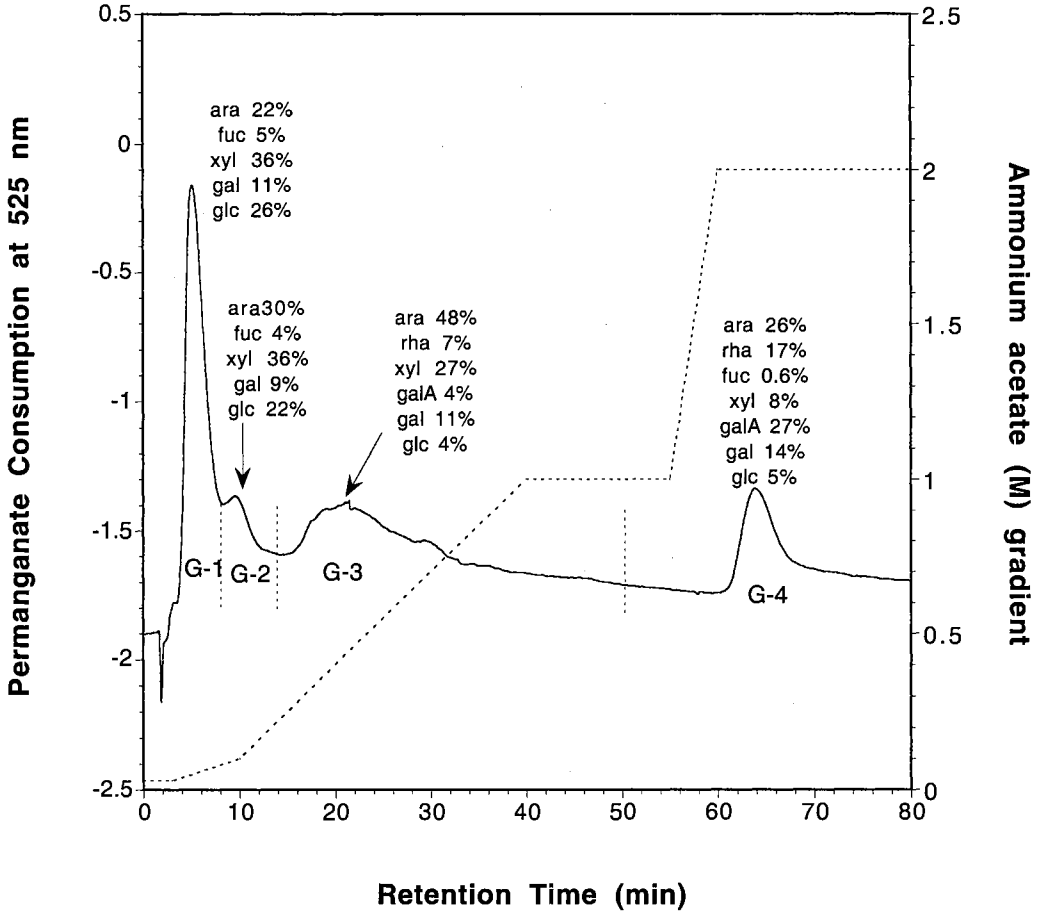

Figure 2-8 HW 65 (S) gel filtration profiles of the extracted cell wall fractions

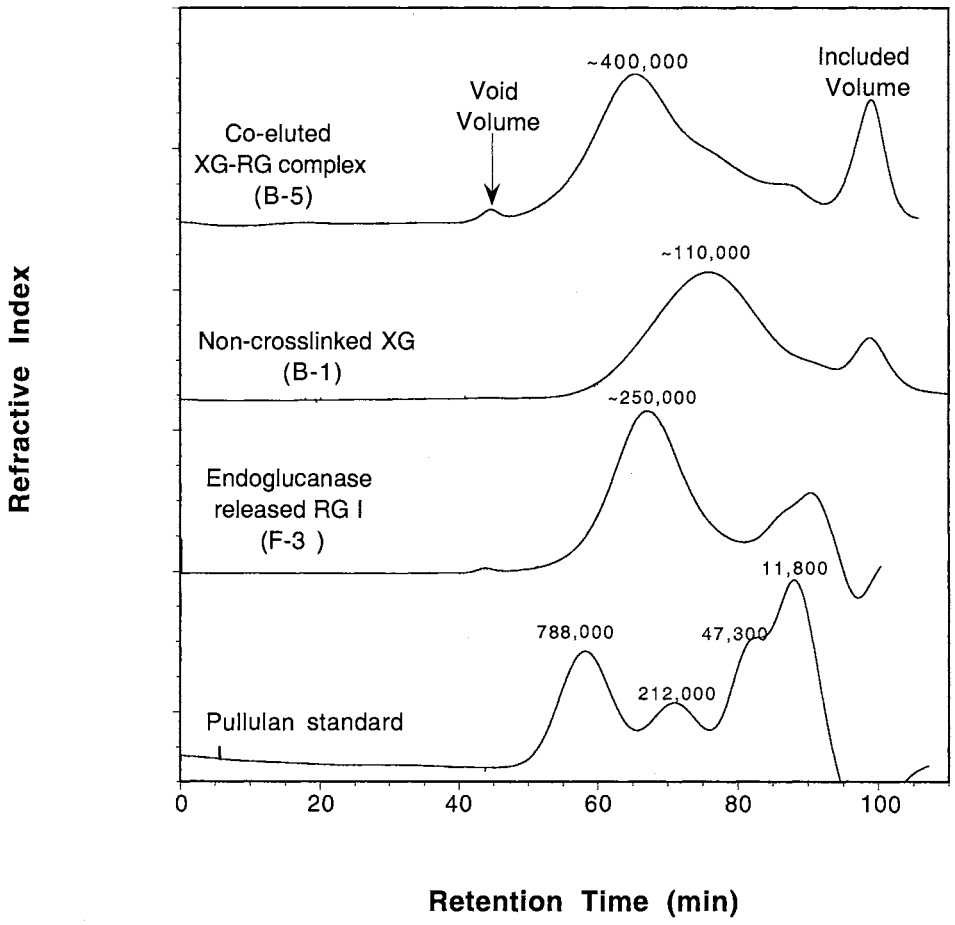

CHAPTER 3 *IN VITRO* BINDING OF XG-RG COMPLEX TO AVICEL CELLULOSE

INTRODUCTION

Xyloglucan (XG) has a cellulose like β-1-4 glucan backbone. It is generally composed of cellotetraose building blocks with three consecutive branches of xyl, gal-xyl or fuc-gal-xyl and an unbranched glc. The unbranched glc residues are normally susceptible to the xyloglucan degrading enzyme: endoglucanase (EG). The endoglucanase generated XG subunits from different species show structural similarity (1). The four basic subunits generated by endoglucanase from cotton XG are illustrated in Fig. 1-1 of chapter 1.

In plant cell walls, xyloglucans are believed not only to bind to the cellulose but also to inter-link different cellulose microfibrils or even weave into the amorphous parts of microfibrils (2). The interactions between XG and cellulose are thought to be through their glucan backbones. Unlike the bare glucan backbone of cellulose, the branches of XG prevent self association of XGs (3) and XG coated microfibrils from forming a larger cellulose complex.

XG can bind to cellulose specifically *in vitro* under acidic conditions (less than pH 6.0). However, the interactions *in vitro* between XG and cellulose are not as strong as the native ones, because 4% KOH was able to extract the *in vitro* bonded XG while 24% KOH was needed to extract the native XG (4, 5). The XG sidechain components and degree of polymerization (DP) of XG have been studied for the binding efficiency. Levy et al. (6) demonstrated that the fucosylated XG has a higher binding rate than the non-

fucosylated XG. Monte Carlo dynamic simulations suggested that trisaccharide sidechains of XG facilitate cellulose binding by forming a planar backbone conformation. Quantitative binding of different DP of XGs to cellulose showed a critical length of at least three repeating XG subunits are required and a preferential adsorption of larger molecules at high XG concentration (7).

In cotton suspension cell walls, approximately 50% of the extracted XG was co-eluted with the extracted RG on the anion exchange column. To further verify that the co-eluted XG and RG are covalently crosslinked to each other, avicel cellulose was used to bind the XG-RG complex.

MATERIALS AND METHODS

Enzyme and chemicals

Endoglucanase and arabinoheptose were purchased from Megazyme (Ireland). Avicel microcrystalline cellulose (PH-101) was purchased from Fluka Chemika-Biochemika (New York, USA). Xyloglucan oligomers were obtained by a partial endoglucanase degradation of extracted cotton XG and subsequent fractionation on a HW50 (S) gel filtration column. XG-RG complex mixture was prepared as described in chapter 2. RG I was obtained as the EPG resistant region of citrus pectin (8).

Preparation of avicel cellulose

Avicel cellulose was washed with 4 M NaOH with constant stirring at room temperature overnight. The suspension was centrifuged at 15,000 g for 10 min. The cellulose pellet was rinsed with water on a nylon filter (0.45 μm) until the pH of the filtrate was neutral. The pre-washed avicel cellulose was then freeze dried and ready for xyloglucan binding experiments.

Avicel cellulose-xyloglucan binding assays

The pre-washed avicel cellulose and xyloglucan sample (100:1 in weight) were mixed in 25 mM NaOAc, pH 5.8, to a concentration of approximately 100 mg/ml. The mixture was incubated at 37 °C with constant rotation for 6 h. The mixture was then centrifuged at 15,000 g for 10 min. The pellet was rinsed with distilled water twice and centrifuged. The supernatants were combined and freeze dried and designated the cellulose unbound fraction.

The cellulose bound fraction was obtained by incubation of the cellulose pellets with 1 M NaOH at room temperature with constant rotation for 6 h. After centrifugation at 15,000 g for 10 min, the alkali supernatant was neutralized with concentrated acetic acid to pH 7 and dialyzed in a 1,000 Da cut off membrane against distilled water. After dialysis the retentate was freeze dried and designated the avicel bound fraction.

An alternate method to release bound XG from avicel was incubation of the cellulose pellets with endoglucanase (Megazyme) in 50 mM ammonium acetate buffer, pH 4.5, to a concentration of approximately 100 mg/ml. One unit of endoglucanase was added to about 1 mg of xyloglucan sample and gently stirred overnight at 37 °C. The suspension was centrifuged at 15,000 g for 10 min, the pellets were rinsed with distilled water twice and centrifuged. The supernatants were combined and freeze dried and designated the endoglucanase released bound fraction.

Analytical methods

For gel filtration chromatography, GLC sugar composition analysis and CZE see methods of chapter 2.

RESULTS

Avicel binding of XG oligomers

Extensive washing of avicel microcrystalline cellulose by strong alkali solubilized about 0.5 % by weight of the total avicel. The sugar composition (mole%) of the solubilized material showed it to contain 73% xyl, 17% man, 8% glc and a trace of ara, gal and 4-O-methyl-glcA. The pre-washed avicel showed a "clean" background, i.e. there was no sugar released by 1 M NaOH.

A mixture of oligomers (XG_2 to XG_{10}) was prepared from partial degradation of the cotton XG with endoglucanase. After incubation of the XG oligomers with the avicel, the unbound sugars were removed by centrifugation. The bound XG was released by 1 M NaOH. Both the unbound and bound fractions were labeled with ANTS. The electropherograms are shown in Fig. 3-1. The majority of XG_2 fragments appeared in the avicel unbound fraction, while the fragments XG_3 and bigger were mainly in the avicel bound fraction. The ANTS labled XG oligomers appeared as clusters of peaks. The small oligomer of XG_2 showed several sharp peaks and the bigger ones merged into bumps. This is because the cotton XG is composed of four subunits (XXXG, XXLG, XXFG and XLFG). The high DP XG can contain more combinations of subunits and the molecular weight differences between them are small. The CZE could not resolve those individual fragments of the high DP XGs, but addition of one subunit of XG is very obvious. The result that XG_3 and bigger oligomers bound to the avicel was consistent with the result of Vincken's although the XG oligomers they used were from non-fucosylated tamarind XG (7).

To examine if avicel cellulose can bind other sugars than XG, RG I and arabinoheptaose were incubated with the pre-washed avicel. None of them showed significant binding to cellulose (data not shown).

Avicel binding of XG-RG complex

The co-eluted XG-RG complex material (B-5) was incubated with the pre-washed avicel for 6 hours with constant rotation. After centrifugation, about 30% of the total weight of the material was left in the avicel unbound supernatant, which indicated that about 70% of the material bound to the avicel. The unbound fraction, from its sugar composition (Table 3-1), appears to be predominantly RG I. The amount of rha in the unbound fraction accounts for 50% of the starting rha amount. Rha recovery is taken into consideration for RG I recovery, because rha is only present in RG I region while galA is present in both RG I and XGA. Thus half of the RG I is in the unbound fraction and the other half, together with most of the XG, bound to the avicel. Since RG I does not bind to the avicel by itself, the presence of RG I in the avicel-bound fraction further indicates that there is a covalent linkage between XG and RG.

Much of the avicel bound XG-RG complex can be re-extracted by 1M NaOH. The yield of the alkali extraction was about 30% of the original complex material. The sugar composition of the alkali released fraction showed it to be enriched in XG (Table 3-1). The relative molar ratio of glc: rha increased from 0.8: 1 in the whole complex to 1.7: 1 in the bound fraction. When chromatographed on an HW65 gel filtration column (fractionation range from 10 kDa to 1000 kDa for dextrans), the avicel unbound fraction (RG I) and the avicel bound fraction (XG-RG complex) showed a similar size range (Fig. 3-2). This also indicates that there is no significant breaking of polymer during the alkali extraction.

The avicel bound XG was reported to be susceptible to endoglucanase digestion (7). In some experiments, endoglucanase instead of 1M NaOH, was used to digest the avicel bound fraction. A control experiment was also carried out using the same amount of enzyme to digest the same amount of washed avicel that was used for binding. Fig. 3-3 shows an HW40 gel filtration column separation of endoglucanase released material from the avicel bound complex and the avicel itself. The endoglucanase purchased from

Megazyme can digest a small amount of avicel (less than 0.3% of the weight) into cellobiose and glucose. However, the endoglucanase released material from the bound complex is much bigger than cellobiose or glucose. The interference from the material released from avicel can be easily subtracted by chromatography. The sugar compositions and weights of endoglucanase released fractions are listed in Table 3-1. About 70% by weight of rha (indicative of RG) was recovered in the endoglucanase released fractions from the avicel bound complex. But the recovered glc (indicative of XG) was only about 10% by weight. The majority of the bound xyloglucan was still associated with the avicel. Further treatment with 1M NaOH solubilized more polymeric XG (but not all the remaining XG). The components of the alkali released polymeric XG showed a relatively high content of XXFG and XLFG after endoglucanase digestion and labeling with ANTS (Fig. 3-4). The endoglucanase released XG subunits are rich in XXXG type. This indicates that XXXG may be a preferential site to be cleaved by endoglucanase, or the fucosylated subunits (XXFG, XLFG) bind tightly with cellulose where they could not be accessed by the enzyme. Because RG does not have a glucan backbone, it would not be directly associated with the cellulose. It could be that RG is linked to the end of the XG chains or on loops where they are away from the cellulose surface and can be cleaved by the enzyme.

DISCUSSION

The total recovery of the XG-RG complex fraction after avicel binding is about 70% in which, 30-50% is in the unbound fraction and 20-40% is in the bound fraction released by 1 M NaOH. In the avicel unbound fraction, there is still a small proportion of XG mixed with RG (Table 3-1). The reason that some of the XG-RG complex did not bind to the cellulose could be insufficient cellulose binding surface, low DP of XG, steric hindrance from crosslinked RG I, or bad adsorption conditions for XG and cellulose. The

remaining 30% of the sample might be lost during the preparations or so strongly bound to the avicel that it could not be extracted by 1 M NaOH.

Avicel binding of the co-eluted XG-RG fraction separated away the free RG I from the true XG-RG complex. The free RG I polymer and the XG-RG complex showed a similar molecular mass on an HW 65 gel filtration column. Because Na_2CO_3 or lower concentration of alkali has been reported to extract RG I, the free RG I polymers mixed in the co-eluted fraction could represent the RG I that was ester-linked in the original walls. Evidence of avicel cellulose binding of XG-RG complex indicates that in cotton suspension cell walls, about half of the extracted RG is covalently crosslinked to half of the extracted XG.

REFERENCES

1. **Hayashi, T.** 1989. Xyloglucans in the primary cell wall. *Annu. Rev. Plant Physiol. Plant Mol. Biol.* 40: 139-168
2. **Carpita, N. C., Gibeaut, D. M.** 1993. Structural models of primary cell walls in flowering plants: consistency of molrcular structure with the physical properties of the walls during growth. *The Plant Journal.* 3(1): 1-30
3. **Reid, J. S. G., Edwards, M. and Dea, I. C. M.** 1988. Enzymatic modification of natural seed gums. *Gums and Stabilizers in the food industry* 4:391-398
4. **Hayashi T. and Maclachlan, G.** 1984. Pea xyloglucan and cellulose, I Macromolecular organization. *Plant physiol.* 75: 596-604
5. **Hayashi T. Marsden, M. P. and Delmer, D. P.** 1987. Pea xyloglucan and cellulose, V Xyloglucan-cellulose interactions *in vitro* and *in vivo*. *Plant physiol.* 83: 384-389
6. **Levy, S., Maclachlan, G. and Staehelin, L.A.** 1997. Xyloglucan sidechains modulate binding to cellulose during in vitro binding assays as predicted by conformational dynamics simulations. *The Plant Journal.* 11(3): 373-386
7. **Vinken, J. P., Keizer, A. Beldman, G. and Voragen, A. G. J.** 1995. Fractionation of xyloglucan fragments and their interaction with cellulose. *Plant Physiol.* 108: 1579-1585
8. **Zhan, D., Janssen, P. and Mort, A. J.** 1998. Scarcity or complete lack of single rhamnose residues interspersed within the homogalacturonan regions of citrus pectin. *Carbohydr. Res.* 308(3-4): 373-380

Table 3-1 Sugar composition of the avicel unbound and bound fractions of the XG-RG complex mixture

	XG-RG complex mixture		Avicel-UB		Avicel-B*	1M NaOH released XG-RG		Endoglucanase released E-1		Endoglucanase released E-2	
	Mole%	mg	Mole%	mg	mg	Mole%	mg	Mole%	mg	Mole%	mg
Ara	25	(4)	31	(1.6)	(2.4)	16	(0.8)	31	(1.0)	3.6	(0.11)
Rha	14	(2.4)	22	(1.2)	(1.2)	10	(0.5)	18	(0.7)	2	(0.07)
Fuc	2.6	(0.4)	0.8	(0.05)	(0.35)	2	(0.11)	2	(0.06)	2	(0.07)
Xyl	18	(2.9)	5	(0.3)	(2.6)	24	(1.1)	6	(0.2)	25	(0.08)
GalA	16	(3.4)	29	(1.9)	(1.5)	18	(1.1)	29	(1.2)	4.7	(0.02)
Gal	11	(2.2)	11	(0.7)	(1.5)	12	(0.7)	11	(0.5)	15	(0.06)
Glc	12	(2.3)	1.6	(0.1)	(2.2)	17	(0.9)	3	(0.1)	46	(0.17)
Twt		(18)		(5.8)	(12.2)		(5.4)		(3.5)		(0.4)
Twt %		100%		30%	70%		30%		20%		2%

Twt: total sugar weight of each fraction calculated from GLC analysis
Twt %: total sugar weight recovery (total sugar weight in each fraction per total sugar weight of the XG-RG complex mixture)
UB: unbound fraction
B*: bound material was obtained from subtraction of the unbound fraction from the total fraction.
Endoglucanase released E-1 and E-2 fractions: fractions separated on HW 40 column (Fig. 3-3)

Figure 3-1 Electropherograms of ANTS labeled avicel unbound and bound XG oligomers A. Cotton XG oligomers B. 1M NaOH released avicel bound XG oligomers C. Avicel unbound XG oligomers

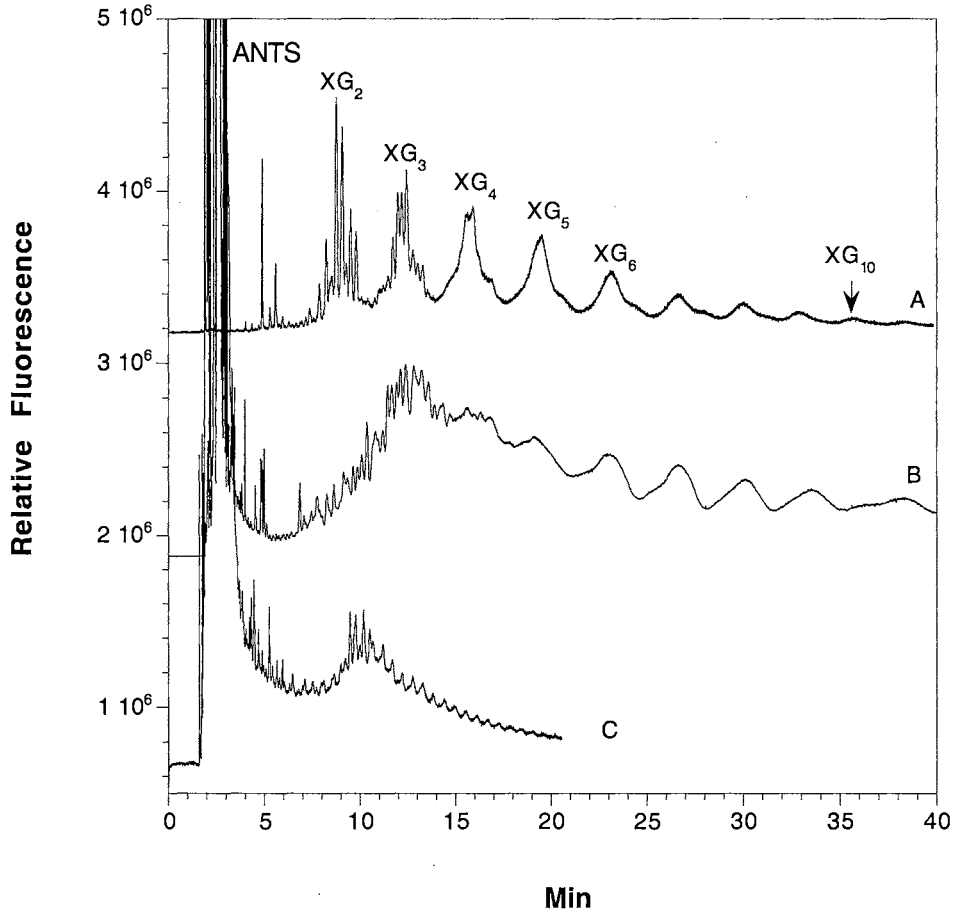

Figure 3-2 HW 65 (S) gel filtration profiles of co-eluted XG-RG complex (A), avicel unbound RG I (B), avicel bound XG-RG complex released by 1M NaOH (C) and Pullulan standard (D)

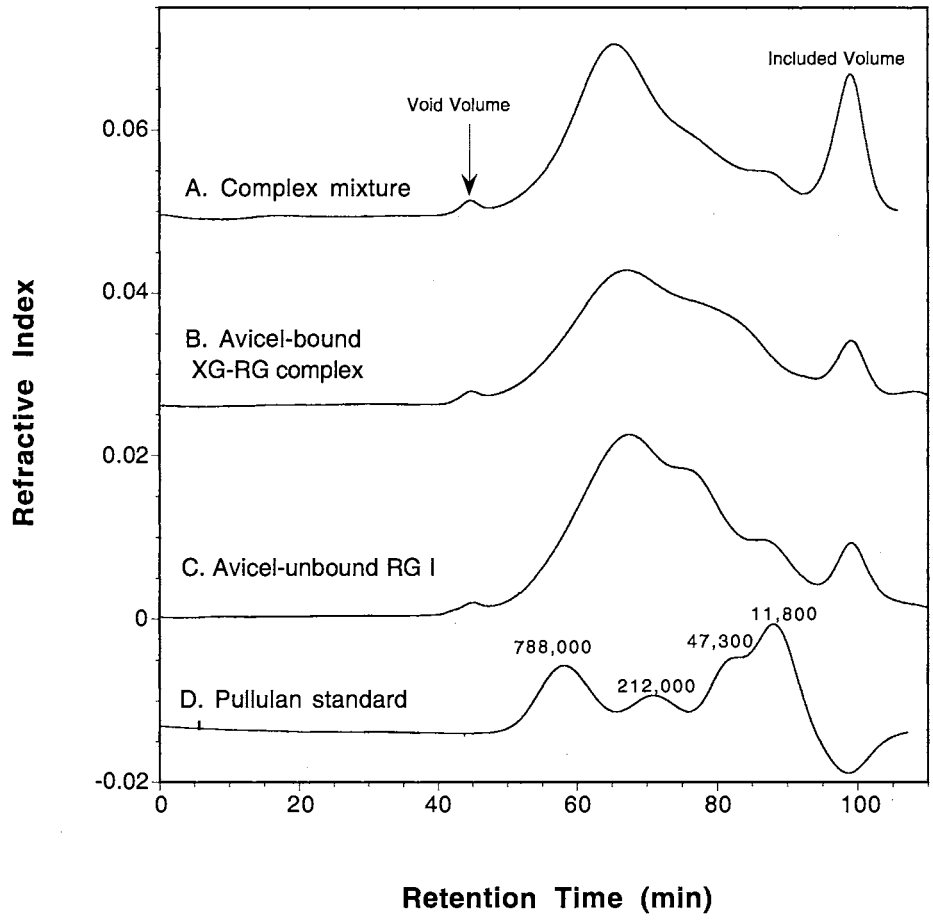

Figure 3-3 HW 40 (S) gel filtration profiles of the endoglucanase solubilized materials from the avicel bound XG-RG complex (A) and the avicel itself (B)

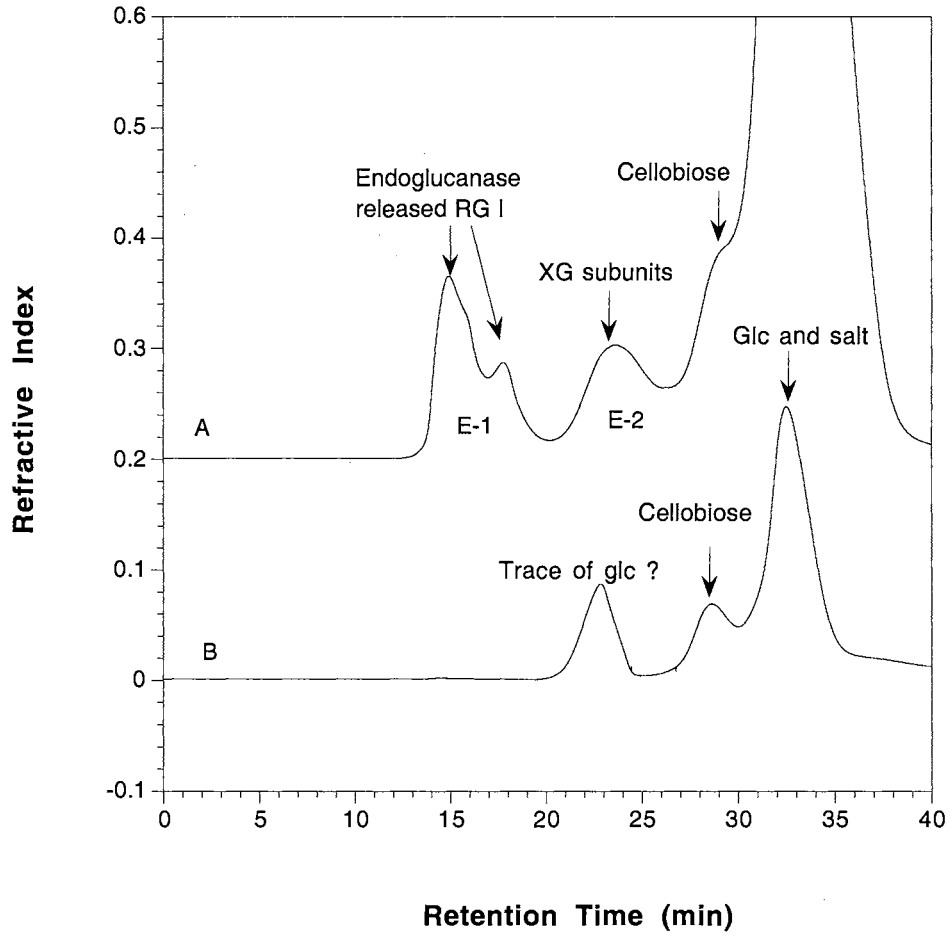

Figure 3-4 Electropherograms of endoglucanase released XG monomer (A) and polymeric XG released by subsequent 1M NaOH which was further digested by endoglucanase (B)

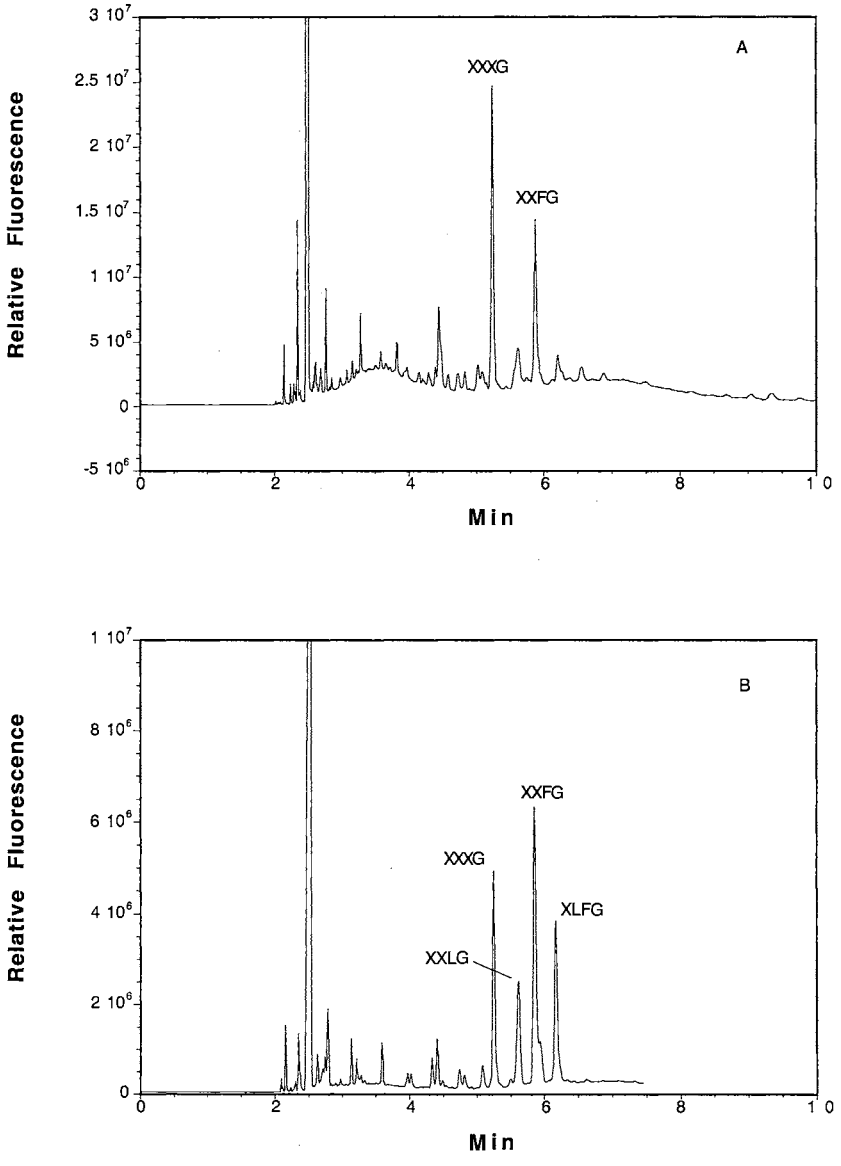

CHAPTER 4 EXPRESSION AND PURIFICATION OF CLONED ENDOARABINASE AND RHAMNOGALACTURONASE IN *PICHIA PASTORIS*

INTRODUCTION

Enzymatic and chemical methods have been widely used to characterize the cell wall structure. To study the XG-RG complex isolated from the cotton suspension cell walls, polysaccharide degrading enzymes were applied to degrade the macromolecular complex into characterizable size fragments. The crosslinks between XG and RG were proposed to be arabinan or arabinogalactan (1). To examine if it is true, arabinan or galactan degrading enzymes (endoarabinanase and endogalactanase, Megazyme) were used to digest the complex. Approximately 50% of the XG was released from the complex, but it was found to have been degraded by contaminating endoglucanase activity. The specificity of the enzymes for structure elucidation is very important. To obtain "pure" enzyme, cloning the enzyme gene and expression of it in an efficient expression system is the best way.

Pichia pastoris is a methylotropic yeast capable of metabolizing methanol in the absence of a repressing carbon source, by generating large amounts of alcohol oxidase. Two genes in *pichia* have been found to code for alcohol oxidase: AOX1 and AOX2. The AOX1 gene is responsible for the majority of alcohol oxidase activity. The AOX1 promoter can be used to drive expression of fusion proteins at high levels. Being an eukaryote, the *pichia* expression system has the advantages of protein processing, protein folding and posttranslational modification. The EasySelect *pichia* expression kit from

Invitrogen provides a simple cloning and selection scheme, and allows a rapid purification of fusion proteins by engineering a His-tag into the protein (2).

MATERIALS AND METHODS

pPICZαA expression vector

pPICZαA vector contains AOX1 promoter, α-factor secretion signal sequence, multiple cloning site, C-terminal myc epitope tag, C-terminal polyhistidine tag and zeocin resistance gene (2). The map of the pPICZαA vector is shown in Fig. 4-1.

Construction of the plasmid of endoarabinase-pPICZαA

A genomic endo-α-1,5-L-arabinase gene from *Bacillus subtilis* (3) was kindly offered from Dr. Sakamoto (Osaka Prefecture University, Japan). PCR primers were designed based on the deduced amino acid sequence of the putative mature protein. The nucleotide sequence of the gene and the primers are listed in Fig. 4-2. The pPICZαA vector was digested by EcoRI and XbaI. The linear vector DNA was filled in to make blunt ends using Klenow polymerase with dNTPs and then dephosphorylated. The PCR amplified DNA was treated with Klenow (without dNTPs) to make blunt ends and ligated into the pPICZαA vector. Wrong direction insertion will be cleaved by restriction enzymes of EcoRI or XbaI due to the introduction of EcoRI and XbaI sites from the primers. The right direction insertion was in frame with both the α-factor signal sequence and the C-terminal His-tag sequence. Fig. 4-3 lists the nucleotide sequence of the constructed plasmid (starting from the start codon of α-factor) and the deduced amino acid sequence.

Construction of the plasmid of RGase-pPICZαA

A rhamnogalacturonan hydrolase (RGase) gene from *Botryotinia fuckeliana* (4) was obtained from Dr. Gross's lab (Horticultural crops quality lab, USDA). PCR primers were designed based on the deduced amino acid sequence of the putative mature protein. The nucleotide sequence of the gene and the primers are listed in Fig. 4-4. EcoRI and XbaI sites were introduced into the upper primer and the lower primer, respectively (bold case indicates the restriction enzyme site).

The pPICZαA vector and the PCR amplified DNA were both digested with EcoRI and XbaI and then ligated. The right direction insertion was in frame with both the α-factor signal sequence and the C-terminal His-tag sequence. The nucleotide sequence of the plasmid (starting from the start codon of α-factor) and the deduced amino acid sequence are listed in Fig. 4-5.

Transformation and expression of recombinant protein in *pichia pastoris*

The recombinant plasmid DNA was transformed into *E. coli* (DH5α) and selected on low salt LB medium with zeocin antibiotics. Transformants were isolated and sequenced in the Core Facility (Oklahoma State University). The plasmid DNA with the correct insertion was integrated into a wildtype strain of *pichia*, X-33.

The transformant phenotype (Mut^+ or Mut^s) of methanol utilization was determined. Mut^+ phenotype colonies (utilizing methanol) were chosen for small-scale expression. A single colony was inoculated in 25 ml BMGY (buffered glycerol-complex medium). After shaking at 30 °C, 300 rpm overnight, the culture was centrifuged at 3000 g for 5 min. The pellets were resuspended in 250 ml BMMY (buffered methanol-complex medium) or MM (minimal methanol medium) and kept in 0.5% methanol by addition of 1.5 ml of methanol every 24 hours. One ml of culture was aliquoted at 0 day, 1 day, 2 days, 3 days, 4 days and 5 days. The aliquoted samples were centrifuged and the supernatants were used for enzyme activity assay.

Enzyme activity assay

Substrates preparation

Arabinoheptaose, tamarind xyloglucan (XG) and endoglucanase were purchased from Megazyme (Ireland).

Xyloglucan dimer was prepared by a partial endoglucanase digestion of the tamarind XG and purified on an HW 40(S) gel filtration column.

Rhamogalacturonan oligomers were prepared by TFA partial hydrolysis of the rhamogalacturonan polymer prepared from citrus pectin (5). The acid hydrolyzed RG fragments were $(GR)_n$ type which contain rha at the reducing end and galA at the non-reducing end. The fragments of $(GR)_7$, $(GR)_8$, and $(GR)_9$ were purified using a PA1 anion exchange column.

ANTS derivatization

Approximately 100 μg of substrates were heated at 90 °C for at least 1 h in a mixture of 50 μl of 23 mM ANTS (in 3:17 v/v of acetic acid: water) and 5 μl of 1 M sodium cyanoborohydride (in dimethylsulfoxide) (6). ANTS derivatized substrates were desalted on an HW40 (S) gel filtration column (15x0.9 cm) monitored by a refractive index detector. The purified substrates were dissolved in water to make a final concentration of 1 nmole/μl (assuming no loss of sugars during the preparation).

APTS derivatization

Approximately 100 nmole of substrates were heated at 75 °C for one hour in a mixture of 10 μl of 0.1 M APTS (in 25% acetic acid) and 10 μl of 0.1 M sodium cyanoborohydride (in THF) (7). APTS derivatized samples were desalted on an HW40 (S) gel filtration column (15x0.9 cm) eluted with 15% of acetonitrile and monitored by a fluorescence detector. The labeled sample was dried under speed vacuum and dissolved in water to make a final concentration of 1 nmole/μl (assuming no loss of sugars during the preparation).

Enzyme activity assay

One nmole of ANTS or APTS labeled substrate was incubated with 50 μl of culture supernatant at 37°C in 50 mM sodium acetate buffer. Different pH (3.0-8.0) buffers were used and a time course of the reaction was collected. Consumption of the substrate was calculated by the equation:

1-(Peak area of the substrate/ Sum of peak areas of both products and substrate)

Capillary zone electrophoresis

The enzyme digestion mixture was run on a custom-built CE instrument with a laser-induced fluorescence detector which used a helium-cadmium laser for excitation and an intensified charge-coupled device camera for detection (8). A fused-silica capillary (Polymicro Technologies, Phoenix, AZ, USA) of 50 μm ID (355 μm OD) was used as the separation column for oligosaccharides. The capillary was 50 cm in length, with 26 cm to the detection window. 0.1 M NaH_2PO_4, pH 2.5, was used as a running buffer. The capillary was rinsed with running buffer after each run and sample was introduced by gravity-driven flow for several seconds. Electrophoresis was conducted at 18 kV with the negative electrode on the injection side.

Purification of His-tagged recombinant proteins

Optimally expressing cell cultures were harvested by centrifugation at 3000 g for 10 min. Supernatants were concentrated to about 10 fold using ultrafiltration with Mr=10,000 cut off ultrafiltration membrane (YM 10, Amicon, Inc. USA). The concentrated supernatants were purified on a poros 20 metal chelate affinity media (Boehringer Mannheim GmbH, Germany) packed in a stainless steel column (8.3 x 1 cm) from Alltech Associates, Inc.

The purification protocol was modified based on the protocols from Boehringer Mannheim (9) and Qiagen (10). The column was saturated with 150 ml of 0.1 M $NiSO_4$, washed by 25 ml of water, 25 ml of 0.5 M NaCl and 25 ml of starting buffer (0.5 M

NaCl-0.02 M sodium phosphate-10 mM imidazole, pH 7.8). After loading of the enzyme medium, the column was washed by 50 ml of starting buffer. The column bound His-tagged proteins were eluted using an imidazole gradient in phosphate buffer (pH 7.8). The proteins were monitored under an UV detector. The eluted proteins were dialyzed against 5 mM phosphate buffer and concentrated using a centricon 10 (Mr=10,000 cut off).

Gel electrophoresis

The purified proteins were separated on a 10% SDS-PAGE gel and stained with commassie blue R-250. A broad molecular weight standard (Bio-Rad) from 6.5 kDa to 200 kDa was used for calibration.

RESULTS AND DISCUSSION

Optimum expression time for recombinant endoarabinase and rhamnogalacturonase

Culture supernatants taken from different time points were mixed with ANTS or APTS labeled substrates and enzyme activity was assayed using CZE. The expressed enzyme activity was compared using the relative consumption rate of the substrate. The expressed endoarabinase shows the highest activity at the 3-4 day culture after induction in the minimal methanol medium. The expressed RGase shows the highest acitivity at the 4-5 day culture after induction (Fig. 4-6). The pH optimum for endoarabinase and RGase is shown in Fig. 4-7. The expression level of both enzymes is about 2-5 μg protein per ml culture based on gel electrophoresis.

Properties of endo-α-1,5-L-arabinase

The purified His-tagged endoarabinase has an apparent molecular weight of 45 kDa. The estimated molecular weight of endoarabinase is about 35 kDa after cleavage of

the signal peptide. The difference of the molecular weight could be contributed from the signal peptide (10 kDa) which is not cleaved, but it is most possibly from the glycosylation since the protein is expressed in an eukaryotic system. Endoarabinase digests the linear ANTS labeled arabinoheptaose into di, tri and tetra-mer. The electropherograms of the substrate and the products are shown in Fig. 4-8. The minimum size of the substrate for endoarabinase is arabinotetramer.

Properties of rhamnogalacturonan hydrolase (RGase)

The purified His-tagged RGase has an apparent molecular weight of 100 kDa, but the estimated molecular weight of the native protein is only 60 kDa after cleavage of the signal peptide. The difference of 40 kDa mass could be contributed from glycosylation. The amino acid sequence of RGase from *Botryotinia fuckeliana* shows very high identity to the sequences of RGase from *Aspergillus niger* and *Aspergillus aculeatus*. Two of four predicted N-glycosylation sites in the sequence of RGase from *Botryotinia fuckeliana* are conserved in the other RGases. N-glycosylation and O-glycosylation were reported to be present in the recombinant RGase from *Aspergillus niger* (11). The crystal structure of RGase from *Aspergillus aculeatus* also illustrates two N-linked glycans and eighteen O-linked mannose (12). This indicates that the RGase expressed in *pichia* could be heavily glycosylated (including N-linked and O-linked) contributing the extra 40 kDa of the molecular mass.

RGase was reported to be able to degrade the alternating rha-galA backbone of the RG I polymer (13). The RG oligomers prepared from TFA hydrolysis have rha at the reducing end and galA at the non-reducing end because the glycosidic bond between rha and galA is more labile under acid condition. The time course of RGase digestion of an ANTS labeled $(GR)_n$ mixture is shown in Fig. 4-9. Degradation of the ANTS labeled substrates was monitored using CZE. After 15 minutes incubation, new peaks appeared between the $(GR)_n$ substrate peaks. This indicates that RGase cleaves at the glycosidic

bond between galA and rha and generates odd number residues of the reducing end products: $(RG)_nR$. The substrates of $(GR)_5$ and larger were degraded very quickly. $(GR)_4$ was degraded very slowly after extended incubation (overnight). However, $(GR)_3$ could not be digested even after addition of excess enzyme or extended incubation.

Studies of the RGase digestion pattern

Mutter et al. (14) reported that RG-hydrolase (*Aspergillus aculeatus*) is able to cleave the RG oligomers with five rha units or more. The RGase cleaves at four or six residues from the first non-reducing end rha. The digestion pattern is illustrated in Fig. 4-10. According to the RGase cleavage pattern, it is very clear that only two types of reducing end fragments will result from complete digestion of the ANTS labeled GR oligomers: $(RG)_2R$ and $(RG)_3R$. The non-reducing end fragments that could not be further degraded are: $G(RG)_2$, $G(RG)_3$, $(RG)_2$ and $(RG)_3$.

However, the non-reducing end products generated by RGase do not have ANTS label. But they can be detected if the RGase digestion mixture is labeled with ANTS again. Fig. 4-11C illustrates the eletropherogram of all products including the originally labeled reducing end fragments and the newly labeled non-reducing end fragments. The reducing end peaks can be distinguished from the non-reducing end peaks by comparing them to the digestion mixture before the second ANTS labeling (Fig. 4-11 B). The separation of fragments using CZE is in part based on the charge density. The ANTS label provides negative charge to all oligomers, however, galA residues also contribute negative charge which increases the velocity of the oligomer. The elution order of these fragments is: $(RG)_2$, $G(RG)_2$, $(RG)_2R$, $(RG)_3$, $(GR)_3$, $G(RG)_3$, $(RG)_3R$ and $(GR)_4$. The fragments $(RG)_2$, $G(RG)_2$ and $(RG)_2R$ show a relatively higher proportion (peak areas) which indicates that RGase preferentially cleaves at four residues rather than six from the first non-reducing rha. This result is also consistent with the result from Mutter (14).

To examine if RGase degrades the substrate from the non-reducing end, purified $(GR)_9$ oligomer was used as substrate instead of the $(GR)_n$ mixture. Fig. 4-12 shows the time course digestion of the APTS labeled $(GR)_9$. A ladder of reducing end products were formed from the start in the order of $(RG)_2R$, $(RG)_3R$, $(RG)_4R$, $(RG)_5R$ and $(RG)_6R$. The products kept a pattern of decreased proportion from $(RG)_2R$ to $(RG)_6R$. All larger reducing end fragments were degraded into final products of $(RG)_2R$ and $(RG)_3R$. If RGase cleaves off two or three RG repeating units from the non-reducing end of $(GR)_9$ (equivalent to $G(RG)_8R$), then the intermediates of $(RG)_6R$, $(RG)_5R$ and $(RG)_4R$ should show higher proportions than the final products of $(RG)_2R$ and $(RG)_3R$. However, the fragments $(RG)_2R$ and $(RG)_3R$ showed continuously higher proportions than the larger ones during the whole degradation process. It could be explained that once RGase makes the first cleavage, it would move along very quickly towards the reducing end and continuously cleave the intermediates until releasing the final products. Because the non-reducing end products could not be detected directly, a second APTS labeling was carried out to detect if any small fragments were cleaved from the non-reducing end. Fig. 4-13 shows the electropherograms of the initial reducing end products from $(GR)_9$ and the APTS labeled all initial products. Unlike ANTS labeled fragments, the APTS labeled non-reducing end fragments of $G(RG)_n$ and the reducing end fragments of $(RG)_nR$ could not be resolved from each other when n is the same number. But if a fragment $G(RG)_2$ is co-eluted with a fragment $(RG)_2R$, the proportion of peak 1 should increase in the second APTS labeling. The result showed that the proportion of peak 1 and 2 decreased while the proportion of peak 3 to 5 increased. Furthermore, no fragments of $(RG)_2$ and $(RG)_3$ were generated initially. This indicates that RGase might not cleave every two or three RG repeating units from the non-reducing end.

A hypothesized cleavage pattern for RGase (*Botryotinia fuckeliana*) is illustrated in Fig. 4-14. RGase binds to the backbone of $(GR)_9$ and cleaves at least two RG repeating units off from the reducing end. The two repeating units or three repeating

units from the reducing end are the preferential cleavage sites. If it is true, then the intermediate fragments of $G(RG)_6$ and $G(RG)_5$ generated from the non-reducing end should be detected. The APTS labeled partial digestion mixture from $(GR)_9$ showed an increased proportion of larger fragments of $(RG)_6R$, $(RG)_5R$ and $(RG)_4R$. It is because the fragments of $G(RG)_6$, $G(RG)_5$ and $G(RG)_4$ are co-eluted with $(RG)_6R$, $(RG)_5R$ and $(RG)_4R$, respectively. A better resolution of separating fragments of $G(RG)_n$ and $(RG)_nR$ is obtained using ANTS labeling. Fig. 4-15 illustrated the ANTS labeled partial digestion mixture of ANTS labeled $(GR)_7$ and $(GR)_8$. The fragments of $G(RG)_4$ and $G(RG)_5$ were eluted a little earlier than $(RG)_4R$ and $(RG)_5R$, respectively. The presence of $G(RG)_4$ and $G(RG)_5$ indicates that RGase cleaves from the reducing end.

The minimum length of substrate for RGase to degrade it is four complete RG repeating units. RGase prefers to degrade the larger oligomer than the small oligomer.

Detection of extraneous activities

The XG dimer was prepared from partial digestion of the tamarind XG polymer. It is a mixture of oligomers composed of two XG subunits and can be degraded by endoglucanase into one subunit. The ANTS labeled XG dimer was used as a substrate to detect the presence of endoglucanase activity. A slight amount of endoglucanase activity was found present in both purified enzymes. No endoglucanase activity was detected in the medium of the untransformed *pichia* strain. The endoglucanase activity could be from contamination during the purification. However, the contaminating endoglucanase is insignificant when compared that found in the commercial enzymes.

REFERENCES

1. **Keegstra, K., Talmadge, K. W., Bauer, W. D., and Albershem, P.** 1973. The structure of plant cell walls. III. A model of the walls of suspension-cultured sycamore cells based on the interconnections of the macromolecular components. *Plant Physiol.* 51: 188-196

2. **EasySelect Pichia Expression Kit.** A manual of methods for expression of recombinant proteins using pPICZ and pPICZα in *pichia pastoris*. Invitrogen Corp. Catalog no. K1740-01

3. **Sakamoto T., Yamada, M., Kawasaki, H. and Sakai, T.** 1997. Molecular cloning and nucletide sequence of an endo-1,5,-α-L-arabinase gene from *Bacillus subtili. Eur. J. Biochem.* 245: 708-714

4. **Chen, H. J., Smith, D. L., Starret, D. A., Zhou, D., Tucker, M. L., Solomos, T. and Gross, K. C.** 1997. Cloning and characterization of a rhamnogalacturonan hydrolase gene from *Botrytis cinerea. Biochem. Mol. Biol. Int.* 43(4): 823-838

5. **Zhan, D., Janssen, P. and Mort, A. J.** 1998. Scarcity or complete lack of single rhamnose residues interspersed within the homogalacturonan regions of citrus pectin. *Carbohydr. Res.* 308(3-4): 373-380

6. **Zhang, Z., Pierce, M. L. and Mort, A. J.** 1996. Detection and differentiation of pectic enzyme activity in vitro and in vivo by capillary electrophoresis of products from fluorescent-labeled substrate. *Electrophoresis* 17(2): 372-378

7. **Evangelista, R. A., Liu, M. and Chen, F.** 1995. Characterization of 9-aminopyrene-1,4,6-trisulfonate-derivatized sugars by capillary electropherosis with laser-induced fluorescence detection. *Anal. Chem.* 67: 2239-2245

8. **Merz, J. M. and Mort, A. J.** 1998. A computer-controlled variable light attenuator for protection and autoranging of a laser-induced fluorescence detector for capillary zone electrophoresis. *Electrophoresis* 19(12): 2239-2242

9. **Schmidbauer, S. B. and Strobel, O. K.** 1997. Purification of Histidine-tagged fusion protein using poros metal chelate perfusion chromatography media: rapid method optimization. *Biochemica Boehringer Maninheim* 3: 22-24

10. **Steinert, K., Wulbeck, M. and ribbe, J.** 1997. Ni-NTA resin-your key to efficient purification of 6xHis-tagged proteins. *Qiagennews* 4: 11-15

11. **Suykerbuyk, M. E. G., Kester, H. C. M., Schaap, P. J., Stam, H., Musters, W. and Visser, J.** 1997. Cloning and characterization of two rhamnogalacturonan hydrolase genes from *Aspergillus niger. Applied and environmental microbiology* 63(7): 2507-2515

12. **Petersen, T. N., Kauppinen, S. and Larsen, S.** 1997. The crystal structure of rhamnogalacturonase A from *Aspergillus aculeatus*: a right handed parallel β helix. *Structure.* 5(4): 533-543

13. **Schols, H. A., Geraeds, C. C. J. M., Searle-Van, Leeuwen M. J. F., Kormelink, F. J. M. and Voragen, A. G. J**. 1990. Rhamnogalacturonase: a novel enzyme that degrades the hairy regions of pectins. *Carbohydr. Res.* 206: 105-115

14. **Mutter M., Renard, M. G. C., Beldman, G., Schols, H. A., Voragen, G. J.** 1998. Mode of action of RG-hydrolase and RG-lyase toward rhamnogalacturonan oligomers. Characterization of degradation products using RG-rhamnohydrolase and RG-galacturonohydrolase. *Carbohydr. Res.* 311: 155-164

Figure 4-1 The map of pPICZαA vector (Invitrogen)

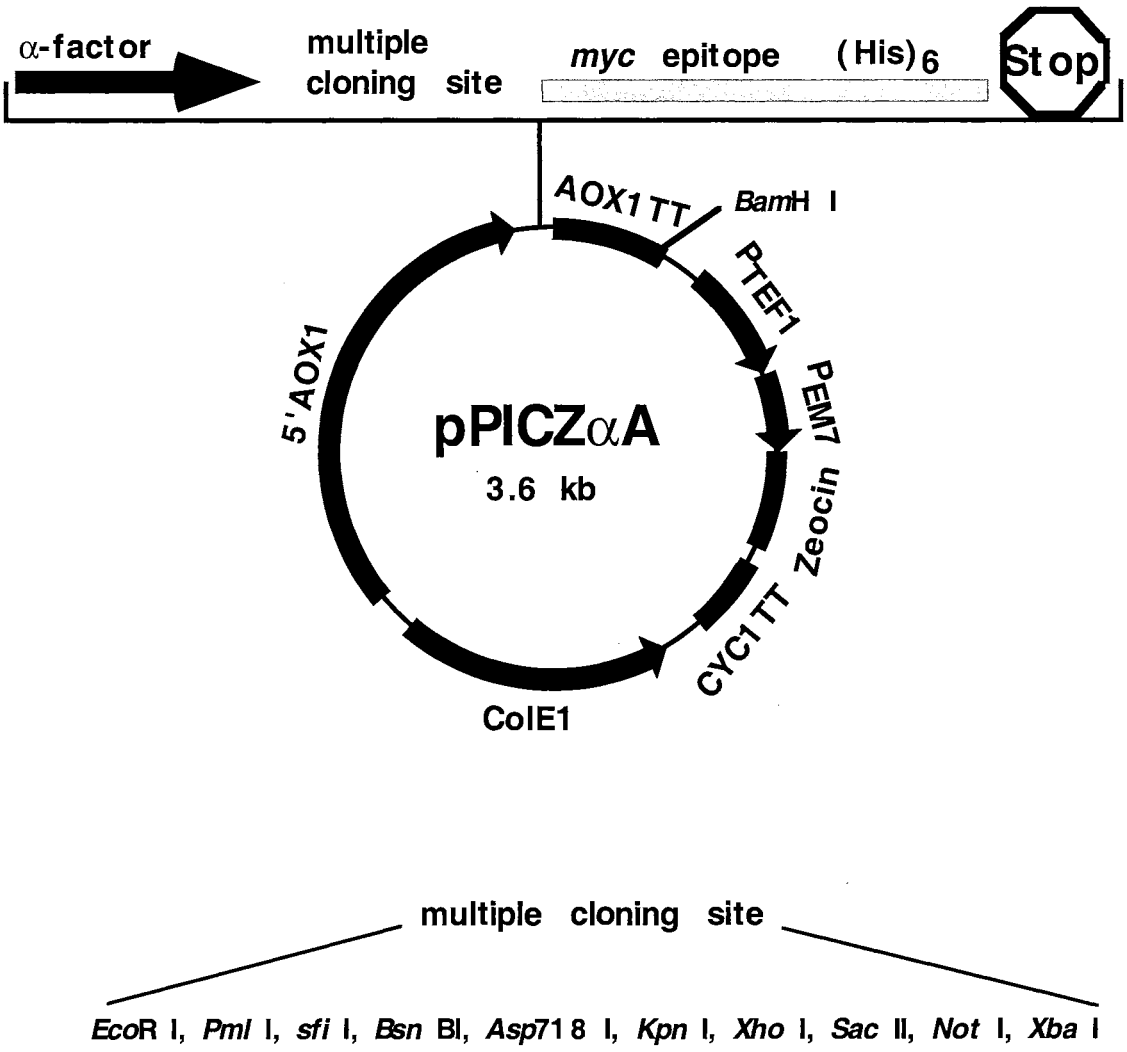

Figure 4-2 Nucleotide sequence of *ppc* from *B. subtilis* IFO 3134 (Sakamoto et al. *Eur. J. Biochem.* 245)

The upper primer and the lower primer sequences are underlined. The upper primer starts from the mature enzyme coding sequence right after the putative signal sequence and an extra A is added on the N-side. The lower primer covers the last amino acid sequence of the protein and extra C A are added on the N-side.

CTGCACCGTGACGATTATGAAAACGCTGTAAAATTAATTACAGAAGTCATTAAGAAGTTAGACCGGCAAAC
GGTTGATGAGATTACGTACCAATAAAGATACGGAGGAATCCGCCTGTTGAGGCGGGTTCTGTTTTTTTGTC
TGTACAAATTGTGGCAGAGTGACTACAATAAAGAAGATACCGAAAATTTCCTGAACTAGATGATATACGAT
ACGCAGCTCATTTGTAAGGAAGGGAGGATCAAACAATATTATTTGTAAGCGCCTTCTAATTTAAAGGAGGT
TGGAAAATGTTGAAAAATAAAAAAACATGGAAACGTTTCTTTCACTTATCTAGTGCCGCTCTGGCTGCAGG
TTTGATATTCACTTCTGCTGCTCCCGCAGAGGCC**GCATTTTGGGGTGCATC**TAACGAGCTGCTTCACGACC
CGACTATGATCAAAGAGGGGAGCTCATGGTATGCGTTAGGAACAGGGCTTAATGAAGAACGGGGACTGCGG
GTTTTGAAGTCTTCGGATGCTAAAAACTGGACCGTCCAAAAATCTATTTTCAGCACACCGCTATCGTGGTG
GTCCAATTATGTGCCGAATTACGAGAAAAACCAGTGGGCGCCGGATATCCAATACTATAACGGAAAGTACT
GGCTGTATTATTCAGTTTCCTCTTTTGGAAACAATACATCTGCCATCGGACTGGCATCCTCAACGAGCATC
AGTTCGGGGAACTGGGAAGACGAAGGCTTGGTCATCCGTTCGACAAGCTCCAATAATTATAACGCGATTGA
TCCGGAGTTGACATTTGACAAGGATGGCAACCCGTGGCTTGCATTCGGCTCGTTTTGGAGCGGAATTAAGC
TGACAAAGCTTGATAAAAGTACGATGAAGCCTACAGGCTCGCCCTATTCGATTGCAGCCAGGCCGAATAAT
AACGGGGCGCTGGAAGCTCCTACTCTTACGTATCAAAATGGCTATTACTATTTAATGGTTTCATTTGATAA
ATGTTGTAACGGGGTAAACAGTACGTACAAAATTGCTTATGGAAGATCTAAAAGCATTACAGGGCCTTATC
TTGATAAAAGCGGGAAAAGCATGCTTGATGGCGGGGGCACCATTTTGGATTCCGGCAACGACCAATGGAAA
GGCCCTGGCGGTCAGGATATTGTAAACGGAAACATTCTTGTTCGTCATGCCTATGACGCCAATGACAACGG
CACTCCGAAGCTTCTCATCAATGATTTGAATTGGAG**TTCGGGCTGGCCGTCCTATT**AAACGAAAAAGCCGG
GAGATCTGTCCCCGGCTTTTTTTAAAAGAAAAGATTGACAGTCTAATAGTCAATTACTATAATAAAGTTGC
TCGTACAAATTAATAGATATCAATTAATTTATTGTCATTAGTACGTATCTTTTGTTATGTTTGAAAGCGTT
TTATTTTATAGGGAAAGGGGCAGTTTACATGCTTCAGACAAAGGATTATGAATTC

Upper primer: A**GCATTTTGGGGTGCATC**
Lower primer: CA**AATAGGACGGCCAGCCCGAA**

Figure 4-3 Nucleotide sequence (1) and deduced amino acid sequence (2) of the constructed endoarabinase-pPICZαA plasmid

Lower case stands for the vector nucleotide sequence or amino acid sequence. Upper case stands for the insert nucleotide sequence or amino acid sequence. PCR primers are shown in bold case and underlined. Signal peptide cleavage site is indicated as *.

(1):

atgagatttccttcaatttttactgctgttttattcgcagcatcctccgcattagctgctccagtcaacactacaacagaagatgaaac
ggcacaaattccggctgaagctgtcatcggttactcagatttagaaggggatttcgatgttgctgttttgccattttccaacagcaca
aataacgggttattgtttataaatactactattgccagcattgctgctaaagaagaaggggtatctctcgagaaaagagaggctgaa
gctgaatt**A<u>GCATTTTGGGGTGCATC</u>**TAACGAGCTGCTTCACGACCCGACTATGATCAAAGA
GGGGAGCTCATGGTATGCGTTAGGAACAGGGCTTAATGAAGAACGGGGACTGCGGGTTT
TGAAGTCTTCGGATGCTAAAAACTGGACCGTCCAAAAATCTATTTTCAGCACACCGCTA
TCGTGGTGGTCCAATTATGTGCCGAATTACGAGAAAAACCAGTGGGCGCCGGATATCCA
ATACTATAACGGAAAGTACTGGCTGTATTATTCAGTTTCCTCTTTTGGAAACAATACAT
CTGCCATCGGACTGGCATCCTCAACGAGCATCAGTTCGGGGAACTGGGAAGACGAAGGC
TTGGTCATCCGTTCGACAAGCTCCAATAATTATAACGCGATTGATCCGGAGTTGACATT
TGACAAGGATGGCAACCCGTGGCTTGCATTCGGCTCGTTTTGGAGCGGAATTAAGCTGA
CAAAGCTTGATAAAAGTACGATGAAGCCTACAGGCTCGCCCTATTCGATTGCAGCCAGG
CCGAATAATAACGGGGCGCTGGAAGCTCCTACTCTTACGTATCAAAATGGCTATTACTA
TTTAATGGTTTCATTTGATAAATGTTGTAACGGGGTAAACAGTACGTACAAAATTGCTT
ATGGAAGATCTAAAAGCATTACAGGGCCTTATCTTGATAAAAGCGGGAAAAGCATGCTT
GATGGCGGGGGCACCATTTTGGATTCCGGCAACGACCAATGGAAAGGCCCTGGCGGTCA
GGATATTGTAAACGGAAACATTCTTGTTCGTCATGCCTATGACGCCAATGACAACGGCA
CTCCGAAGCTTCTCATCAATGATTTGAATTGGAG**<u>TTCGGGCTGGCCGTCCTATT</u>**TGctaga
acaaaaactcatctcagaagaggatctgaatagcgccgtcgaccatcatcatcatcattga

(2):

mrfpsiftavlfaassalaapvntttedetaqipaeavigysdlegdfdvavlpfsnstnngllfinttiasiaakeegvslekrea
ea*elAFWGASNELLHDPTMIKEGSSWYALGTGLNEERGLRVLKSSDAKNWTVQK
SIFSTPLSWWSNYVPNYEKNQWAPDIQYYNGKYWLYYSVSSFGNNTSAIGLASS
TSISSGNWEDEGLVIRSTSSNNYNAIDPELTFDKDGNPWLAFGSFWSGIKLTKLD
KSTMKPTGSPYSIAARPNNNGALEAPTLTYQNGYYYLMVSFDKCCNGVNSTYKI
AYGRSKSITGPYLDKSGKSMLDGGGTILDSGNDQWKGPGGQDIVNGNILVRHAY
DANDNGTPKLLINDLNWSSGWPSYlleqkliseedlnsavdhhhhhh

Figure 4-4 Nucleotide sequence of rhamnogalacturonan hydrolase from *Botryotinia fuckeliana* (Gross et al. horticultural crops quality lab, USDA)

The upper primer and the lower primer sequences are underlined. EcoRI and XbaI sites (in bold case) are introduced into the upper primer and the lower primer, respectively. The PCR product covers the entire mature enzyme coding sequence (right after the putative signal sequence) and in frame with the opening frame of the pPICZαA vector at the EcoR I and XbaI sites.

ATGCAATTCGGCACATTATCAGCCCTCGCGGCAATTGTCCTCCCAGCTGTAGTATCAGCACAGTTGACTGG
TTCAGTTGGCCCCTTGACTTCAAGAGAATCTAAGGCCACAAAAGTTTGCAGTGTTTTGGACTATGGTGGAA
AAGCAAGCAAGACTTCAGATATTGGCCCGGCGCTTACTTCTGCATTCGCTGCTTGCAAGACTGGTGGAACA
GTTTATGTCCCACCTGGAGATTATGGTATGTCTACTTGGATTACACTCAGCGGAGGTTCGGCATGGGCACT
TAAGCTTGATGGTATCATTTATCGCACTGGTAGTGATGATGGAAACATGATCATGATCAAACACACCACCG
ATTTCGAAATGTACAGTAGTACCTCTGCAGGTGCCATTCAGGGTTATGGTTATGAATTTCACAAAGACGGA
GCTTATGGTGCACGCCTCCTCCGATTTTACGACGCTACCAACTGGTCCATCCACGACATTGCTTTGGTCGA
CGCCCCTCAATTCCATTTTTCCATTGATACCTGCGTTAACGGAGAAGTTTACAACATGATCATTCGTGGTG
GCAACGAGGGTGGTCTTGATGGTATTGATGTTTGGGGAACCAACATCTGGATTCACGATGTTGAAGTTACT
AATAAGGATGAGTGTGTTACTGTCAAGAATCCTTCCGATCATATTCTCATTGAAGATATCTACTGTAACAG
TTCAGGAGGCTGTGGTATGGGATCTCTTGGAGCAGATACTGCCATCTCTAACATCGTCTACAACAATATTT
ACACTTACGGATCCAACCAAATGTACATGATCAAATCAAACGGTGGTAGCGGTACAGTTTCTGACTGTCAA
TTCAACAACTTCATCGGTCGCTCCAATGCCTACAGTTTGAACATTAATGCAGCCTGGCCTCAAGCAAGCAA
GGCTTCCGGTAATGGTGTCATCTACGAGAACCTCTCTTTTAACAACTGGAAGGGAACATGTACCAGTACCT
CTGAACGTGGACCAATCAACCTCCTCTGCTCATCCACCGCTCCATGCACAAACGTCACCATCACTGACTTT
GCCATCGGAACTGAATCCGGCAGCACCGGAAAATACGTCTGCCAAAATGCTTACGGTTCAGGAGGATGTCT
CAAAGCCGATACCGATTCCCCATCCGCTTACACTACAACTCAATCTTGGTCCTCTATGCCAACCGGCTACG
AAGCTTCTACCATGGCCCAAGATTTGGCTACTCCTTTCGCCGTGAGCGTAAGCATTCCTATCCCAACCATC
CCAACCTCTTTCTTCCCAGGTAGAACTCCTGTCTCCGCTCTCATGGCCAATGGCGGCAAGTCCTCAGCTTC
AGTTGCATCCCACGTAGCTATCACCACCTCTTCAAAAGCCGCAGTAGCCACCTCGACCGCCGTCGCTTCCT
CCTCAAAGGTCGCCGCTACCAGCAAAGCTTCTTCTTCCGCTGCTGTCGTTTCCGCCAGCAAGACTACTCTC
GCCACCCAAAAATCTAGCACTACTCTTGCTACTTCCGCTAAACCAGCTGCTACAACCGCTGCTTCATCTTC
TGGCTCGGTCCCTTTGTACGGTAGCTGCACCGGGGGACAGTCCTGCTCTGCCGACGGCGGAGAAGTTTCTT
CAACCGAGATTGCCAGCTCGGTTGCTCCTGCTCCAACTGATGCAACGGATGCGAGTGGAGAGGAAGATGAT
GAGTGTGAAATCTAGACGTCTAAACGTCACTCTAGATATGGGGACGCAAGGAAAGAAAACACATATATATA
AGGAGGGGATAGATTCATTGTATTATAGTTAGAACAGTATCTTGATTGTAAATATTGGAATGAAGAAAACA
TTTCCTGCTGCCCTGTTGAATGGGGCGGAGGATGATTGAATTTTAAAAAAAAAAAAAAAAAA

Upper primer GTA**GAATTC**GCACAGTTGACTGG
Lower primer CGTCTAG**TCTAGA**CACTCATC

Figure 4-5 Nucleotide sequence (1) and deduced amino acid sequence (2) of the constructed RGase-pPICZαA plasmid

Lower case stands for the vector nucleotide sequence or amino acid sequence. Upper case stands for the insert nucleotide sequence or amino acid sequence. PCR primers are underlined. EcoRI and XbaI sites are shown in bold case. Signal peptide cleavage site is indicated as *.

(1):

atgagatttccttcaatttttactgctgttttattcgcagcatcctccgcattagctgctccagtcaacac
tacaacagaagatgaaacggcacaaattccggctgaagctgtcatcggttactcagatttagaaggggatt
tcgatgttgctgttttgccattttccaacagcacaaataacgggttattgtttataaatactactattgcc
agcattgctgctaaagaagaaggggtatctctcgagaaaagagaggctgaagct**gaattC**GCACAGTTGAC
TGGTTCAGTTGGCCCCTTGACTTCAAGAGAATCTAAGGCCACAAAAGTTTGCAGTGTTTTGGACTATGGTG
GAAAAGCAAGCAAGACTTCAGATATTGGCCCGGCGCTTACTTCTGCATTCGCTGCTTGCAAGACTGGTGGA
ACAGTTTATGTCCCACCTGGAGATTATGGTATGTCTACTTGGATTACACTCAGCGGAGGTTCGGCATGGGC
ACTTAAGCTTGATGGTATCATTTATCGCACTGGTAGTGATGATGGAAACATGATCATGATCAAACACACCA
CCGATTTCGAAATGTACAGTAGTACCTCTGCAGGTGCCATTCAGGGTTATGGTTATGAATTTCACAAAGAC
GGAGCTTATGGTGCACGCCTCCTCCGATTTTACGACGCTACCAACTGGTCCATCCACGACATTGCTTTGGT
CGACGCCCCTCAATTCCATTTTTCCATTGATACCTGCGTTAACGGAGAAGTTTACAACATGATCATTCGTG
GTGGCAACGAGGGTGGTCTTGATGGTATTGATGTTTGGGGAACCAACATCTGGATTCACGATGTTGAAGTT
ACTAATAAGGATGAGTGTGTTACTGTCAAGAATCCTTCCGATCATATTCTCATTGAAGATATCTACTGTAA
CAGTTCAGGAGGCTGTGGTATGGGATCTCTTGGAGCAGATACTGCCATCTCTAACATCGTCTACAACAATA
TTTACACTTACGGATCCAACCAAATGTACATGATCAAATCAAACGGTGGTAGCGGTACAGTTTCTGACTGT
CAATTCAACAACTTCATCGGTCGCTCCAATGCCTACAGTTTGAACATTAATGCAGCCTGGCCTCAAGCAAG
CAAGGCTTCCGGTAATGGTGTCATCTACGAGAACCTCTCTTTTAACAACTGGAAGGGAACATGTACCAGTA
CCTCTGAACGTGGACCAATCAACCTCCTCTGCTCATCCACCGCTCCATGCACAAACGTCACCATCACTGAC
TTTGCCATCGGAACTGAATCCGGCAGCACCGGAAAATACGTCTGCCAAAATGCTTACGGTTCAGGAGGATG
TCTCAAAGCCGATACCGATTCCCCATCCGCTTACACTACAACTCAATCTTGGTCCTCTATGCCAACCGGCT
ACGAAGCTTCTACCATGGCCCAAGATTTGGCTACTCCTTTCGCCGTGAGCGTAAGCATTCCTATCCCAACC
ATCCCAACCTCTTTCTTCCCAGGTAGAACTCCTGTCTCCGCTCTCATGGCCAATGGCGGCAAGTCCTCAGC
TTCAGTTGCATCCCACGTAGCTATCACCACCTCTTCAAAAGCCGCAGTAGCCACCTCGACCGCCGTCGCTT
CCTCCTCAAAGGTCGCCGCTACCAGCAAAGCTTCTTCTTCCGCTGCTGTCGTTTCCGCCAGCAAGACTACT
CTCGCCACCCAAAAATCTAGCACTACTCTTGCTACTTCCGCTAAACCAGCTGCTACAACCGCTGCTTCATC
TTCTGGCTCGGTCCCTTTGTACGGTAGCTGCACCGGGGGACAGTCCTGCTCTGCCGACGGCGGAGAAGTTT
CTTCAACCGAGATTGCCAGCTCGGTTGCTCCTGCTCCAACTGATGCAACGGATGCGAGTGGAGAGGAAGAT
GATGAGTG**TCTAga**acaaaaactcatctcagaagaggatctgaatagcgccgtcgaccatcatcatcatca
tcattg

(2):

mrfpsiftavlfaassalaapvnttttedetaqipaeavigysdlegdfdvavlpfsnstnngllfinttiasiaakeegvslekreaea*eFAQLTGSV
GPLTSRESKATKVCSVLDYGGKASKTSDIGPALTSAFAACKTGGTVYVPPGDYGMSTWITLSGGS
AWALKLDGIIYRTGSDDGNMIMIKHTTDFEMYSSTSAGAIQGYGYEFHKDGAYGARLLRFYDATN
WSIHDIALVDAPQFHFSIDTCVNGEVYNMIIRGGNEGGLDGIDVWGTNIWIHDVEVTNKDECVTV
KNPSDHILIEDIYCNSSGGCGMGSLGADTAISNIVYNNIYTYGSNQMYMIKSNGGSGTVSDCQFNN
FIGRSNAYSLNINAAWPQASKASGNGVIYENLSFNNWKGTCTSTSERGPINLLCSSTAPCTNVTITD
FAIGTESGSTGKYVCQNAYGSGGCLKADTDSPSAYTTTQSWSSMPTGYEASTMAQDLATPFAVSV
SIPIPTIPTSFFPGRTPVSALMANGGKSSASVASHVAITTSSKAAVATSTAVASSSKVAATSKASSSA
AVVSASKTTLATQKSSTTLATSAKPAATTAASSSGSVPLYGSCTGGQSCSADGGEVSSTEIASSVAP
APTDATDASGEEDDEC leqkliseedlnsavdhhhhhh

Figure 4-6 Time course of expressed enzyme in minimal methanol medium

Endoarabinase activity values are calculated based on a consumption of 1 nmole of APTS labeled ara_7 in 1 hour per 50 µl of culture supernatant, pH adjusted to 6.0. RGase activity values are calculated based on a consumption of 0.25 nmole of APTS labeled $(GR)_9$ in 24 h per 50 µl of culture supernatant, pH adjusted to 4.0.

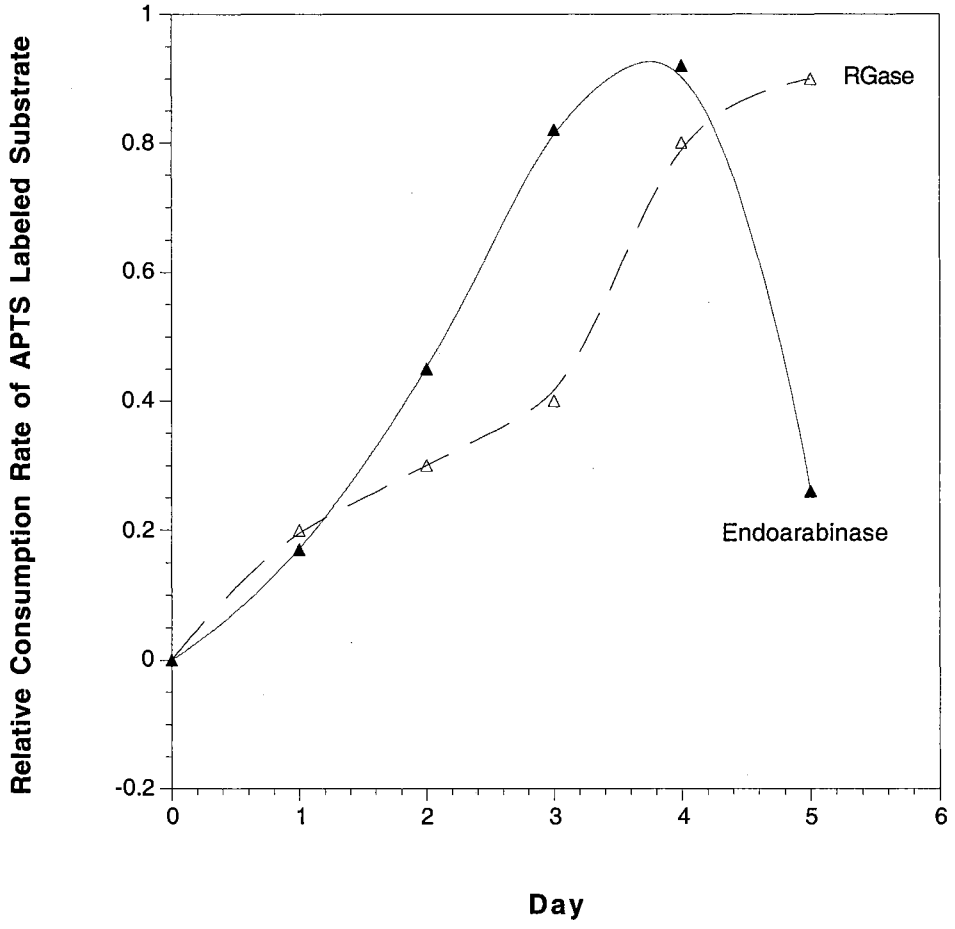

Figure 4-7 Effect of pH on enzyme activity

Endoarabinase activity values are calculated based on a consumption of 1 nmole of APTS labeled ara_7 in 60 min. RGase activity values are calculated based on a consumption of 1 nmole of APTS labeled $(GR)_9$ in 60 min. 50 mM sodium acetate buffers with different pH are used.

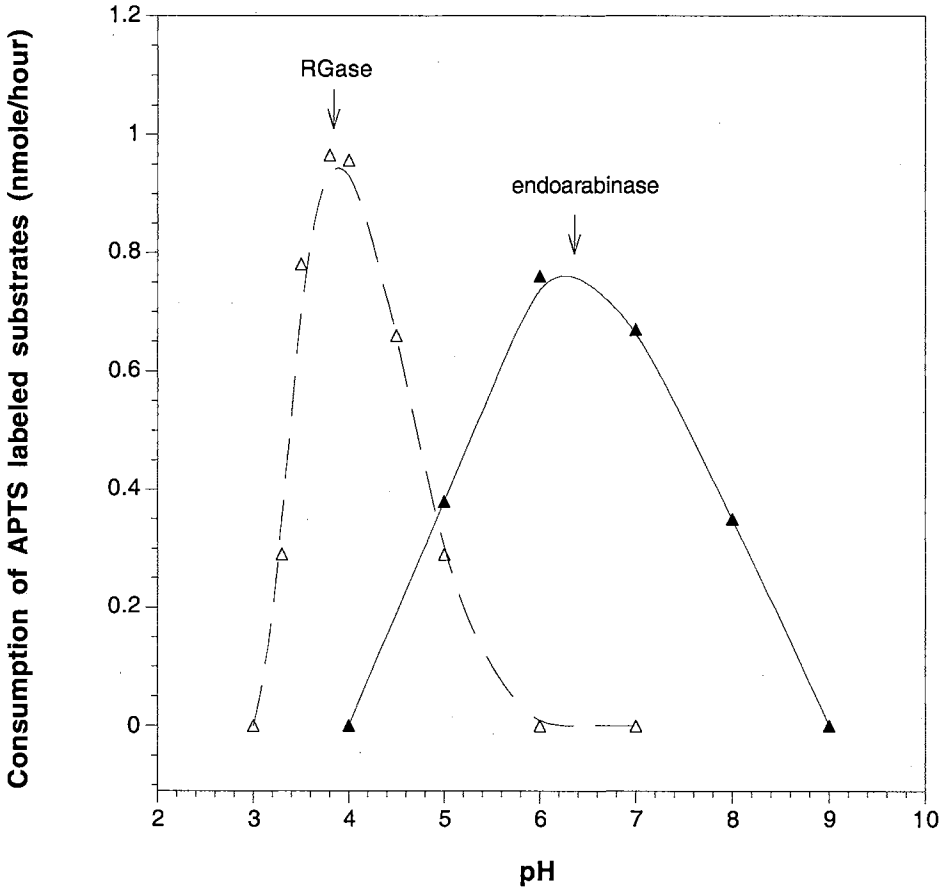

Figure 4-8 Time course of endoarabinase digestion of ANTS labeled arabinoheptaose

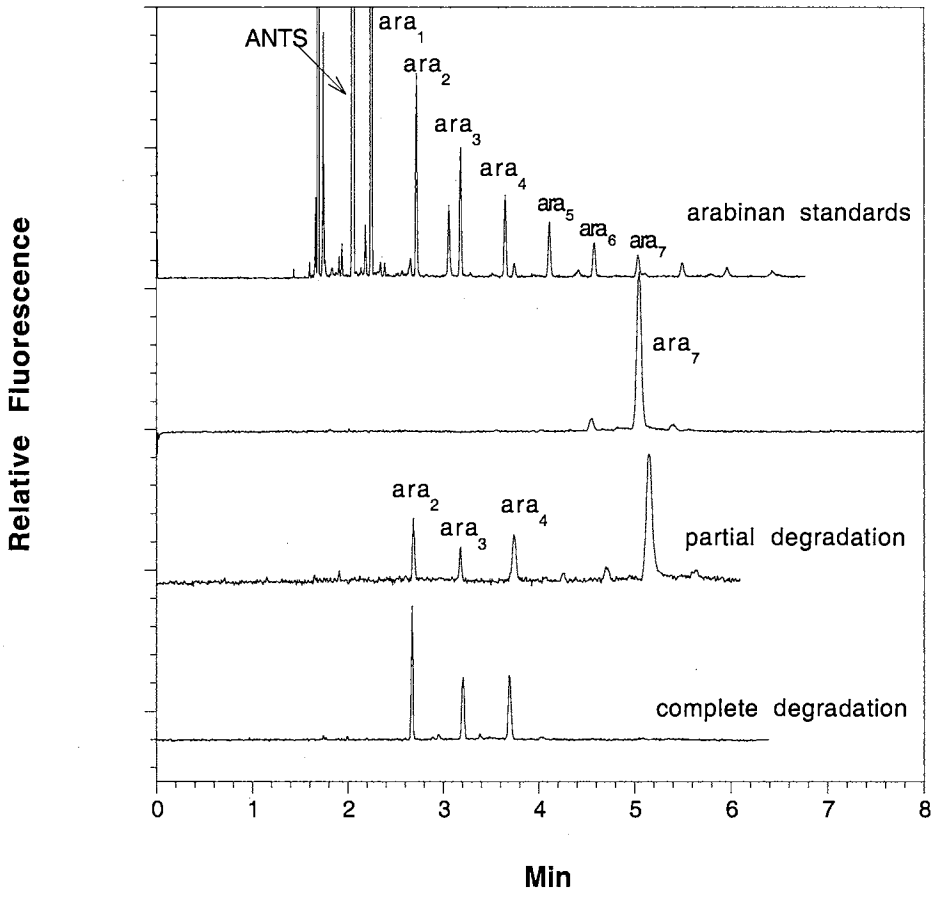

Figure 4-9 Time course of RGase digestion of ANTS labeled $(GR)_n$ mixture

About 5 μg of ANTS labeled GR mixture was incubated with 1 μl of concentrated RGase in 50 mM sodium acetate buffer, pH 4.0. Peaks marked with * are reducing end products generated by RGase.

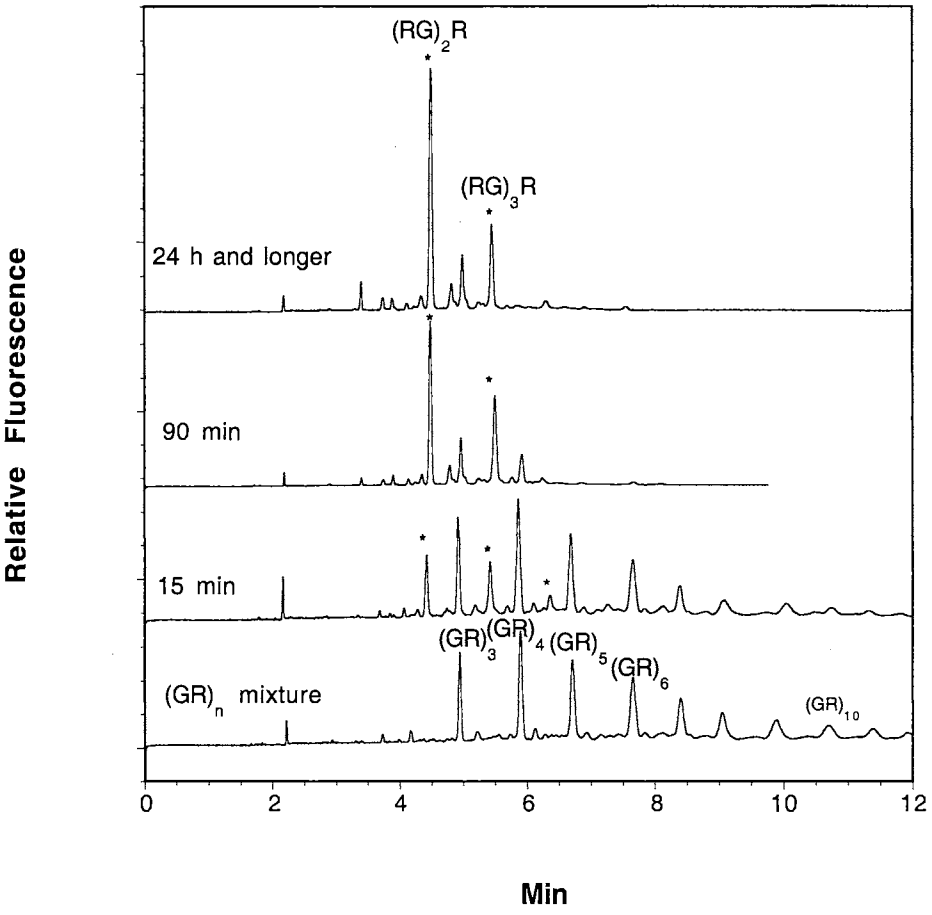

Figure 4-10 RGase digestion pattern (Mutter et al.)

The reducing end rha is labeled with ANTS.

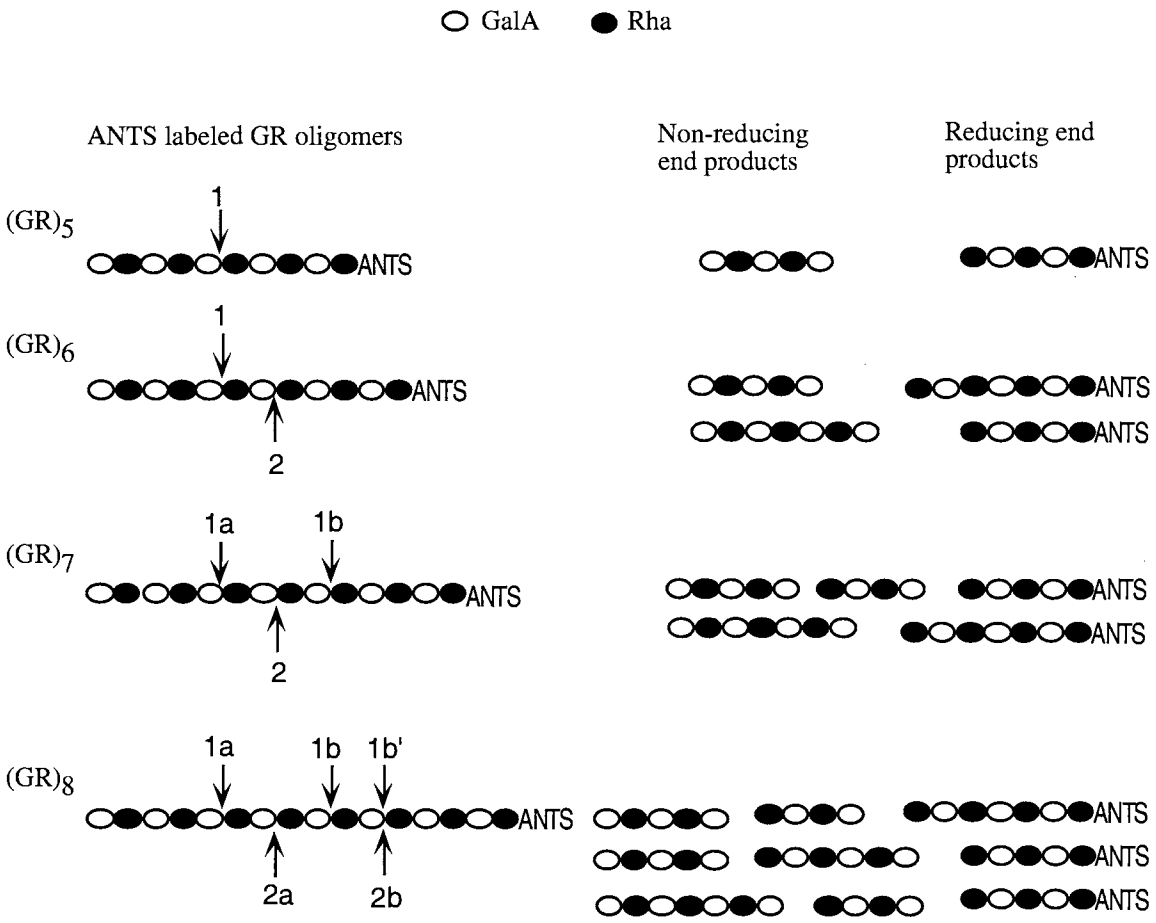

Figure 4-11 Electropherograms of the reducing end and non-reducing products of RGase digested ANTS labeled $(GR)_n$ mixture

A. ANTS labeled $(GR)_n$ substrates. B. Reducing end fragments (marked with *). C. Non-reducing end and reducing end fragments after second ANTS labeling. $(GR)_3$ and $(GR)_4$ are marked with X and are RGase resistant substrates.

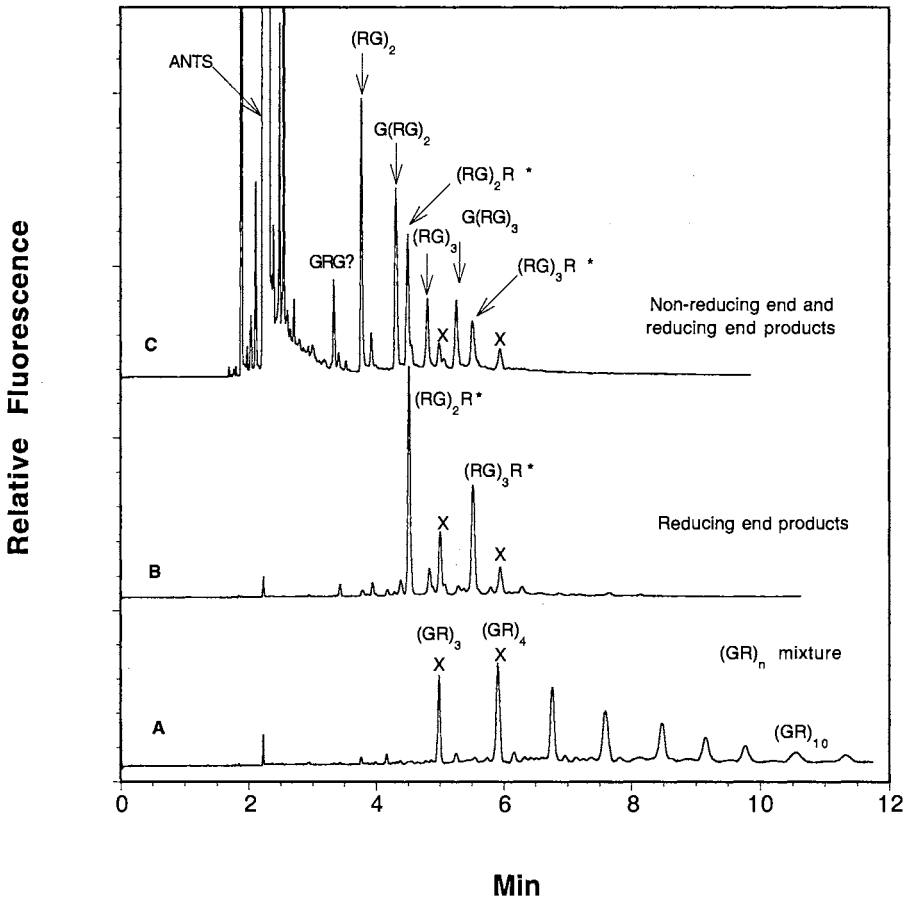

Figure 4-12 Time course of RGase digestion of an APTS labeled $(GR)_9$

Enzyme activity assay is carried out at room temperature. 1 nmole of substrate is incubated with 0.25 μl of concentrated RGase (~10 ng/μl) in 30 μl of 50 mM sodium acetate buffer, pH 4.0

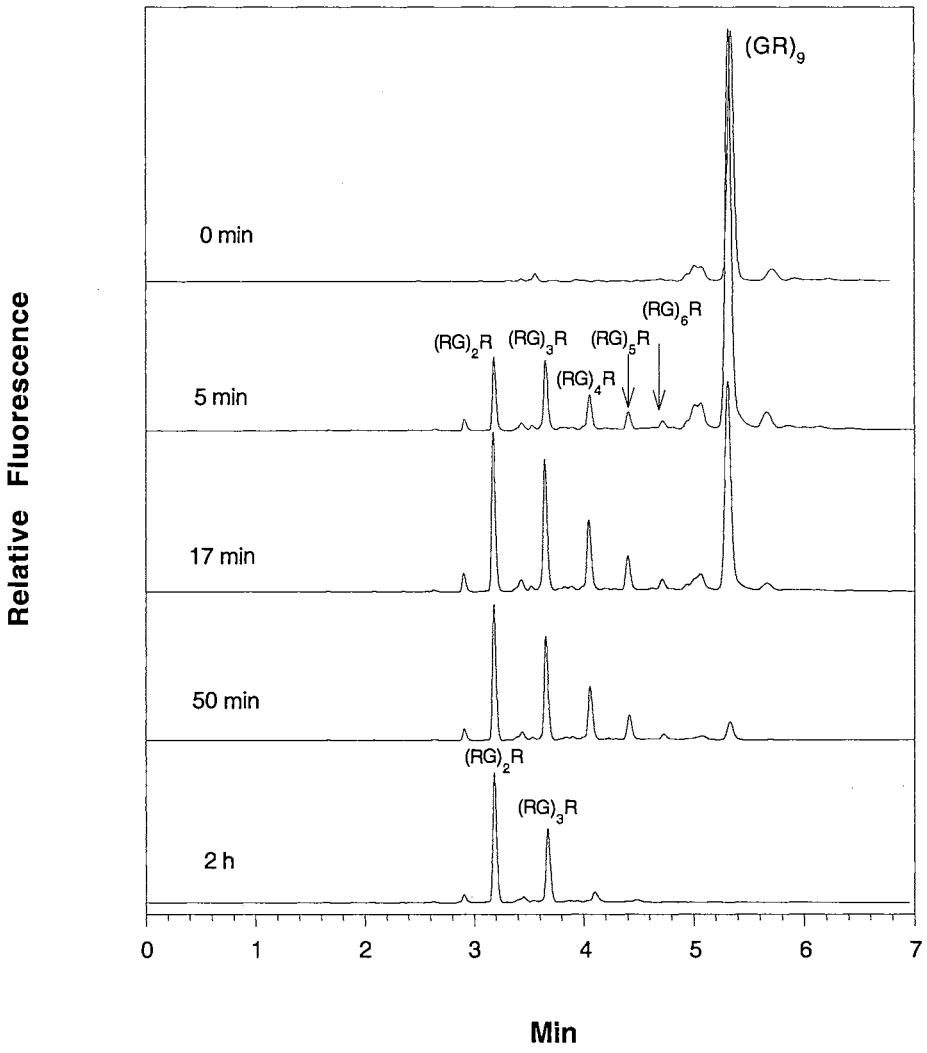

Figure 4-13 Intermediate fragments generated by RGase from APTS labeled $(GR)_9$

A. Non-reducing end fragments and reducing end fragments after second APTS labeling.
B. Reducing end fragments generated by RGase directly.
1: $(RG)_2R$, 2: $(RG)_3R$, 3: $(RG)_4R$, 4: $(RG)_5R$, 5: $(RG)_5R$.
1': $G(RG)_2$, 2': $G(RG)_3$, 3': $G(RG)_4$, 4': $G(RG)_5$, 5': $G(RG)_6$.

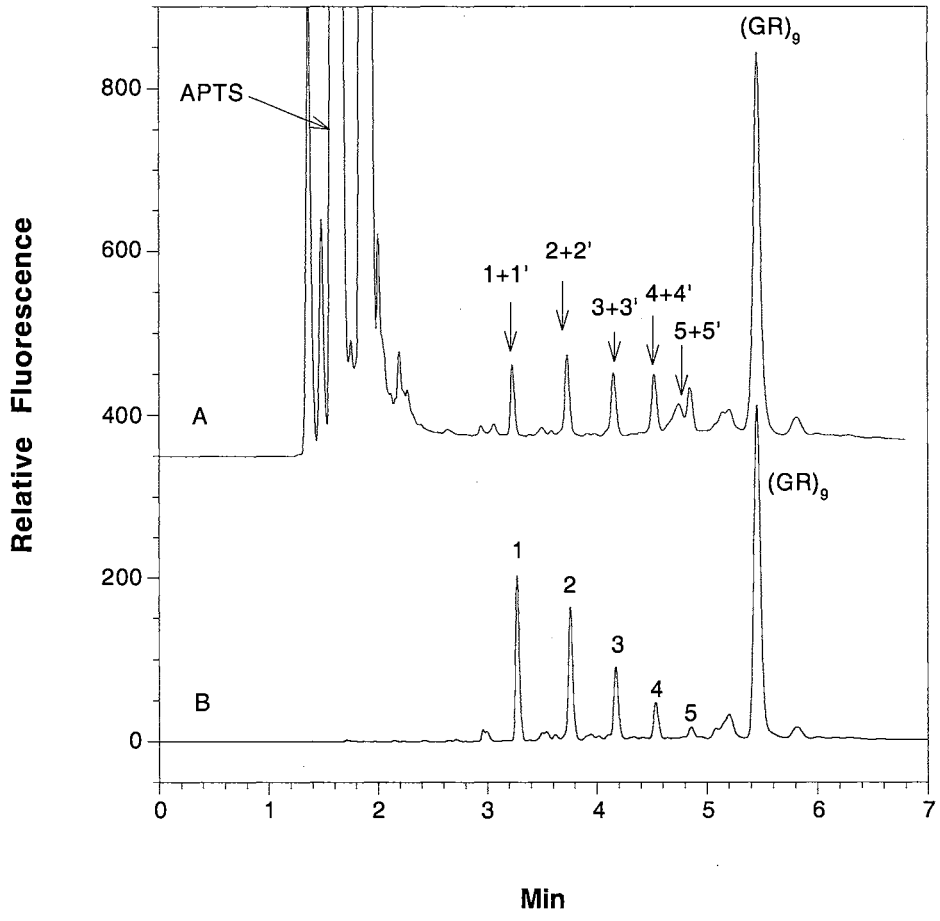

Figure 4-14 RGase digestion of APTS labeled $(GR)_9$

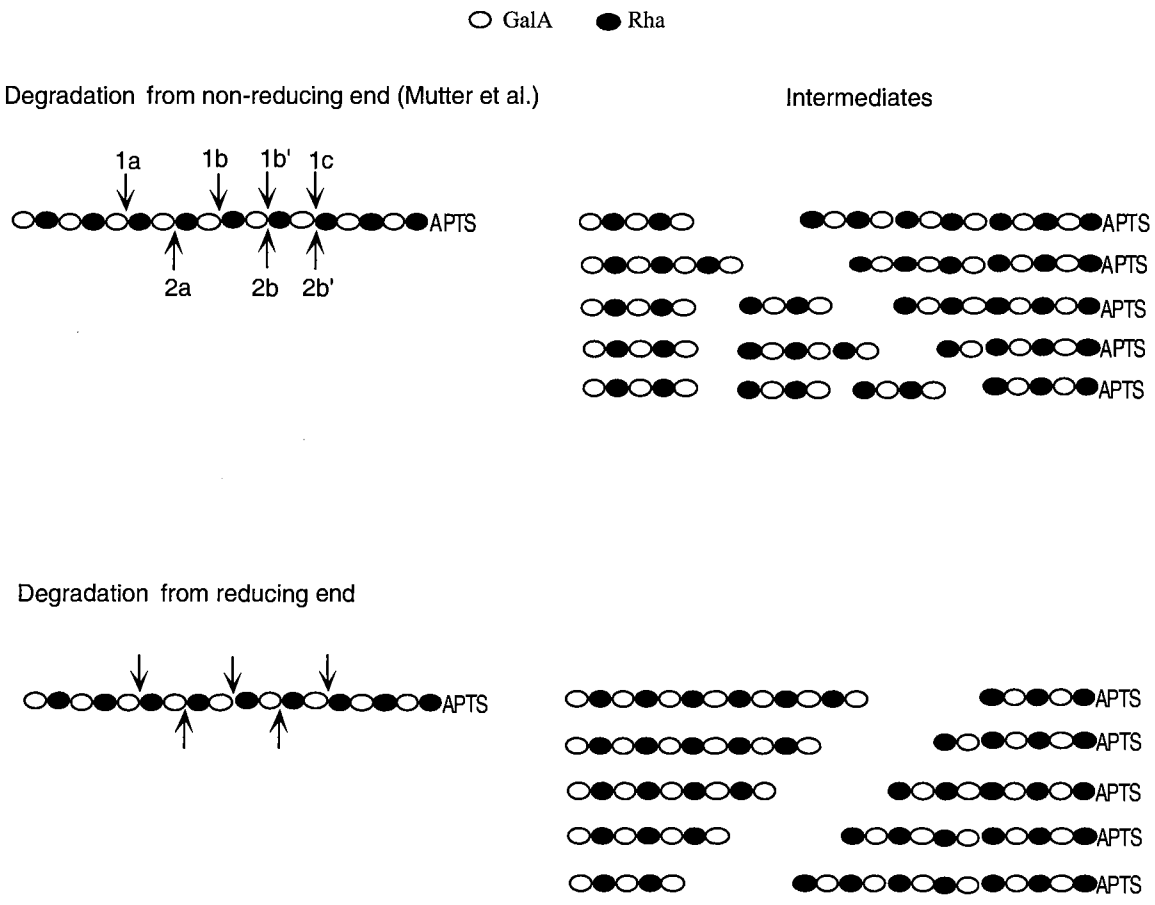

Figure 4-15 Intermediate fragments generated by RGase from ANTS labeled $(GR)_7$ and $(GR)_8$ mixture

A. Non-reducing end fragments and reducing end fragments after second ANTS labeling.
B. Reducing end fragments generated by RGase directly.
1: $(RG)_2R$, 2: $(RG)_3R$, 3: $(RG)_4R$, 4: $(RG)_5R$
1': $G(RG)_2$, 2': $G(RG)_3$, 3': $G(RG)_4$, 4': $G(RG)_5$

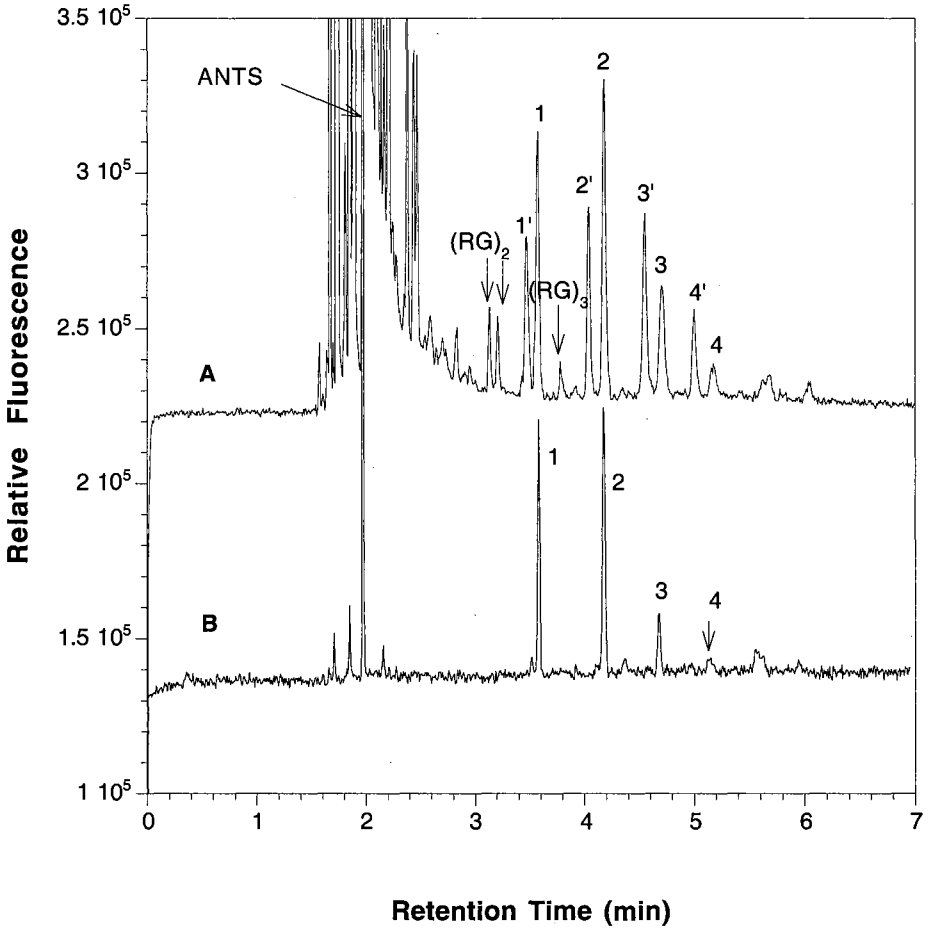

CHAPTER 5 PARTIAL CHARACTERIZATION OF THE XG-RG COMPLEX USING POLYSACCHARIDE DEGRADING ENZYMES

INTRODUCTION

To characterize the XG-RG crosslinked complex, one expects to isolate the crosslink fragments by degrading the XG and RG polymer without destroying the crosslink, or to separate the XG from the RG by breaking the crosslink. Polysaccharide degrading enzymes have better specificity towards the glycosidic linkages than chemical methods. However, the commercial enzymes from Megazyme show limited specificity. Endoarabinanase and arabinosidase are able to degrade α-1, 5 linked arabinan or branched arabinan, endogalactanase is able to degrade β-1, 4 linked galactan, but all of these commercial enzymes contain significant endoglucanase activity. This eliminates the possibility of using these enzymes to examine the proposed arabinan or arabinogalactan crosslinks between XG and RG (1). Endoglucanase is able to degrade the cotton XG polymer into four basic units of XXXG, XXLG, XXFG and XLFG (2). Degradation of the XG-RG complex by endoglucanase can remove most of the XG and leave the remaining RG moiety with a molecular weight of about 250 kD (chapter 2). The RG polymer has a very complicated structure due to its various sidechains. Once the XG has been removed, the crosslink between XG and RG is difficult to track. So, to isolate the XG-RG crosslink, the better way is to degrade the RG polymer without degrading the XG polymer, then use the XG polymer as an indicator to isolate the crosslink fragment for further characterization.

Rhamnogalacturonase (RGase), first reported by Schols et al., is able to degrade the modified hairy region (a novel enzyme resistant RG I region) prepared from apple cell walls (3). Later they found three distinguishable units can be released from the modified hairy region by RGase: a polymeric xylogalacturonan unit, an intermediate size arabinan-rich RG I unit and RG I oligomers (4). However, it was reported that RGase could not degrade the "native" RG I isolated from sycamore suspension cell walls, but it could degrade it into RG oligomers after removal of the RG I sidechains by a combination of enzymes (5). This indicates that the RG I region varies from different sources and the variation may be mostly from the substitution of the sidechains which will affect the RGase degradation.

A cloned RGase (*Botryotinia fuckeliana*) was successfully expressed in *Pichia*. The purified RGase can cleave linear RG oligomers into RG dimer and trimer. Another enzyme, endoarabinase was also expressed in *Pichia* and purified. Characterization of the XG-RG complex was carried out by applying various cell wall degrading enzymes including the cloned RGase and endoarabinase.

MATERIALS AND METHODS

Enzymes

Endoglucanase, endoarabinase, arabinosidase, endogalactanase were purchased from Megazyme (Ireland). Cloned RGase (*Botryotinia fuckeliana*) and endoarabinase (*Bacillus subtilis*) were expressed and purified as described in chapter 4.

Substrates

The XG-RG complex was prepared as described in chapter 2. The avicel unbound RG I was isolated as described in chapter 3.

Enzymatic digestion

100 mg of the XG-RG complex was incubated with the purified RGase in 50 mM sodium acetate, pH 4.0 at 40 °C for 24 h. The amount of RGase added was adequate to digest 6 μmole of linear $(RG)_8$ in one hour. 100 mg of the complex contains the equivalent of 12 μmole of $(RG)_8$. The digestion mixture was heated at 90 °C for 15 min to inactivate the enzyme before chromatographic separation.

MALDITOF-MS

Oligosaccharides were dissolved in aqueous 2% acetonitrile containing 0.1% trifluoroacetic acid. This solution was mixed with an equal volume of dihydroxybenzoic acid and dried on the sample plate in air. Spectra were obtained on a Perseptive Biosystems Voyager matrix-assisted laser desorption time-of-flight mass spectrometer in the negative ion mode (University of Oklahoma Health Sciences Center Laser Mass Facility).

NMR spectroscopy

^1H NMR spectra of samples in D_2O were recorded at 30 °C on a varian Unity Inova 400 NMR spectrometer.

For ANTS derivatization and CZE, GLC sugar composition analysis, gel filtration chromatography see methods of chapter 2.

RESULTS

Digestion of the XG-RG complex mixture with RGase

The procedure of degradation of the XG-RG complex is illustrated in Fig. 5-1. The anion exchange column co-eluted XG-RG complex mixture contains the XG-RG

complex and the free RG I. The XG-RG complex can be separated from the free RG I by *in vitro* binding it to avicel. But using 1 M NaOH to release the XG-RG complex from the avicel causes desalting problems and the recovery is only half of the bound material. For large quantities, the XG-RG complex mixture was used for RGase degradation. A control experiment of RGase degradation of the free RG I was carried out for a comparison.

Fig. 5-2 shows the chromatograms of separation of RGase digested XG-RG complex mixture and the free RG I on an HW55 (S) gel filtration column. Degradation of the XG-RG complex mixture (Fig. 5-2A) gave three major fractions: (1) high molecular weight (HMW) fraction (size range 100,000 Da-200,000 Da), (2) low molecular weight (LMW) fraction (size range 1,000 Da-50,000 Da) and (3) included volume fraction (size lower than 1000 Da). The sugar composition of each fraction is listed in Table 5-1. If one takes rha as an indication for RG I and glc for XG, approximately 90% of the total RG I in the complex mixture can be degraded by RGase into the LMW fraction while 85% of the total XG stays in the HMW fraction.

In the co-eluted XG-RG fraction, about half of the rha by weight is in the avicel unbound free RG I fraction and half is in the avicel bound XG-RG complex. To examine if the free RG I can be completely digested by RGase or not, the unbound RG I was treated with RGase and separated on the same HW55 (S) gel filtration column (Fig. 5-2B). The chromatogram shows one major peak in the LMW (1,000 Da-50,000 Da) region and a small bump eluted in the HMW (100,000 Da-200,000 Da) region. The sugar composition of these two fractions is listed in Table 5-2. The majority of the unbound RG I was degraded into the LMW fragments and only a small proportion remained in the HMW fraction. The sugar composition of this small fraction shows 9% ara, 9% rha, 3% fuc, 30% xyl, 23% galA, 12% gal and 12% glc. The presence of glc and fuc indicates that this low proportion fraction could be digestion products of the XG-RG complex which was left unbound to the avicel. So, we can assume that the avicel unbound free

RG I can be completely digested by RGase into the LMW fragments. If one subtracts 50% of the total RG I in the LMW fraction as being from the free RG I, there is about 40% of the RG I cleaved off from the "real" XG-RG complex. The remaining 10% RGase resistant RG is associated with most of the XG and contributes to the HMW fraction.

Digestion of the RGase resistant XG-RG complex with endoglucanase

To test whether the XG is still crosslinked to the rest of the RG I after RGase digestion, the HMW fraction was re-chromatographed on a PA1 anion exchange column (Fig. 5-3). The chromatogram shows two major peaks, a non-adsorbed fraction and an adsorbed fraction. The non-adsorbed fraction is mainly XG and it accounts for about 10% of the total XG in the HMW. This small amount of XG could be cleaved off from the complex by a trace of contaminating endoglucanase present in the purified RGase. However, the majority of the XG in the HMW fraction still co-eluted with the RG. In comparison to the elution profile of the adsorbed fraction, the RGase resistant XG-RG complex eluted at a lower concentration of ammonium acetate than the undigested complex mixture. This is because the RGase resistant complex contains much less RG I and thus shows much less binding to the anion exchange column.

The RGase resistant XG-RG complex was enriched in XG and showed a high *in vitro* binding to the avicel cellulose. This further indicates that the RGase resistant RG is crosslinked to the XG. Endoglucanase was used to digest the avicel bound complex and the released fraction was separated on an HW40 (S) gel filtration column (Fig. 5-4). The released pectic sugars are mainly in the void volume fraction and the XG are mostly in the later fractions as XG monomers and a trace of dimers. The void volume fraction contains 2% ara, 16% rha, 2% fuc, 27% xyl, 40% galA, 5% gal and 6% glc. This fraction could be the XG-RG crosslink-containing fraction. The relative molar ratio of rha: galA: xyl is 1: 2.6: 1.7. If one takes a 1: 1 of galA: rha for RG I, then the remaining molar ratio

of galA to xyl is about 1.6: 1.7. The high content of xyl and galA may indicate the presence of xylogalacturonan (XGA), but xyl: galA ratio is much higher than the average ratio (1: 3) for XGA. Since this fraction was released by endoglucanase, there is not much XG left and thus not much xyl from XG. The high content of xyl could be contributed from other types of xyl containing fragments like xylan. The electropherogram of ANTS labeled putative crosslink-containing fraction (Fig. 5-5) shows a series of peaks. These fragments could have a difference of several sugar residues between each other. Because xyl and galA are the most abundant sugars in this fraction, a series of xylan or XGA containing fragments is expected. However, further digestion of this fraction with xylanase or exo-polygalacturonase (which can cleave XGA from its non-reducing end) did not show a significant change (data not shown). The MALDI-MS data gave a series of mass fragments abundant in the 2,000 Da-8,000 Da region (Fig. 5-6). A major series of 396 mass differences was obtained. Two relatively small peaks were also present within the 396 difference mass peaks, but the mass differences between each were not consistent and did not fit those expected abundant sugars. More material of this crosslink-containing fraction should be prepared for a further detailed characterization.

Digestion of the RGase resistant XG-RG complex with endoarabinase

Arabinan or arabinogalactan were hypothesized to be the crosslinks between XG and RG I (1). To investigate if it is the case in cotton suspension cell walls, endoarabinase was used to digest the XG-RG complex. If endoarabinase can release the XG from the complex by breaking the arabinan crosslink, then the neutral XG fraction can be separated from the acidic RG I fraction on an anion exchange column. The commercial endoarabinase from Megazyme contains significant endoglucanase activity which can degrade the XG backbone, but not through the potential "arabinan crosslink". A specific cloned endoarabinase was used to digest the RGase resistant XG-RG complex.

Since RGase removed 90% of the total ara and 80% of the total gal into the LMW RG I fragments, the remaining XG-RG complex has much less interference from the RG I sidechains in comparison to the total complex mixture. The endoarabinase digestion showed a trace of XG cleavage from the RGase resistant XG-RG complex. Minimal release of XG from the complex by endoarabinase would have several explanations. First, no such arabinan crosslinks exists between XG and RG I. Second, if these crosslinks are present, they might be highly branched, and so, resistant to endoarabinase. More specific enzymes like arabinosidase, endogalactanase, or others will be needed for further investigation. Third, the involvement of XGA and potential xylan increases the complexity of the crosslink junction, and thus further degradation of XGA and RG I is needed to isolate the real crosslink fragments. The possibility of the potential arabinan or arabinogalactan crosslinks still could not be ruled out.

Characterization of the LMW fraction

To investigate the small fragments generated by RGase, the LMW fraction was separated on a PA1 anion exchange column (Fig. 5-7). The chromatogram shows a series of peaks eluted between 0.03 M and 1 M of ammonium acetate. Each peak was collected as one fraction and its sugar composition is listed in Table 5-3. The electropherogram of each ANTS labeled fraction is illustrated in Fig. 5-8.

Fraction 1 is an unadsorbed fraction. It is mainly composed of neutral sugars: ara, xyl, gal, glc, rha, fuc and a trace of galA. Re-chromatography of this fraction on an HW55 (S) gel filtration column shows a major peak around 10 kDa (Fig. 5-9A). A small proportion of XG rich material was eluted earlier before the major peak. The major peak fraction contains 80% of ara and a trace of RG and XG sugars. The sugar composition indicates that this major fraction could be arabinan-rich RG I fragments. To examine if arabinan or arabinose is directly linked to rha, endoarabinase and arabinosidase (both from Megazyme) were used to digest this fraction. Three fractions were obtained after

separation on an HW40 (S) gel filtration column (Fig. 5-9B). Fraction I contains much of the XG and can be digested by endoglucanase into XG subunits. Fraction III is mainly arabinose released by enzymes. Fraction II shows an average molecular mass of 1000. The sugar composition of fraction II shows 24% ara, 19% rha, 8% xyl, 12% galA, 20% gal and 16% glc. The ANTS labeled electropherograms of fraction II and endoglucanase digested fraction I are illustrated in Fig. 5-10. From the sugar composition and the ANTS labeled electropherogram, fraction II could be a mixture of RG I oligomers with arabinosyl or galactosyl sidechains. A small proportion of XG subunits contaminated fraction II due to the endoglucanase activity present in the commercial enzymes. The fraction II samples were tried on MALDI-MS, but no good MS data were obtained to confirm either an arabinosyl or galactosyl substitution on RG I.

PA1 fraction 2 and fraction 3 have a similar sugar composition to fraction 1. These two fractions could also be a mixture of RG I fragments linked with large arabinan, galactan or arabinogalactan sidechains. Fig. 5-8A shows no ANTS labeled peaks in the 30 min run. This indicates, by comparing to the migration time of the ANTS labeled polysaccharide standard, the samples in fractions 1 to 3 could be larger than 10 kDa.

PA1 fraction 4 to fraction 13 are relatively small fragments because the electropherograms (Fig. 5-8 B, C, D) show sharp peaks within 10 min. Several fragments were identified by MALDI-MS as RG dimer and trimer with or without single gal substituted. No ara substitution on RG I has been indicated from the MS data. Fractions 7, 10 and 13 were confirmed by NMR spectroscopy to be mainly $(RG)_2$, $(RG)_3$ and $(RG)_4$, respectively. However, the sugar composition of fractions 4 to13 showed a high content of ara, especially in fractions 4 to 6 which contained 50-70% ara. The high content of ara could be contamination from arabinan rich fragments which spread over the later fractions on the anion exchange column. When labeled with ANTS, small oligomers are much easier to be detected than big polymers.

According to the sugar composition of each fraction, fractions 1 to 6 are considered to be arabinan or galactan rich fractions and account for 30% of the total LMW sugar weight. Fractions 7 to 16 are considered to be small oligomers and account for about 50% of the total sugar weight.

Fraction 17 was eluted under a higher concentration of ammonium acetate (0.6 M-1 M). The sugar composition was 13% ara, 12% rha, 2% fuc, 18% xyl, 24% galA, 18% gal and 7% glc. It could be a junction of RG I, XGA and/or XG. Further digestion of this fraction with endogalactanase, endoarabinase and arabinosidase to remove the RG I sidechains followed by RGase, generated a few oligomers, but the majority of the material remained unchanged (Fig. 5-11). The sugar composition of the enzyme modified fraction 17 is also listed in Fig. 5-11.

Characterization of enzyme treated LMW fraction

The LMW fraction generated from the XG-RG complex mixture by RGase contains abundant RG I fragments with arabinan and galactan sidechains attached. The complexity of the sidechains may inhibit RGase digestion. The LMW fraction was treated with a combination of endogalactanase, endoarabinase and arabinosidase (all from Megazyme) to remove the sidechains on RG I, and then RGase. The enzyme treated LMW fraction was separated on a PA 1 column (Fig. 5-12). In comparing the PA1 profile of the LMW material and the enzyme treated LMW material, the later one shows less material eluted before 0.2 M of ammonium acetate. This indicates that the combination of enzymes removed much of the large sidechains on RG I. The sugar composition of each separated fraction is listed in Table 5-4. The electropherograms of ANTS labeled fractions are showed in Fig. 5-13. Major fragments in these fractions were identified by MALDI-MS and listed in Table 5-4.

Fraction E1 contains mainly neutral sugars generated by enzymes. Fraction E2 is a small proportion fraction which contains rha, galA, xyl and gal. Fraction E3 shows

61% of galA, 16% of rha and 13% of gal. It is a mixture of galA monomer and gal substituted RG dimer. Fraction E4 to fraction E13 shows a similar sugar ratio of rha: galA: gal: ara of 1: 1: 0.6: 0.07. The sugar composition of these fractions indicates that they are mainly RG I oligomers with some gal substitution. The gal substitution was confirmed from MALDI-MS data. But ara substitution on RG I was not found. Fractions eluted later than E10 could be further degraded if more RGase was added. These fragments contain more than four RG repeating units. The sugar composition of fraction E15 is close to that of the enzyme modified fraction 17 (Fig. 5-11). This indicates that the enzyme resistant region is the junction of XGA and RG.

DISCUSSION

The complexity of RG I

RGase digestion of the XG-RG complex mixture (free RG I and XG-RG complex) released 90% of the total RG I into LMW fragments. In the LMW fraction, three types of RG I were distinguished according to the separation on a PA1 anion exchange column. Type I, arabinan/galactan rich RG I fragments; type II, simple RG I oligomers with some gal substitution; type III, RGase resistant RG I-XGA junction (Table 5-5).

Because of the diversity of the sidechains on the RG I backbone, rha distribution is used to reflect the RG I composition rather than using total fraction sugar weight. Approximately 15% of the total rha is linked with large sidechains, 37% is linked with single gal, 35% with no sidechains and 13% is involved in the junction with XGA.

Treatment of the LMW fraction with RG I sidechain degrading enzymes followed by RGase resulted in generation of more type II fragments. No type I fragments were obtained. This indicates that most of the large sidechains on RG I could be degraded by the combination of enzymes toward arabinan or galactan. The type III fragments have a

characteristic sugar content of about 20% rha, 10% xyl, 30% galA. 5% ara and 15% gal. The presence of XGA and highly branched sidechains on RG I could be the reason for the enzyme resistance.

The crosslink between XG and RG I

RGase digestion of the XG-RG complex mixture (~400 kDa) degrades much of the RG I and leaves the XG intact. Further degradation by endoglucanase removes most of the XG and leaves the crosslink-containing fraction about several kDa. The sugar composition of this enzyme resistant putative crosslink-containing fraction indicates that every one rha is associated with 2.6 galA, 1.7 xyl and 0.4 glc. The high molar ratio of galA and xyl to rha suggests that XGA might be involved in the crosslink fraction. A fungal medium (*Aspergillus nidulan*) containing exo-polygalacturonase (exo-PG) is able to degrade XGA. The ANTS labeled crosslink fraction was treated with the fungal medium filtrate. A dimer peak was generated and it might be a xyl substituted galA fragment. If XGA is at the non-reducing end of the XGA-RG-XG complex, then exo-PG would be able to degrade the junction further to give smaller crosslink containing pieces. Pure exo-PG should be obtained for a further characterization.

A cloned endoarabinase has been applied to digest the RGase resistant XG-RG complex. The result showed no significant release of the XG from the complex by endoarabinase digestion. A specific arabinosidase will be needed to examine if the crosslink is through a highly branched arabinan.

The finding of the XGA closely associated with the crosslink brings us closer to finding out the nature of the crosslink between RG and XG. Further study should put effort towards degrading the RG-XGA junction. More specific enzymes and more specific methods are needed to isolate and characterize the real crosslink.

REFERENCES

1. **Keegstra, K., Talmadge, K. W., Bauer, W. D., and Albershem, P.** 1973. The structure of plant cell walls. III. A model of the walls of suspension-cultured sycamore cells based on the interconnections of the macromolecular components. *Plant Physiol.* 51: 188-196

2. **El Rassi, Z., Tedford, D., An, J. and Mort, A. J.** 1991. High performance reversed-phase chromatographic mapping of 2-pyridylamino derivatives of xyloglucan oligosaccharides. *Carbohydr. Res.* 215: 25-38

3. **Schols, H. A., Geraeds, C. C. J. M., Searle-Van L., Marjo, F., Kormelink, F. J. M., Voragen, A. G. J.** 1990. Hairy (ramified) regions of pectins. Part II. Rhamnogalacturonase: a novel enzyme that degrades the hairy regions of pectins. *Carbohydr. Res.* 206: 105-15

4. **Schols, H. A., Bakx, E. J., Schipper, D. and Voragen, A. G., J.** 1995. A xylogalacturonan subunit present in the modified hairy regions of apple pectin. *Carbohydr. Res.* 279: 265-279

5. **An, J., Zhang, L., Oneil, M. A., Albersheim, P. and Darvill, A. G.** 1994. Isolation and structural characterization of endo-rhamnogalacturonase-generated fragments of the backbone of rhamnogalacturonan I. *Carbohydr. Res.* 264: 83-96

Figure 5-1 Scheme of enzymatic degradation of the XG-RG complex mixture

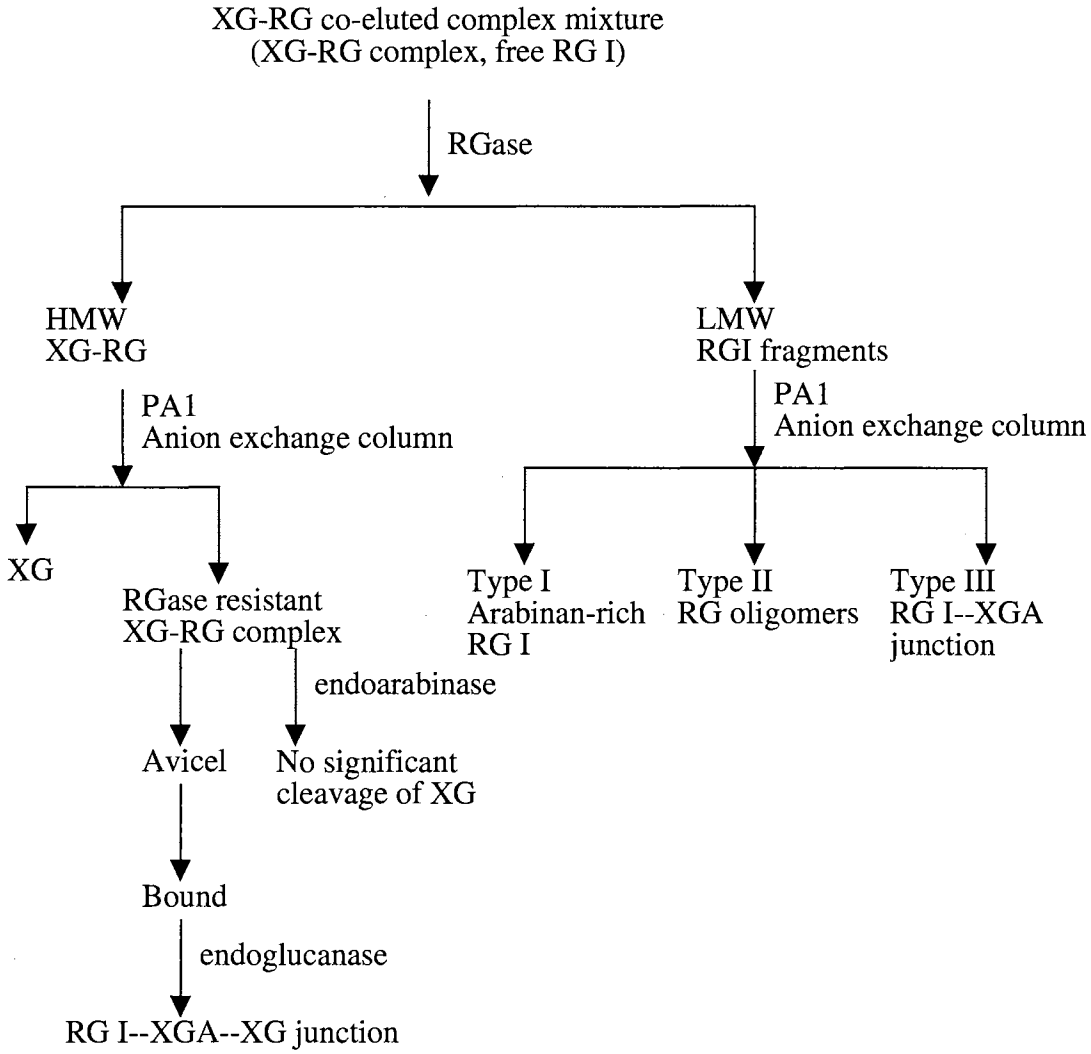

Figure 5-2 HW 55 (S) gel filtration profile of RGase digested co-eluted XG-RG complex mixture (A), RGase digested the avicel unbound free RG I (B) and pullulan polysaccharides standard (C)

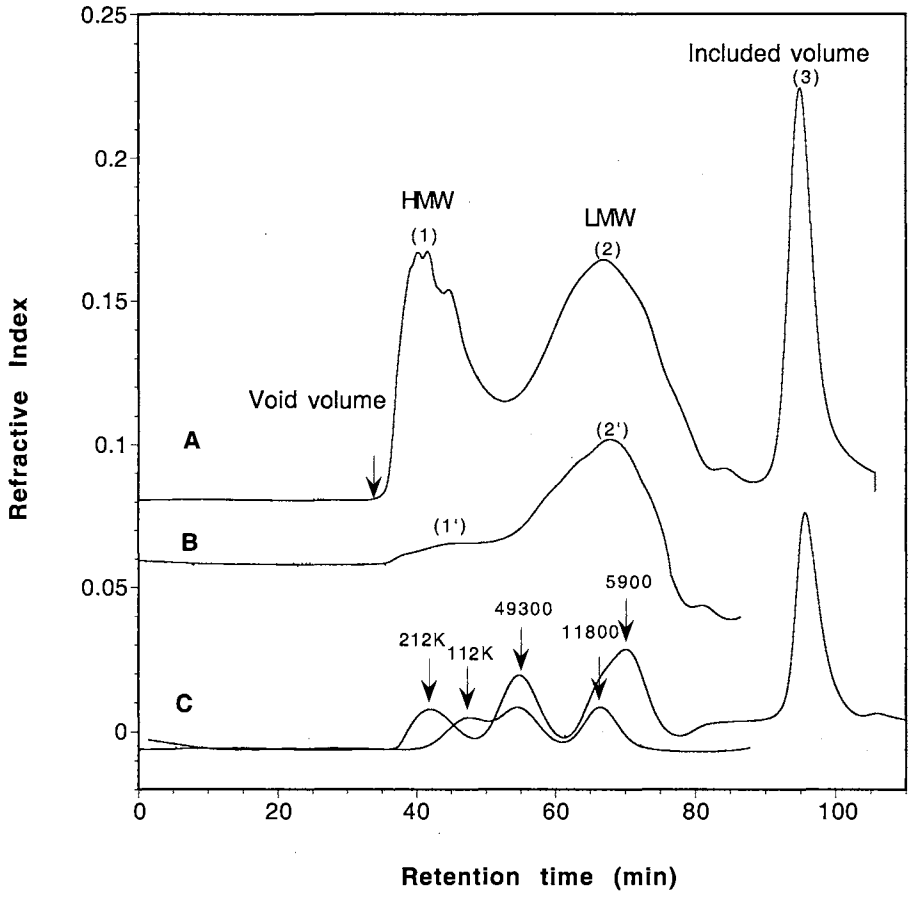

Table 5-1. Sugar composition of HW55 (S) gel filtration column separated fractions of RGase digested XG-RG complex mixture

Fraction	Sugar composition in mole%							Fraction wt%	XG wt%	RG wt%
	Ara	Rha	Fuc	Xyl	GalA	Gal	Glc			
XG-RG complex mixture	30	13	2	17	16	14	8	100	100	100
HW55 (1)	4	3	5	37	8	16	27	31	85	7
HW55 (2)	41	16	n.d.	6	16	19	2	66	15	90
HW55 (3)	27	22	n.d.	n.d.	30	10	n.d.	3	0	3

Fraction wt %: total sugar weight in each fraction per total sugar weight in the complex
XG wt %: glc sugar weight in each fraction per total glc sugar weight in the complex
RG wt %: rha sugar weight in each fraction per total rha sugar weight in the complex
n. d.: not detected

Table 5-2. Sugar composition of HW55 (S) gel filtration column separated fractions of RGase digested the unbound RG I fraction

Fraction	Sugar composition in mole%							Fraction wt%	XG wt%	RG wt%
	Ara	Rha	Fuc	Xyl	GalA	Gal	Glc			
XG-RG complex mixture	30	13	2	17	16	14	8	100	100	100
Unbound RG fraction	31	22	0.8	5	29	11	1	30	4	50
HW55 (1')	9	9	3	30	23	12	12	3	4	3
HW55 (2')	39	20	n.d.	3	22	13	1	27		47

Fraction wt%: total sugar weight in each fraction per total sugar weight in the unbound RG fraction
XG wt %: glc sugar weight in each fraction per total glc sugar weight in the complex
RG wt %: rha sugar weight in each fraction per total rha sugar weight in the complex
n. d.: not detected

Figure 5-3 PA1 anion exchange column separation of the HMW fraction after RGase digestion of the co-eluted XG-RG complex mixture (A) and the co-eluted XG-RG complex mixture only (B)

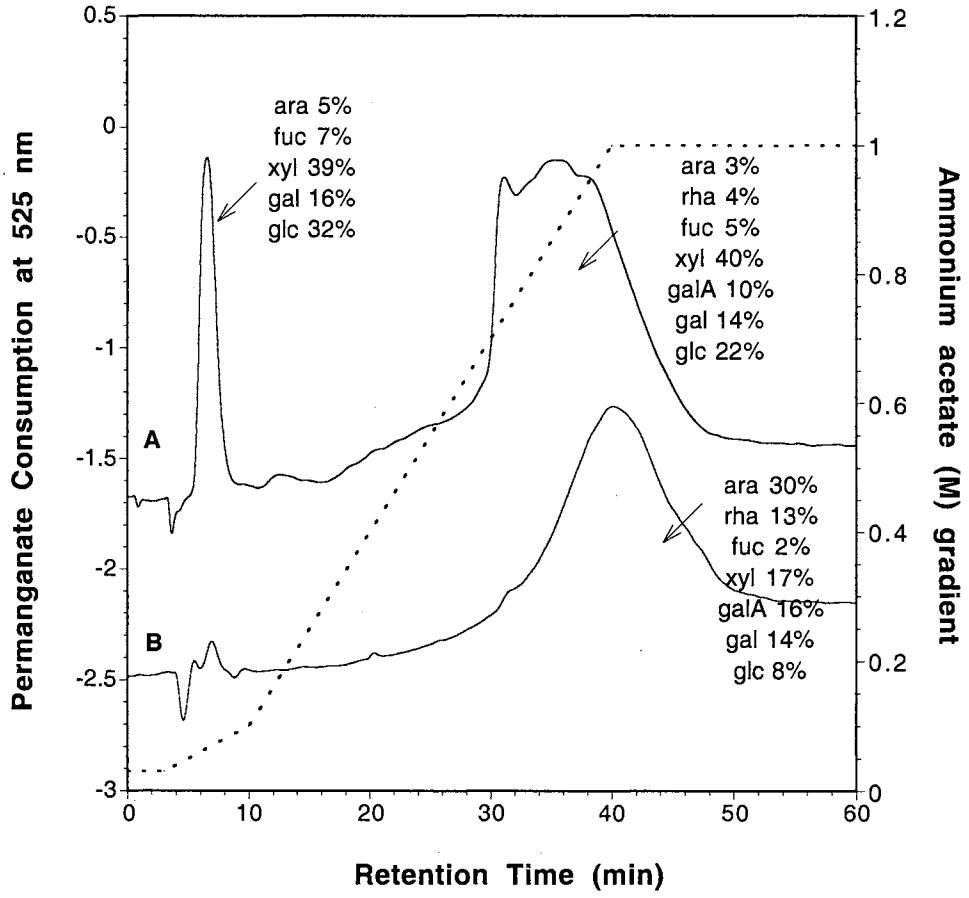

Figure 5-4 HW 40 (S) gel filtration profile of the endoglucanase released material from the avicel bound RGase resistant XG-RG complex

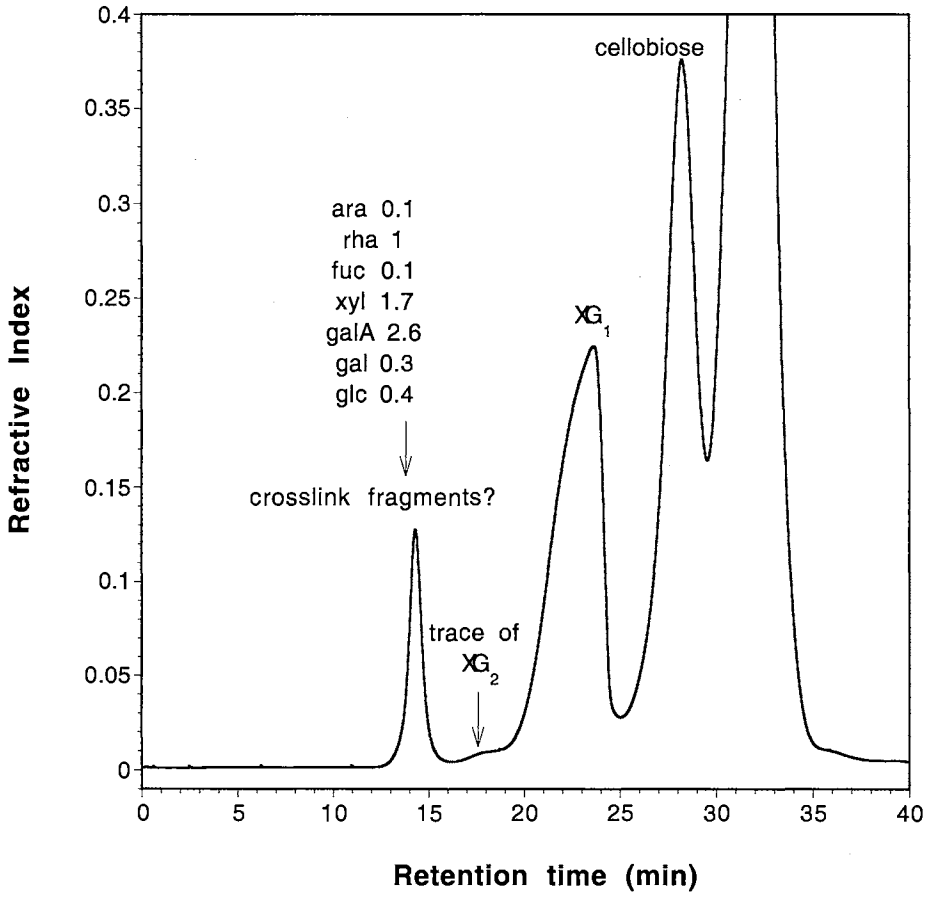

Figure 5-5 Electropherogram of the ANTS labeled the putative crosslink-containing fraction

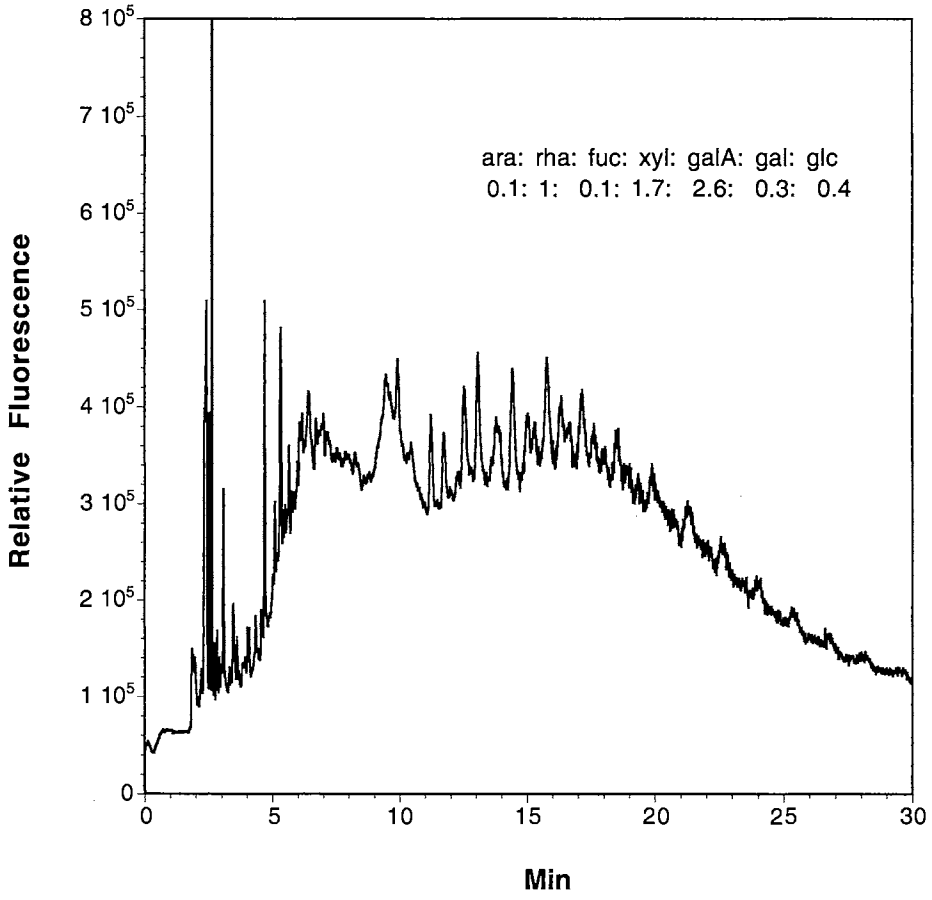

Fig. 5-6 MALDI-MS spectrum of the putative crosslink-containing fraction from the XG-RG complex treated by RGase and endoglucanase

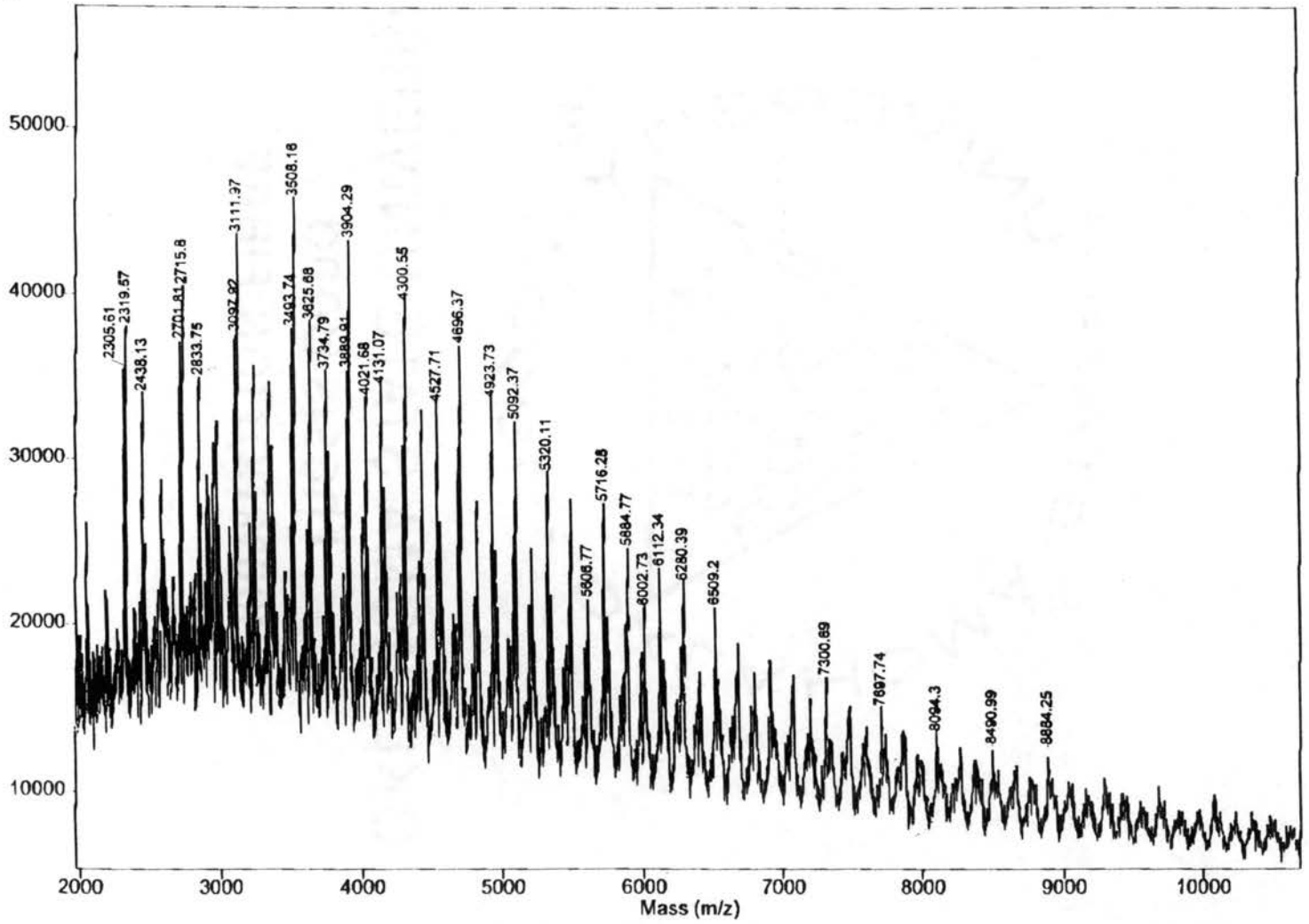

Figure 5-7 PA1 anion exchange column profile of the LMW fraction

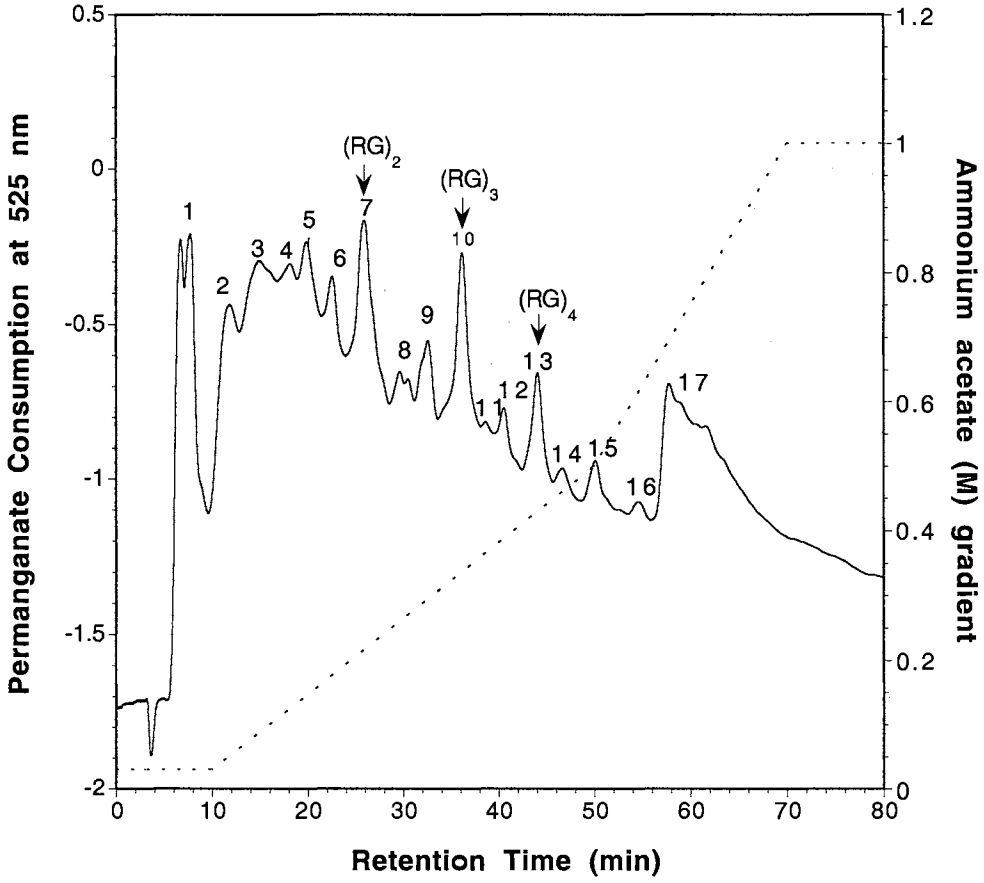

Figure 5-8 Electrophoregrams of the ANTS labeled PA1 fractions of the LMW material

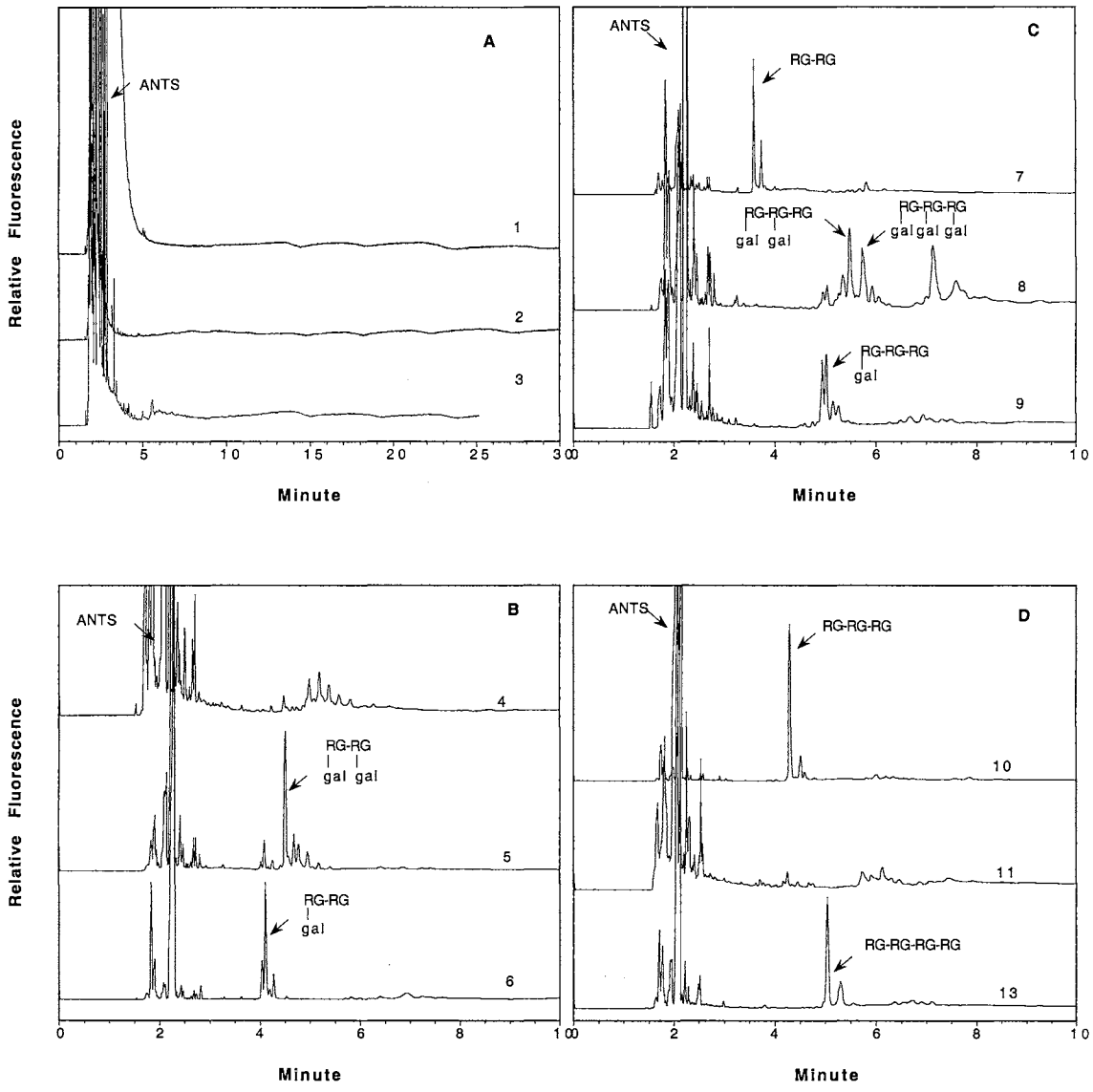

Figure 5-9 HW 55 (S) gel filtration profile of PA1 fraction1 (A) and HW40 (S) gel filtration profile of endoarabinase/arabinosidase digested arabinan-RG fraction (B)

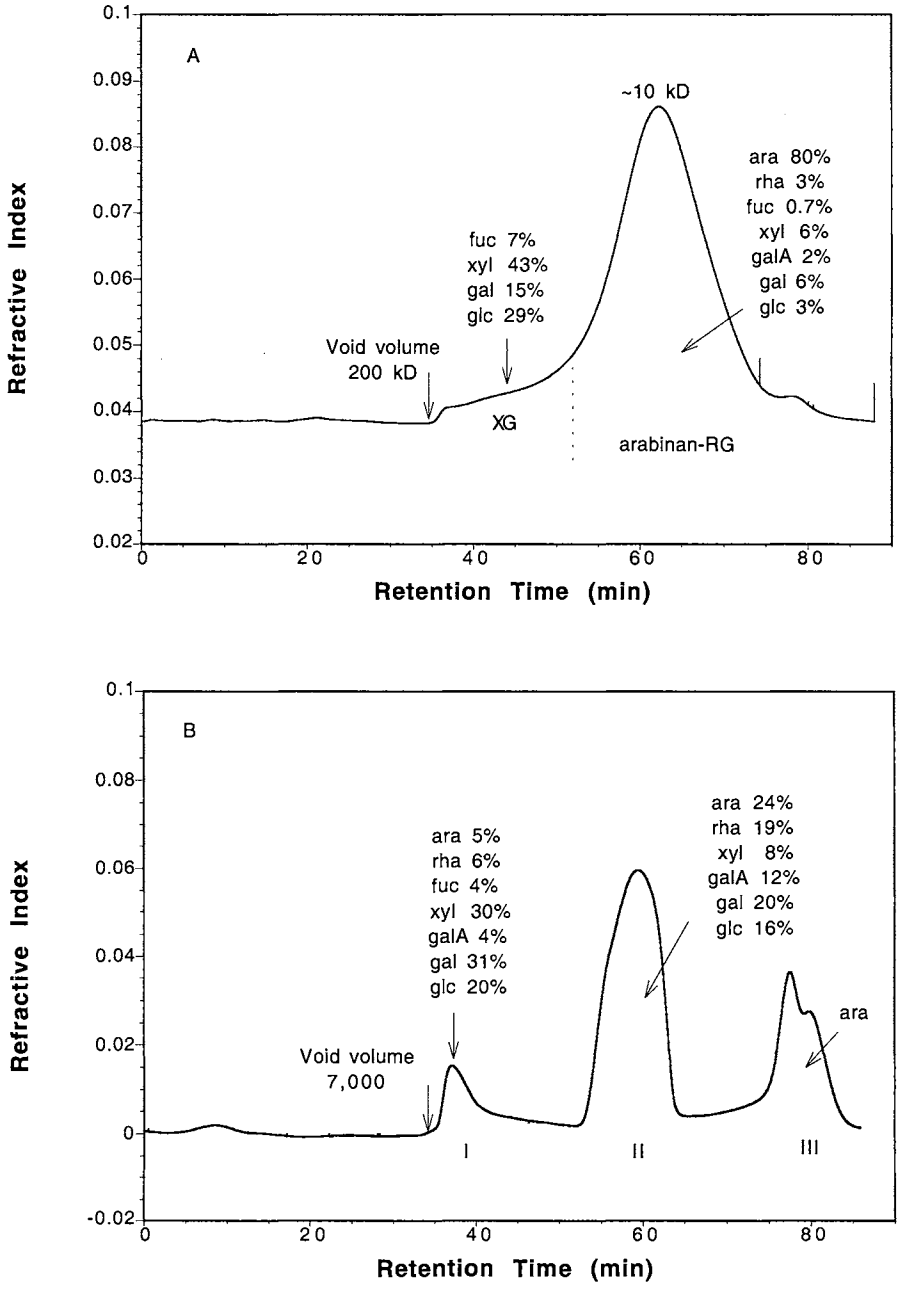

Figure 5-10 Electropherograms of ANTS labeled fraction II of figure 5-9B and endoglucanase further treated fraction I of figure 5-9B

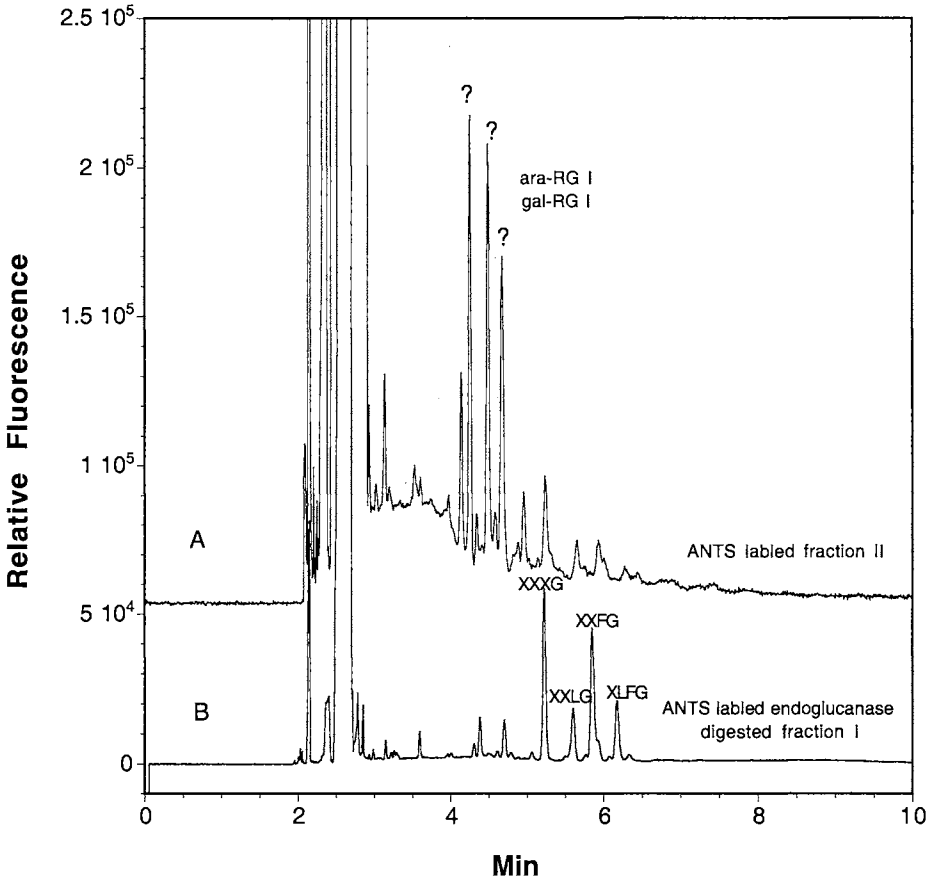

Figure 5-11 PA1 anion exchange column profile of the LMW fraction of RGase digested XG-RG complex (A) and the enzyme treated PA1-17 fraction (B)

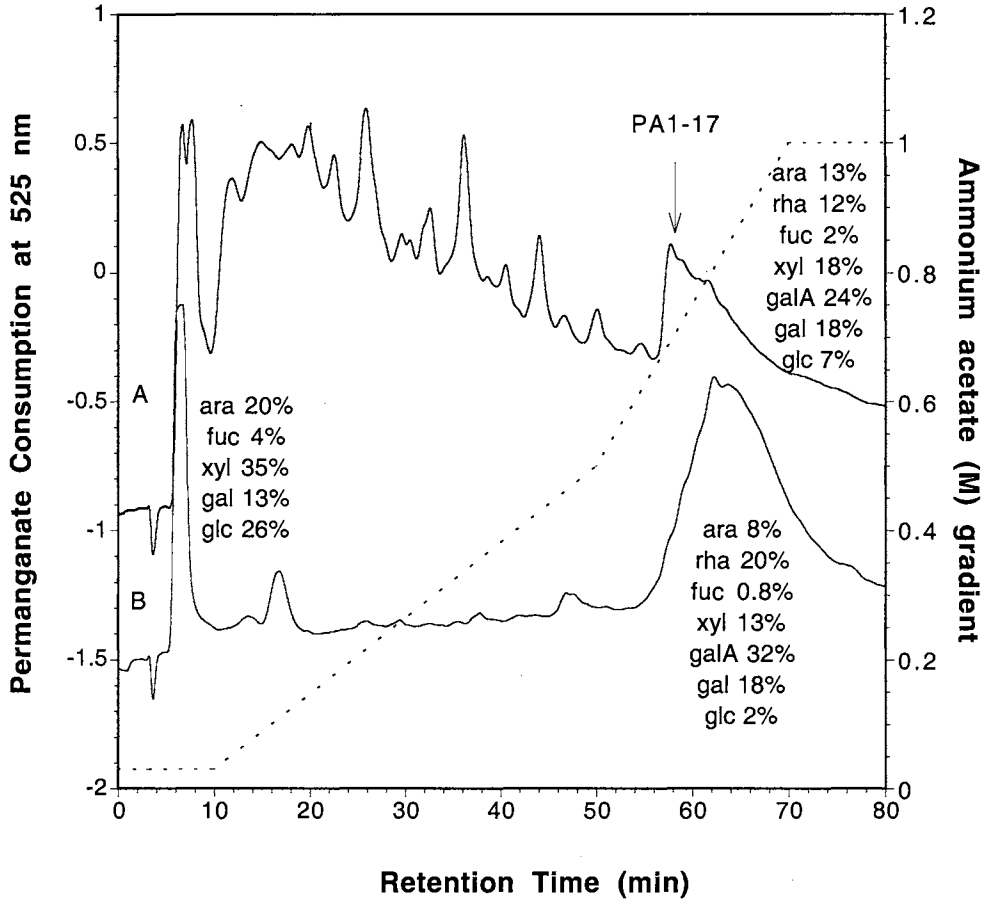

Figure 5-12 PA1 anion exchange column profile of enzyme (endogalactanase, endoarabinase, arabinosidase, RGase) treated LMW fraction

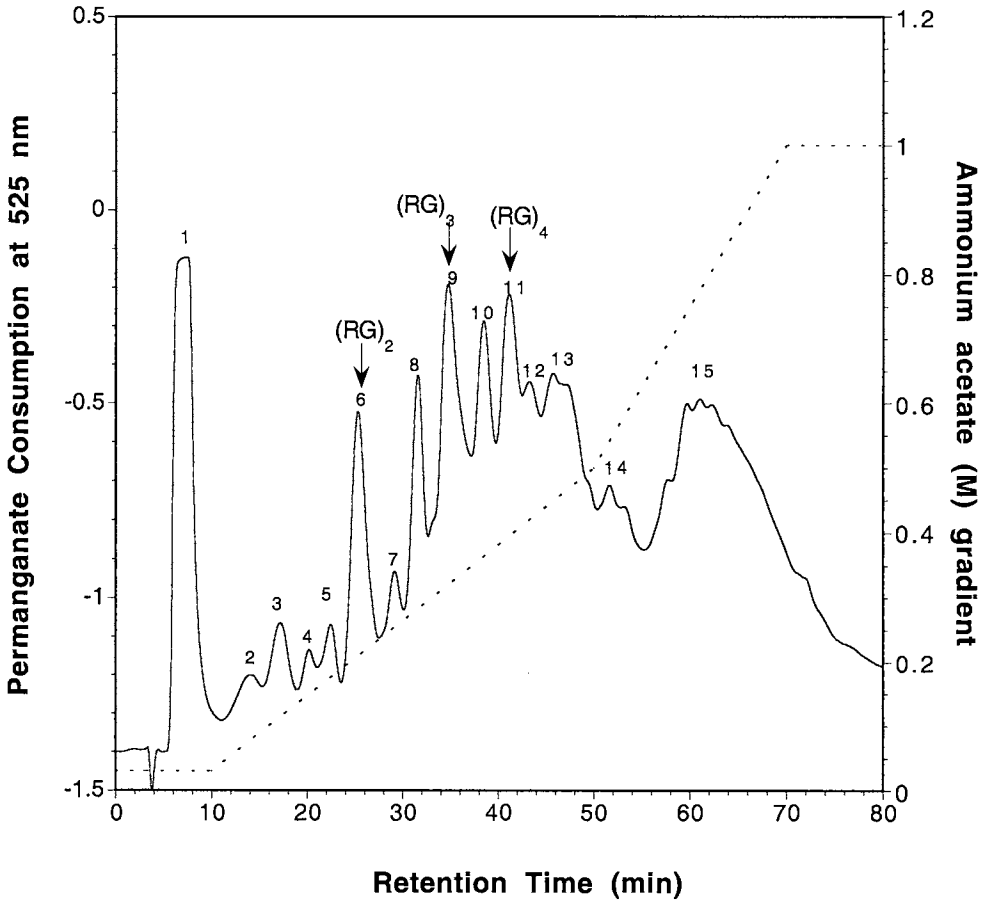

Figure 5-13 Electrophoregrams of the ANTS labeled PA1 fractions from the enzyme treated LMW material

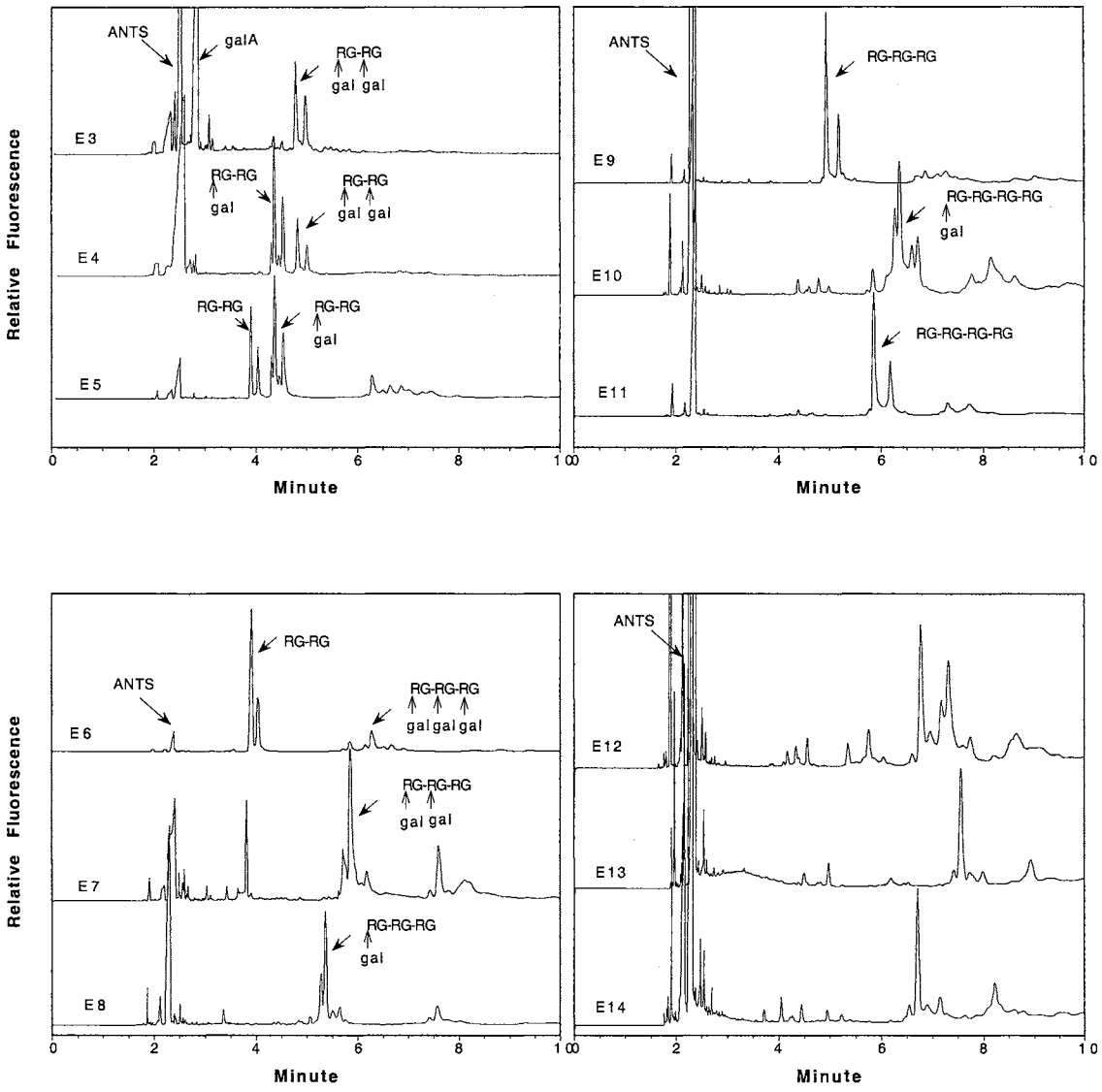

Table 5-3. Sugar composition of PA1 fractions of the LMW material

Fraction	Sugar composition in mole%							Fraction wt (mg)	Rha wt (mg)
	Ara	Rha	Fuc	Xyl	GalA	Gal	Glc		
PA1-1	55	3	2	11	4	13	12	6	0.17
PA1-2	68	6	0.8	?	7	16	2	2	0.10
PA1-3	77	7	0.8	?	5	9	2	3.1	0.16
PA1-4	70	9		3	6	12	0.5	3.1	0.25
PA1-5	60	13		4	9	15		2.8	0.24
PA1-6	56	15		2	10	16	1	3	0.42
PA1-7	44	21		2	17	16	0.6	5	1.0
PA1-8	41	19		3	15	20	1.8	2.6	0.4
PA1-9	33	21		4	18	21	1	1.7	0.3
PA1-10	25	28		3	25	18	0.7	3	0.7
PA1-11	29	22		3	20	24	1	1.5	0.3
PA1-12	24	24		4	23	23	1	1.5	0.3
PA1-13	20	29		4	26	20	1	2.8	0.7
PA1-14	23	24		5	23	23	1	1.3	0.25
PA1-15	17	25		5	27	20	1	2.3	0.5
PA1-16	17	22		6	23	20	3	1.4	0.2
PA1-17	13	12	2	18	24	18	7	11.5	0.9
Total sugar weight								55	6.9

Fraction wt: total sugar weight of each fraction calculated from GLC analysis
Rha wt: rha sugar weight of each fraction calculated from GLC analysis

Table 5-4. Sugar composition of PA1 fractions of the enzyme treated LMW material

Fraction	Sugar composition in mole%							Major fragments
	Ara	Rha	Fuc	Xyl	GalA	Gal	Glc	
E-1	23	3	3	32	1	17	17	ara, XG subunits
E-2	3	40		20	27	9		galA, rha? XGA?
E-3	2	16		8	61	13		galA, $(RG)_2gal_2$
E-4	2	30		13	30	20	3	$(RG)_2gal$, $(RG)_2gal_2$
E-5	2	31		10	34	20	2	$(RG)_2gal$, $(RG)_2$
E-6	2	32		7	32	20		$(RG)_2$, $(RG)_3gal_2$,$(RG)_3gal_3$
E-7	2	32		6	35	21		$(RG)_3gal_2$, $(RG)_4gal_4$?
E-8	2	34		6	37	20		$(RG)_3gal$, $(RG)_4gal_4$?
E-9	3	33		5	36	21	1	$(RG)_3$
E-10	3	35		5	33	23		$(RG)_4gal$
E-11	3	35		5	38	18	3	$(RG)_4$
E-12	3	35		4	36	21	1	
E-13	3	35		4	35	21	1	
E-14	2	28		3	45	21	1	
E-15	4	26	1	11	35	15	2	RG I-XGA junction

Table 5-5 RG I fragments in the LMW fraction generated by RGase

	Sidechain	Mass	Fragment	Fraction wt%	Rha wt%
Type I	arabinan galactan arabinogalactan	~10,000		30%	15%
Type II	no sidechain	662	$(RG)_2$		
		984	$(RG)_3$	20%	35%
		1306	$(RG)_4$		
	single gal	824,986	$(RG)_2gal_{1-2}$		
		1146,1308,1470	$(RG)_3gal_{1-3}$	30%	35%
		1468,1630,1792,1954	$(RG)_4gal_{1-4}$		
Type III	ara, gal?	~5,000	RG I-XGA?	20%	15%

Fraction wt%: total sugar weight of each fraction per total sugar weight of all fractions
Rha wt%: total rha weight of each fraction per total rha weight of all fractions

CHAPTER 6 DEGRADATION OF THE XG-RG COMPLEX BY LITHIUM/ETHYLENEDIAMINE REACTION

INTRODUCTION

Lithium/ethylenediamine reaction was first reported to selectively destroy the uronic acids of the extracellular polysaccharide made by *Bradyrhizobium japonicum* (1). Treatment of RG I with this reaction was also reported to selectively cleave the galA residues of the RG I, leaving intact the neutral glycosyl residues and their glycosidic linkages (2). To characterize the crosslinks between XG and RG, intact crosslink fragments need to be isolated. However, RGase degradation of the RG I polymer could not completely remove RG I. Xylogalacturonan (XGA) was found to be tightly associated with the RGase resistant XG-RG crosslink fragments. If lithium/ethylenediamine reaction can cleave the galA on both RG I and XGA and leave the crosslinks between XG and RG intact, then the crosslink-XG fragments will be isolated for further characterization.

MATERIALS AND METHODS

Materials

Lithium wire was obtained from Alfa Products. Ethylenendiamine was purchased from Aldrich. Endoglucanase, endoarabinanase and arbinosidase were purchased from Megazyme (Ireland).

Lithium/ethylenediamine reaction

About 50 mg of dried XG-RG complex was suspended in 5 ml of ethylenediamine and the mixture was stirred until the carbohydrate had dissolved. Two or three lithium wire pieces (cut into 2-3 mm long) were added into the solution. The solution turned dark blue after stirring for about 5 min. Additional lithium wire pieces were added to maintain the blue color for 1 h. The reaction was stopped by addition of 5 ml of distilled water on ice. The reaction mixture was dried in a speed vacuum, then a few drops of toluene were added to co-evaporate ethylenediamine in a speed vacuum. The resulting white powder was dissolved in water, neutralized with concentrated acetic acid and then applied on a Toyopearl HW50 (S) gel filtration column. The eluted polymeric fractions were collected and lyophilized.

2-Aminobenzoic Acid (AA) derivatization and CZE

About 100 nmoles of monosaccharides (or oligosaccharides) were dissolved in 5 μl of reaction solution containing 0.2 M 2-AA and 1 M sodium cyanoborohydride in methanol. The mixture was heated at 70 °C for 1 h. An alternate method with better solubility for oligosaccharides was also used. 50 μl of 23 mM 2-AA (in 3:17 v/v of acetic acid: water) and 5 μl of 1 M sodium cyanoborohydride (in dimethylsulfoxide) were applied for about 100 μg of oligosaccharides and heated at 90 °C for 1 h. The reaction mixture was dried in a speed vacuum. The dried 2-AA labeled oligosaccharides were then hydrolyzed by 2 M TFA at 90 °C for 2 h. All samples were dried in a speed vacuum and dissolved in water before injection. The samples were analyzed on a capillary electrophoresis instrument using conditions from previous reports (3, 4).

Samples were run on a custom-built instrument with a Spellman CZE 1000 R high voltage power supply (Spellman High Voltage Electronics Co., Plainfield, NY) with an online spectrofluorescence detector (FL-750 HPLC.PLUS, McPherson Instrument, CA). The excitation wavelength was set at 245 nm. A fused-silica capillary (Polymicro

Technologies, Phoenix, AZ, USA) of 50 μm ID (355 μm OD) was used as the separation column. The capillary was 80 cm in length, with 50 cm to the detection window. 200 mM boric acid-50 mM NaH_2PO_4, pH 7.0, was used as a running buffer. The capillary was rinsed with running buffer after each run and samples were introduced by gravity-driven flow for several seconds. Electrophoresis was conducted at 13 kV with the positive electrode on the injection side.

For ANTS derivatization and CZE, GLC sugar composition analysis, gel filtration chromatography see methods of chapter 2. MALDI-MS see methods of chapter 5.

RESULTS AND DISCUSSION

Lithium treatment of the XG-RG complex mixture

The flow chart of lithium/ethylenediamine treatment of the XG-RG complex mixture is illustrated in Fig. 6-1. The lithium treated XG-RG complex mixture was separated on an HW50 (S) gel filtration column (Fig. 6-2). The polymeric sugar fraction (size from 1,000 Da-10,000 Da) was collected. The recovered sugars in the polymeric fraction were 30% of the starting material. The sugar compositions of the XG-RG complex mixture and the recovered fraction after lithium treatment are listed in Table 6-1. The mole percentage of galA decreased from 16% to 1.5% after lithium reaction. The sugar weight recovery of galA was about 4%. Glc, xyl and fuc showed 50-70% recovery of the sugar by weight. This indicates that the XG is kept "intact" or polymeric during the lithium reaction. Gal had a much lower sugar weight recovery (30%), because gal is mainly present in the RG I region as a terminal substitution on rha and could be cleaved off by lithium as gal-rha dimer. During desalting on an HW50 (S) gel filtration column, small fragments could not be recovered from the salts. This also explains the low recovery of rha (3%). No rhamnitol was found although rhamose might be reduced by the reaction. The ara recovery was about 30%. Ara is mostly present as large arabinan

sidechains on RG I, the low recovery of ara could be a non-specific cleavage of arabinan and the cleaved small arabinan fragments were lost during desalting.

The efficiency of galA cleavage by lithium varies from time to time and sample to sample. It could be due to a solubility problem of the polysaccharide in ethylenediamine. The XG-RG complex mixture has an average apparent molecular weight of 400 kDa and the solubility of the macromolecules in ethylenendiamine is not very good. If the first lithium treatment did not cleave many of galAs, a second lithium treatment may give a better result (Fig. 6-2).

Isolation of the XG-crosslinks containing fragments

The hypothesized lithium cleavage pattern of the XG-RG complex is illustrated in Fig. 6-3. The lithium treated products have a broad size range. If lithium leaves the XG with the crosslinks intact, then the XG fragments which contain the crosslinks need to be separated from other fragments. Avicel cellulose was applied to bind the XG fragments. After removal of the unbound fraction, the avicel bound fraction was recovered by 1M NaOH or by endoglucanase. The endoglucanase released fragments were separated on an HW40 (S) gel filtration column (data not shown). The sugar compositions of the avicel unbound fraction and bound fraction are listed in Table 6-2.

In the avicel unbound fraction, the most abundant sugar is ara (76 mole%) and the second is gal (11 mole%). This unbound fraction could be rha-linked arabinan or arabinogalactan fragments cleaved by lithium. The ANTS labeled electropherograms of the unbound and bound fractions are shown in Fig. 6-4. The unbound fraction shows a series of peaks. To determine if these serial fragments contain a rha reducing end (resulting from a specific cleavage at galA) or a ara reducing end (resulting from a non-specific cleavage), the reducing end of these fragments needed to be identified.

Analysis of the reducing end of the avicel unbound fragments

2-aminobenzoic acid (2-AA) labeled monosaccharides can be determined by CZE (3). The avicel unbound fragments were derivatized with 2-AA and then hydrolyzed by 2M TFA into monosaccharides. Complete acid hydrolysis can release the 2-AA labeled reducing end residue. In comparison to the 2-AA labeled monosaccharide standards, the reducing end residue of the oligomer can be determined. The result shows that the reducing end of the avicel unbound fragments is mainly ara (Fig. 6-5). A small proportion of the reducing end could be rha (data is not very promising). This indicates that the avicel unbound serial fragments could be generated by a non-specific cleavage by lithium of the α-1-5 linked arabinan.

Analysis of the avicel bound fraction

The avicel bound fraction released by 1M NaOH shows an enriched XG content (Table 6-2). Endoglucanase digestion of the avicel bound complex results in three fractions on an HW40 (S) gel filtration column (Fig. 6-6). The E-1 fraction was eluted in the void volume. It contains 42% ara, 9% rha, 15% galA, 7% xyl, 11% gal and 16% glc. The sugar weight of E-1 fraction accounts for only one tenth of the sugar weight of E-2 and E-3 fractions. Fractions E-2 and E-3 are mostly endoglucanase generated XG dimer and monomer, respectively. The XG dimer can be further degraded into XG monomer if more endoglucanase is added (Fig. 6-7). The XG dimers are rich in fucosyl substituted XG subunits (XXFG, XLFG), which are reported to be less favored by endoglucanase (5).

Faction E-1, from its sugar composition, seems to be the crosslink fragments. The high content of ara could indicate a putative arabinan crosslink between XG and RG. However, further treatment of fraction E-1 with endoarabinase and arabinosidase did not show a convincing result (no degradation of the ANTS labeled E 1 fragments).

Lithium treatment of the RGase resistant XG-RG complex

The RGase resistant XG-RG complex has a much smaller apparent molecular weight (100-200 kDa) and a much lower galA content (7%) in comparison to the XG-RG complex mixture (~400 kDa and 16% galA content). The purpose of lithium treatment is to further degrade the RGase resistant junction region of RG I-XGA, and to isolate the XG-crosslink fragments.

After lithium treatment, the RGase resistant complex was separated on an HW50 (S) gel filtration column. Fig. 6-8 shows a broad peak of an average mass of 10 kD compared to pullulan standard. The sugar composition of the recovered fraction is listed in Table 6-3. Lithium treatment further decreased the galA content from 7% to 1.5%. The recovery of glc, xyl, gal and fuc was 60%, 50%, 50% and 60%, respectively. This indicates that the reaction did not affect the XG polymer much. The recovery of ara was about 40% and rha was about 10%.

Since most of the ara and gal sidechains linked on RG I had been removed by RGase, in the recovered polymeric fraction, less interference should come from ara or gal sidechains than without the RGase treatment following lithium treatment, unless they are in big pieces. A small proportion of the recovered sugars was tested for avicel binding and the result showed most of it can bind to the avicel. Due to the low recovery after avicel binding and insufficient amount of the sample, the recovered fraction was digested by endoglucanase directly. Three fractions were obtained after separation on an HW40 (S) gel filtration column (Fig. 6-9). The first fraction contains 30% xyl, 22% gal, 20% ara, 7% rha, 13% galA and a trace of fuc and glc. This fraction could be the putative crosslink fragments. The second fraction on HW40 (S) column is mainly endoglucanase generated XG monomer.

The putative crosslink fraction was labeled with ANTS. The electropherogram (Fig. 6-10) shows series of peaks, which seems to be a set of small peaks interspersed between a set of big peaks. The sample was run on an MALDI-MS to determine the

mass of the fragments. The MS data also show a primary pattern of 396 mass differences and two 132 mass differences within the 396 set (Fig. 6-11). The mass difference of 132 could be an ara or xyl. This is consistent with the most abundant sugar composition of this fraction. The results from the ANTS labeled electropherogram and the MS spectrum indicate that these fragments could be different in their residue numbers of ara and/or xyl. No indication of a mass of XG linked could be found from the mass data.

Concerns about this lithium treatment

The lithium reaction is one of the possibilities to further degrade the RGase resistant RG I-XGA region. However, the specificity of the cleavage needs to be considered. The mechanism of the cleavage of galA by lithium is not clear and thus the application of this method for degradation of the RG I is limited.

Control experiments need to be done to examine if lithium can non-specifically cleave the arabinan, arabinogalactan, xylan and xyloglucan. If lithium cleavage shows high specificity towards the galA residues, then large amounts of the RGase resistant complex should be treated by lithium to isolate enough of the putative XG-crosslink fragments. Further analysis of the putative crosslink fragments can be carried out using MS, CZE, NMR, enzyme treatment and reducing end sugar analysis.

REFERENCES

1. **Mort, A. J., Bauer, W. D.** 1982. Application of two new methods for cleavage of polysaccharides into specific oligosaccharide fragments. Structure of the capsular and extracellular polysaccharides of Rhizobium japonicum that bind soybean lectin. *J. Biol. Chem.* 257(4): 1870-1875
2. **Lau, J. M., McNeil, M., Darvill, A. G. and Albersheim, P.** 1987. Treatment of rhamnogalacturonan I with lithium in ethylenediamine. *Carbohydr. Res.* 168(2): 245-274
3. **Sato, K., Sato, K., Okubo, A., Yamazaki, S.** 1997. Determination of monosaccharides derivatized with 2-aminobenzoic acid by capillary electrophoresis. *Anal. Biochem.* 251(1): 119-121

4. **Sato, K., Sato, K., Okubo, A., Yamazaki, S.** 1998. Optimization of derivatization with 2-aminobenzoic acid for determination of monosaccharide composition by capillary electrophoresis. *Anal. Biochem.* 262(2): 195-197

5. **Vinken, J. P., Keizer, A. Beldman, G. and Voragen, A. G. J.** 1995. Fractionation of xyloglucan fragments and their interaction with cellulose. *Plant Physiol.* 108: 1579-1585

Figure 6-1 Flow chart of lithium/ethylenediamine treatment of the XG-RG complex mixture

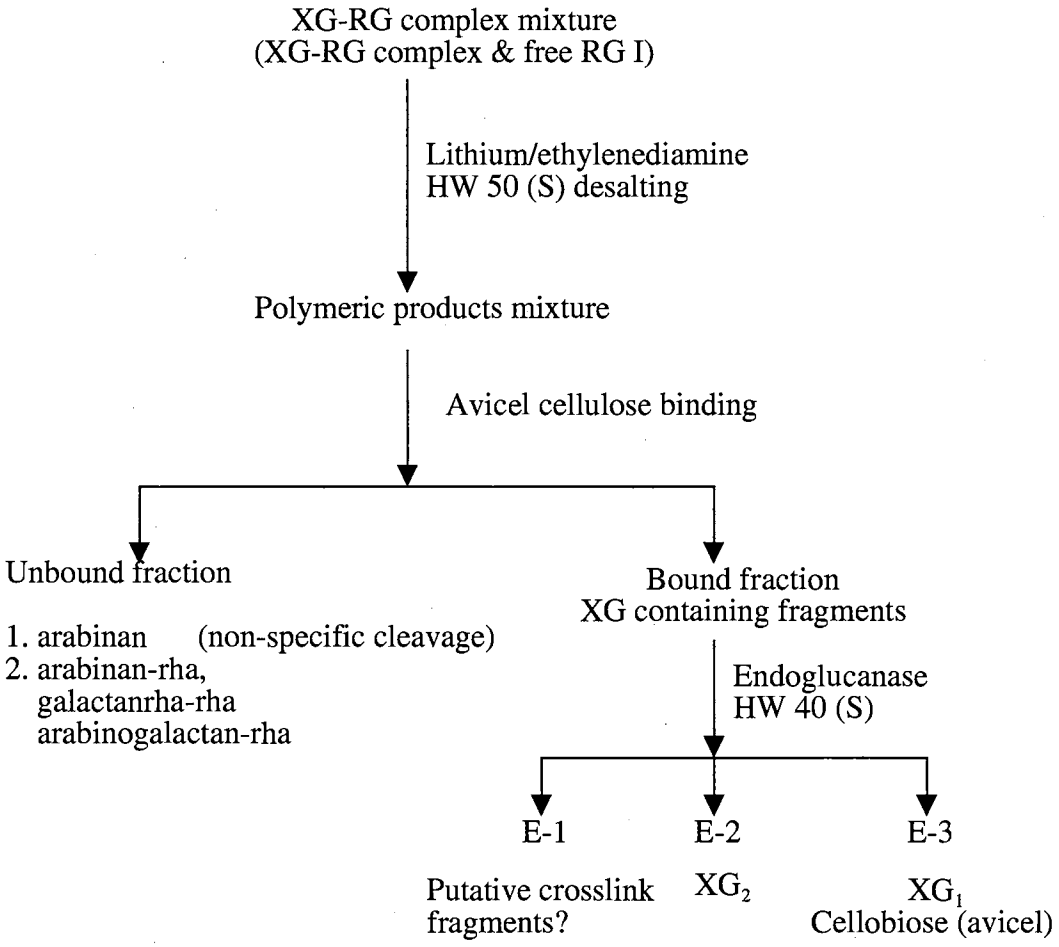

Figure 6-2 HW 50 (S) gel filtration profile of the lithum treated XG-RG complex mixture

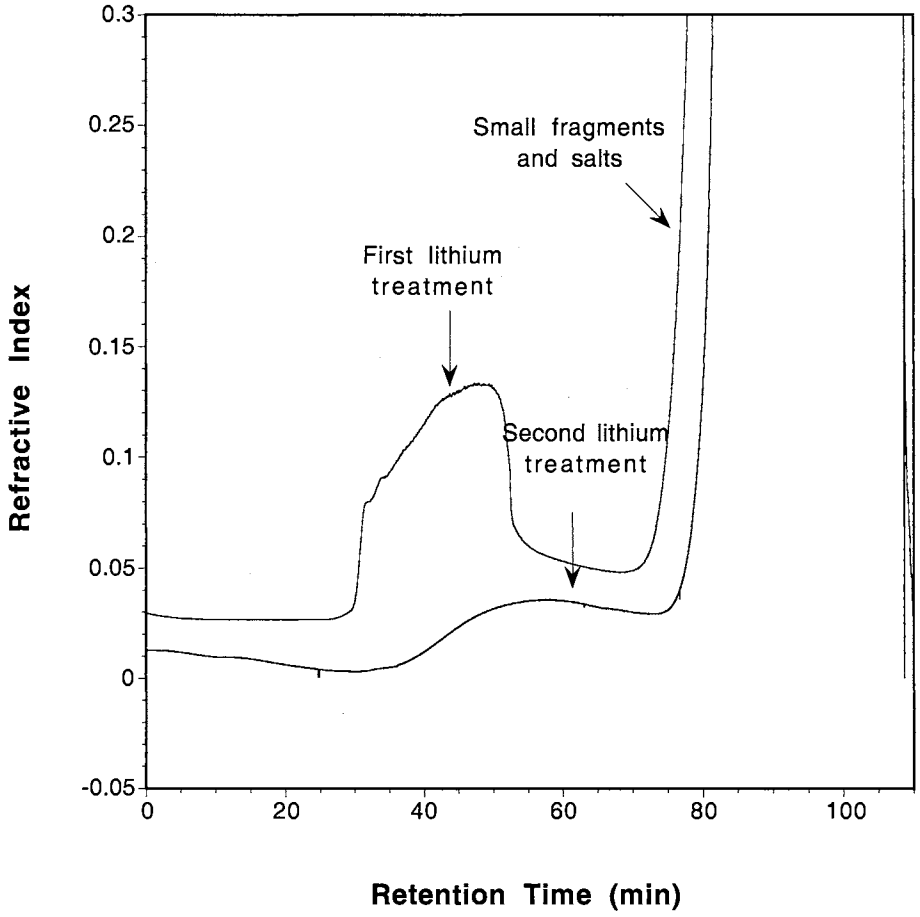

Figure 6-3 Hypothesized lithium cleavage pattern of the XG-RG complex
Cleavage site is marked with a solid arrow.

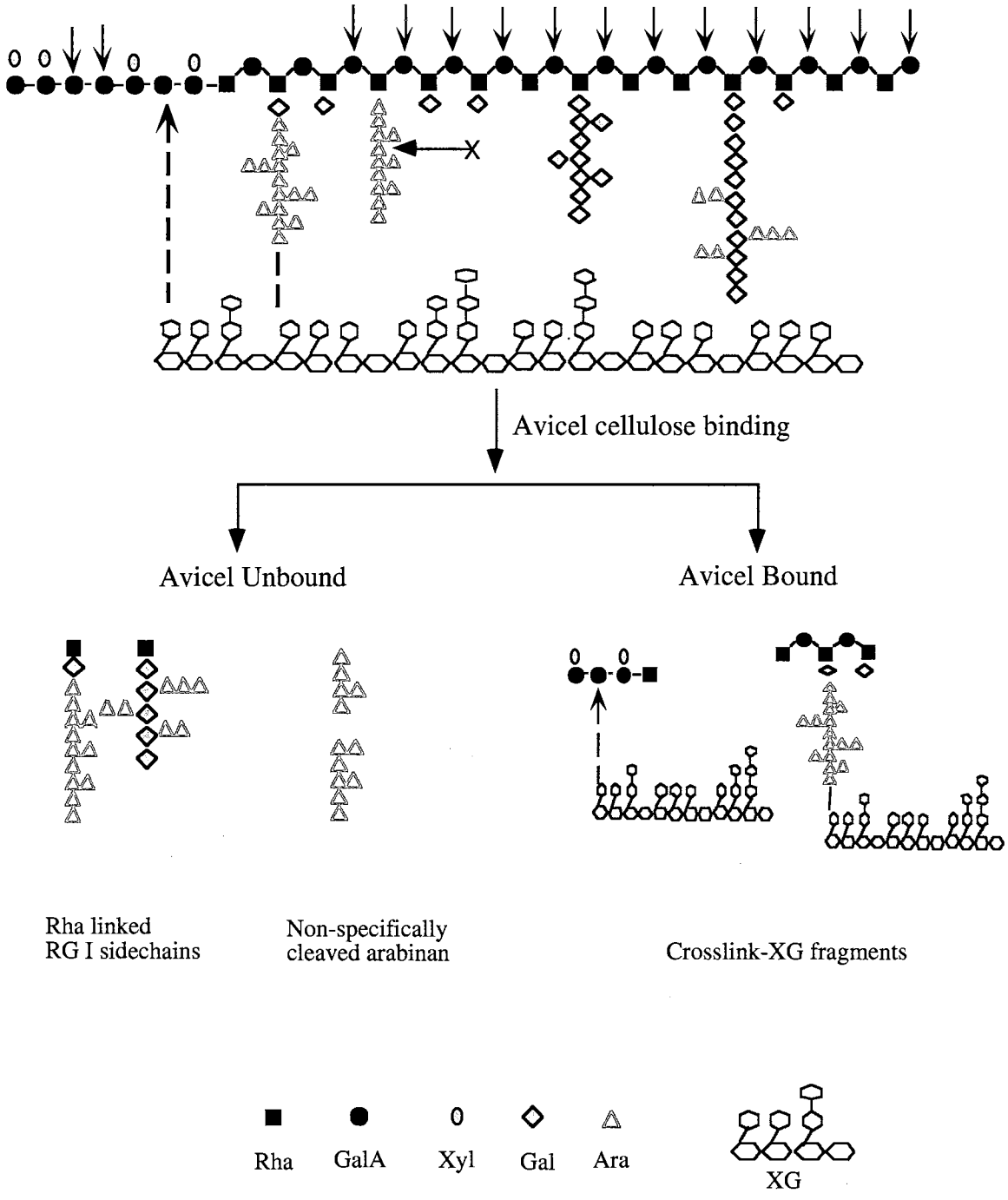

Table 6-1 Sugar composition of the XG-RG complex mixture before and after lithium treatment

Sugar	XG-RG complex mixture		Polymeric fraction after lithium treatment		Recovery (%)
	mole %	mg	mole %	mg	
Ara	25	16	30	4.3	30
Rha	14	9.8	1.5	0.3	3
Fuc	3	1.8	4	0.9	50
Xyl	18	11	29	6.5	60
GalA	16	13	1.5	0.5	4
Gal	11	9	12	3	30
Glc	12	9	20	6	70
Total sugar wt		71		21	30

mole%: molar percentage of sugars accounted for in the GLC analysis
mg: sugar weight in mg calculated from GLC analysis
Total sugar wt: total sugar weight calculated from GLC analysis
Recovery: sugar weight of the polymeric fraction after lithium treatment per sugar weight of the total complex

Table 6-2 Sugar composition of the avicel unbound and bound fractions of lithium treated XG-RG complex mixture

Sample	Sugar composition in mole%						
	Ara	Rha	Fuc	Xyl	GalA	Gal	Glc
Li treated XG-RG complex	30	1.5	4	29	1.5	12	20
Avicel unbound	76	4	1	2	3	11	3
Avicel bound (1M NaOH)	2	tr.	5	42	1	11	36
E-1*	42	9	tr.	7	15	11	16
E-2	9	0.8	6	31	2	11	39
E-3	0.6	0.2	2	28	2	5	59

mole%: molar percentage of sugars accounted for in the GLC analysis
tr: trace
E-1*: the void volume fraction of the endoglucanase released avicel bound material separated on an HW40 (S) gel filtration column
E-2, E-3: second and third fraction on an HW40 (S) gel filtration column

Figure 6-4 ANTS labeled electropherograms of the avicel unbound fraction (A) and the bound fraction of the lithium treated XG-RG complex mixture released by 1M NaOH (B)

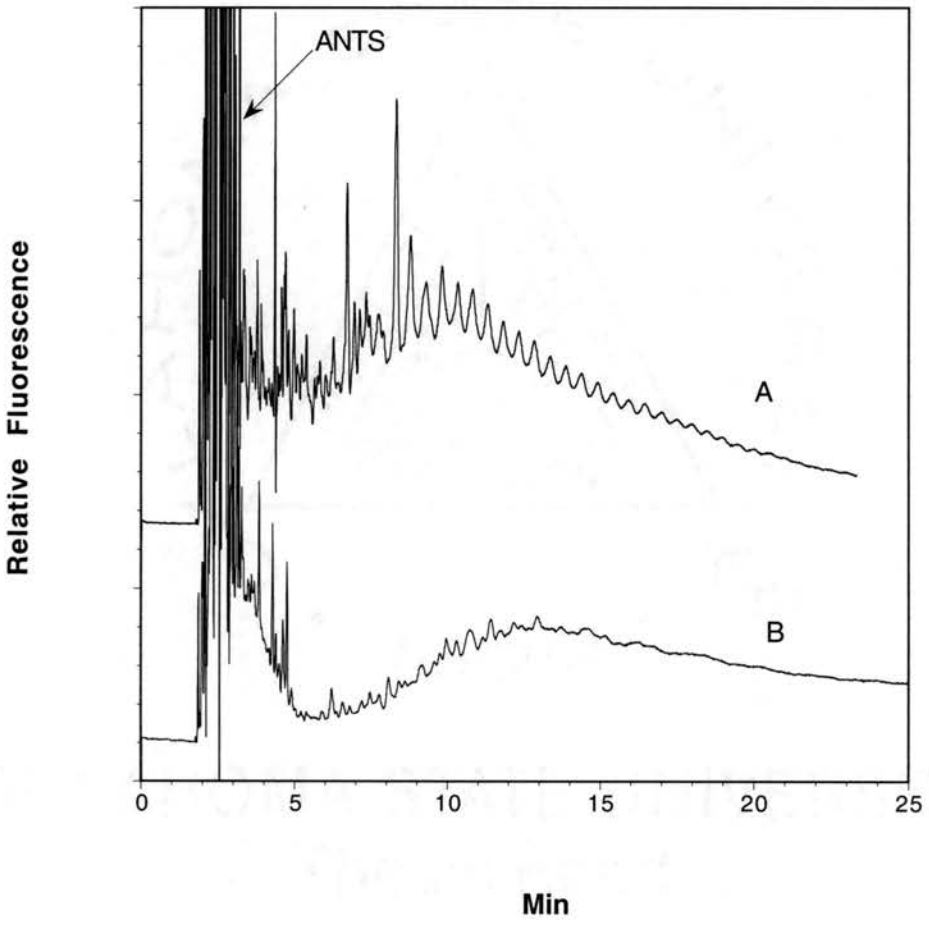

Figure 6-5 Electropherograms of 2-AA-derivatized monosaccharide standards (A) and 2-AA-derivatized avicel unbound fragments hydrolyzed by 2 M TFA (B)

1: 3-O-methyl-glc 2: ara 3: fuc 4: rha 5: man 6: gal 7: xyl 8: glc 9: galA

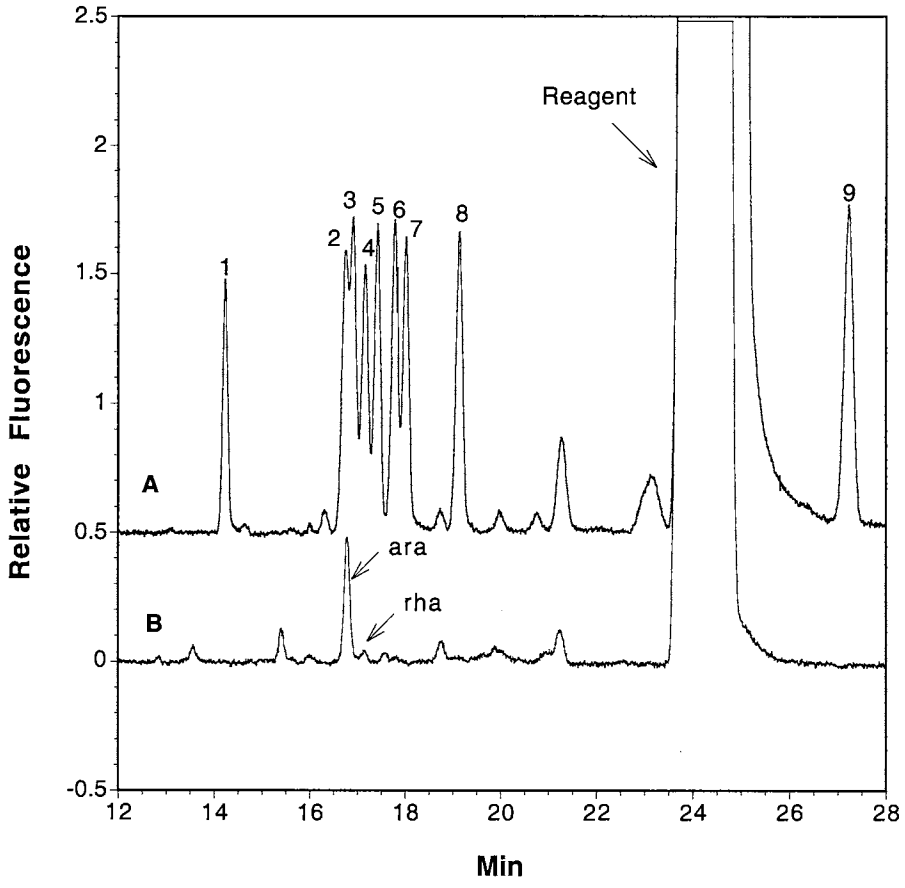

Figure 6-6 HW40 (S) gel filtration profile of the avicel bound fraction released by endoglucanase

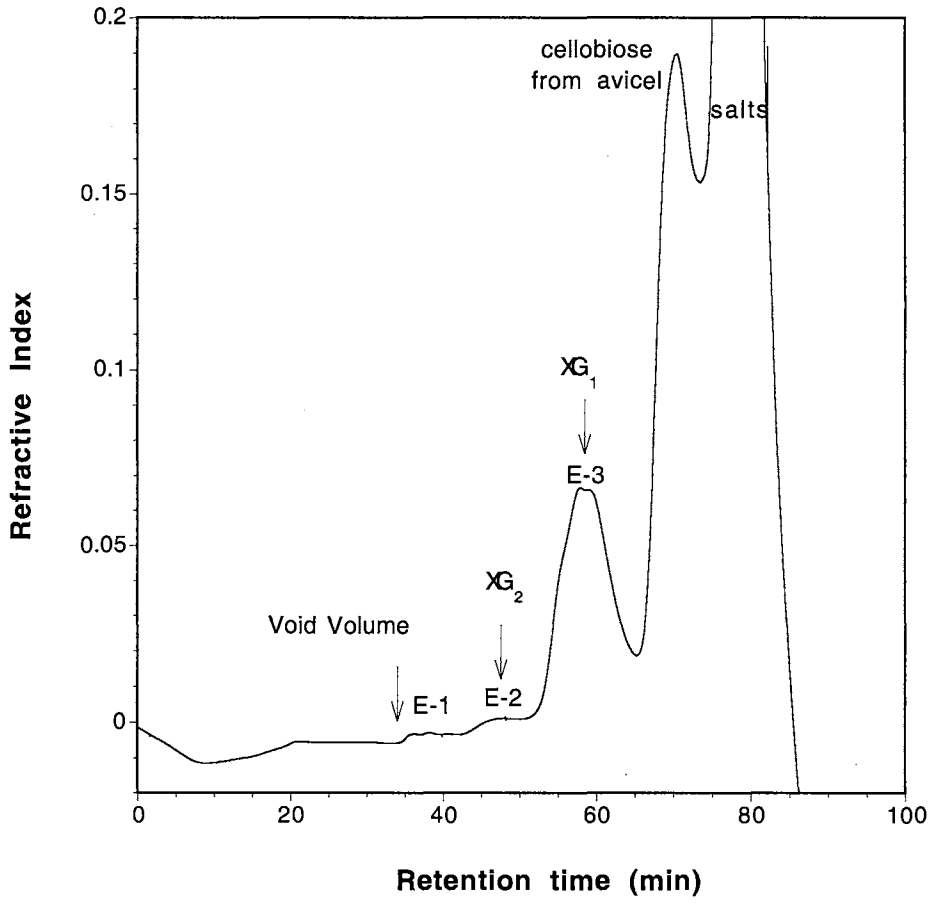

Figure 6-7 ANTS labeled electropherograms of the XG dimer released by endoglucanase from the avicel bound lithium treated complex (A) and the monomers after addition of endoglucanase (B)

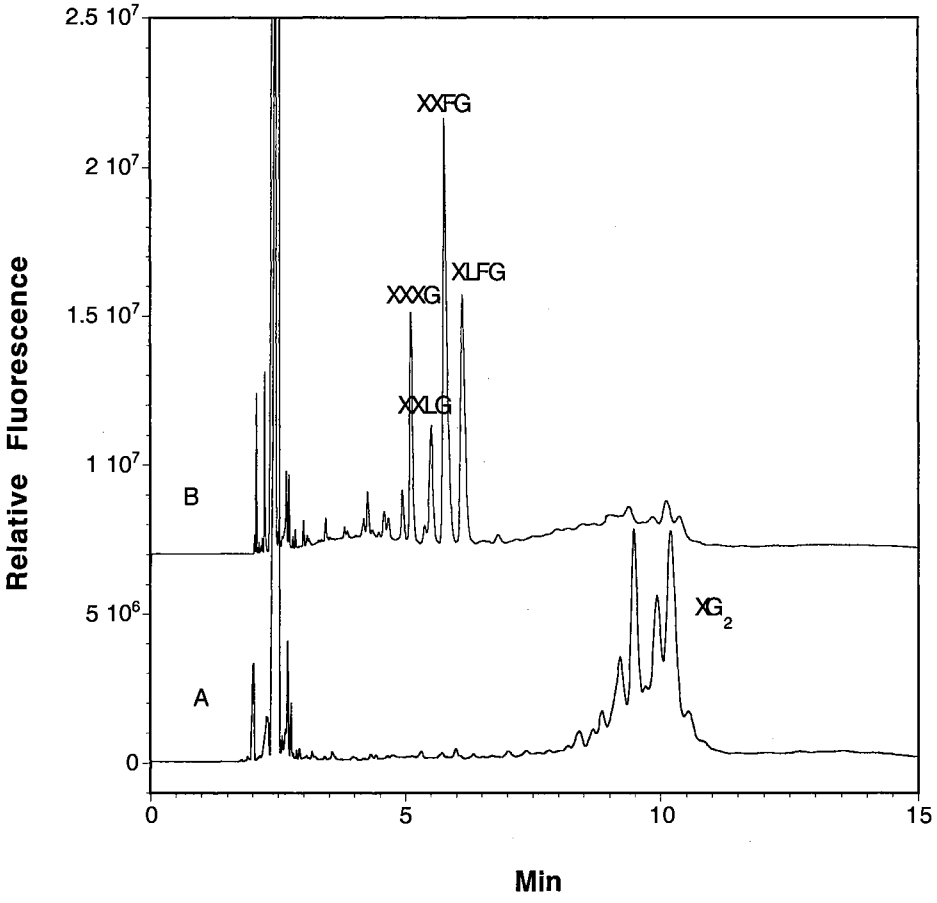

Figure 6-8 HW50 (S) gel filtration profile of the lithium treated RGase resistant XG-RG complex

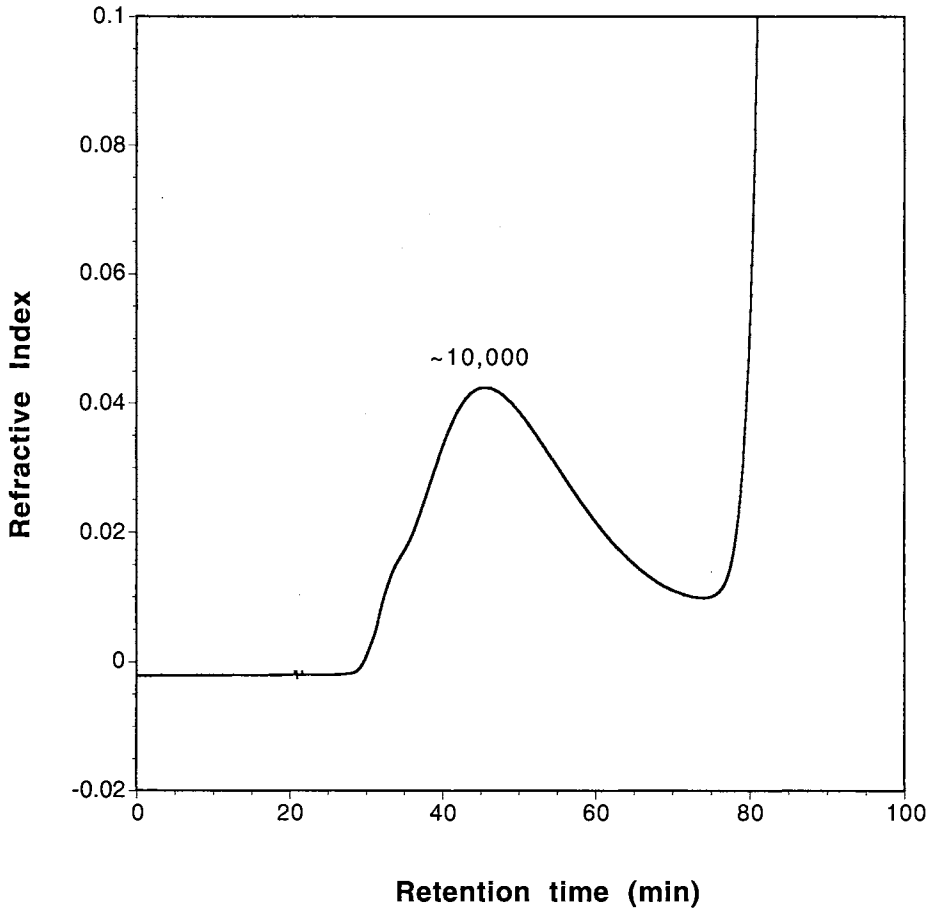

Table 6-3 Sugar composition of the RGase resistant XG-RG complex before and after lithium treatment

Sugar	RGase resistant XG-RG complex		Polymeric fraction after lithium treatment		Recovery (%)
	mole %	mg	mole %	mg	
Ara	4	0.7	4	0.3	40
Rha	3	0.5	0.8	0.06	10
Fuc	5	0.8	6	0.5	60
Xyl	42	6.5	44	3.1	50
GalA	7	1.6	0.6	0.05	3
Gal	12	2.3	15	1.2	50
Glc	25	4.7	31	2.8	60
Total sugar wt		18		8	45

mole%: molar percentage of sugars accounted for in the GLC analysis
mg: sugar weight in mg calculated from GLC analysis
Total sugar wt: total sugar weight of each fraction
Recovery: sugar weight of the polymeric fraction after lithium treatment per sugar weight of the strating material

Figure 6-9 HW40 (S) gel filtration profile of the endoglucanase released avicel bound fraction from the lithium treated RGase resistant complex

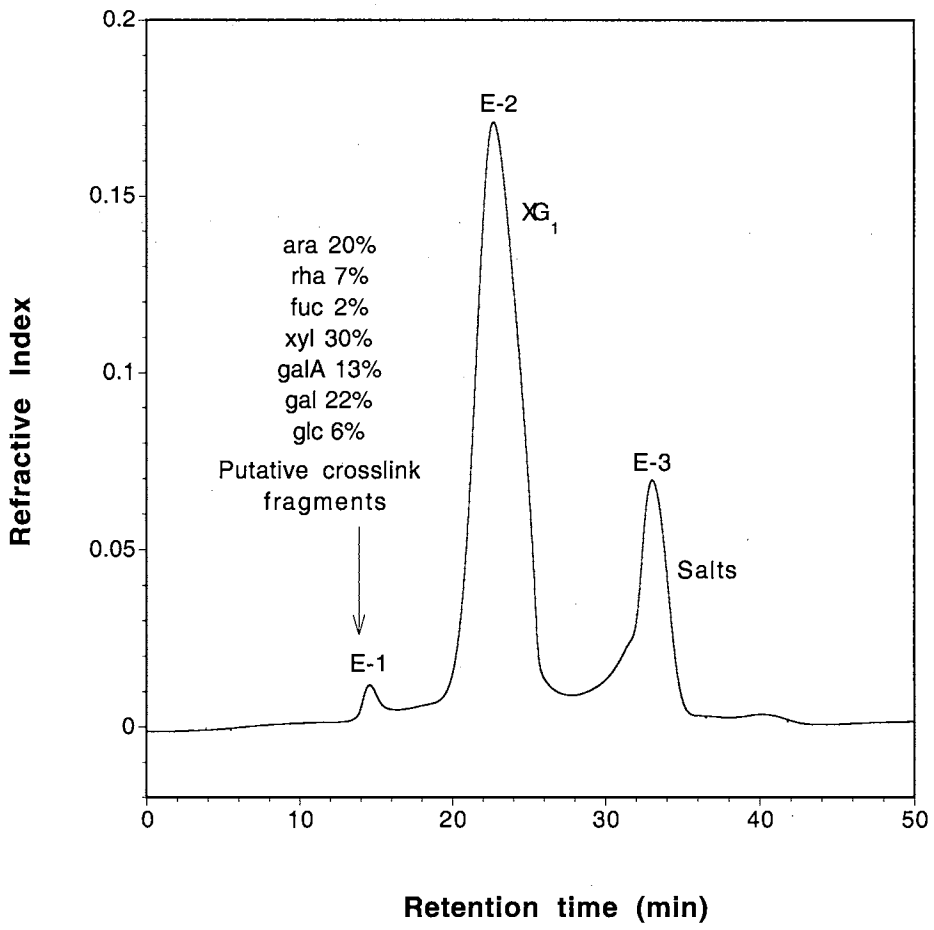

Figure 6-10 ANTS labeled electropherogram of the putative crosslink fraction from the RGase resistant complex treated by lithium and endoglucanase

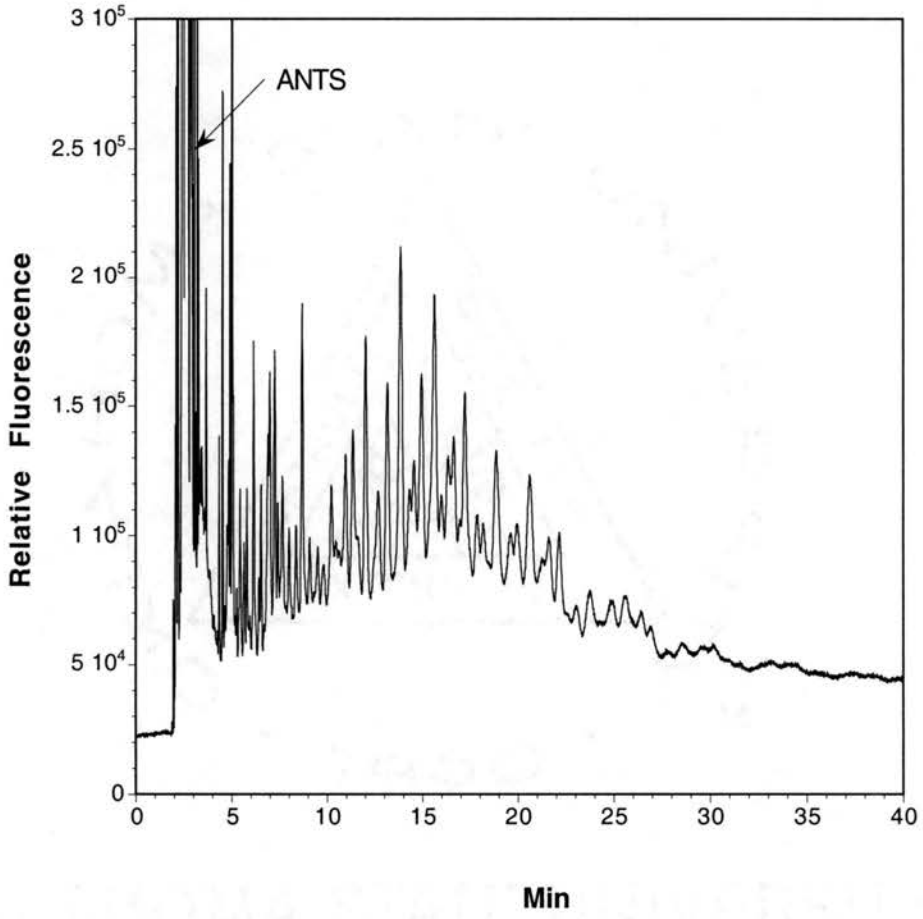

Figure 6-11 MALDI-MS spectrum of the putative crosslink-containing fraction from the RGase resistant complex treated by lithium and endoglucanase

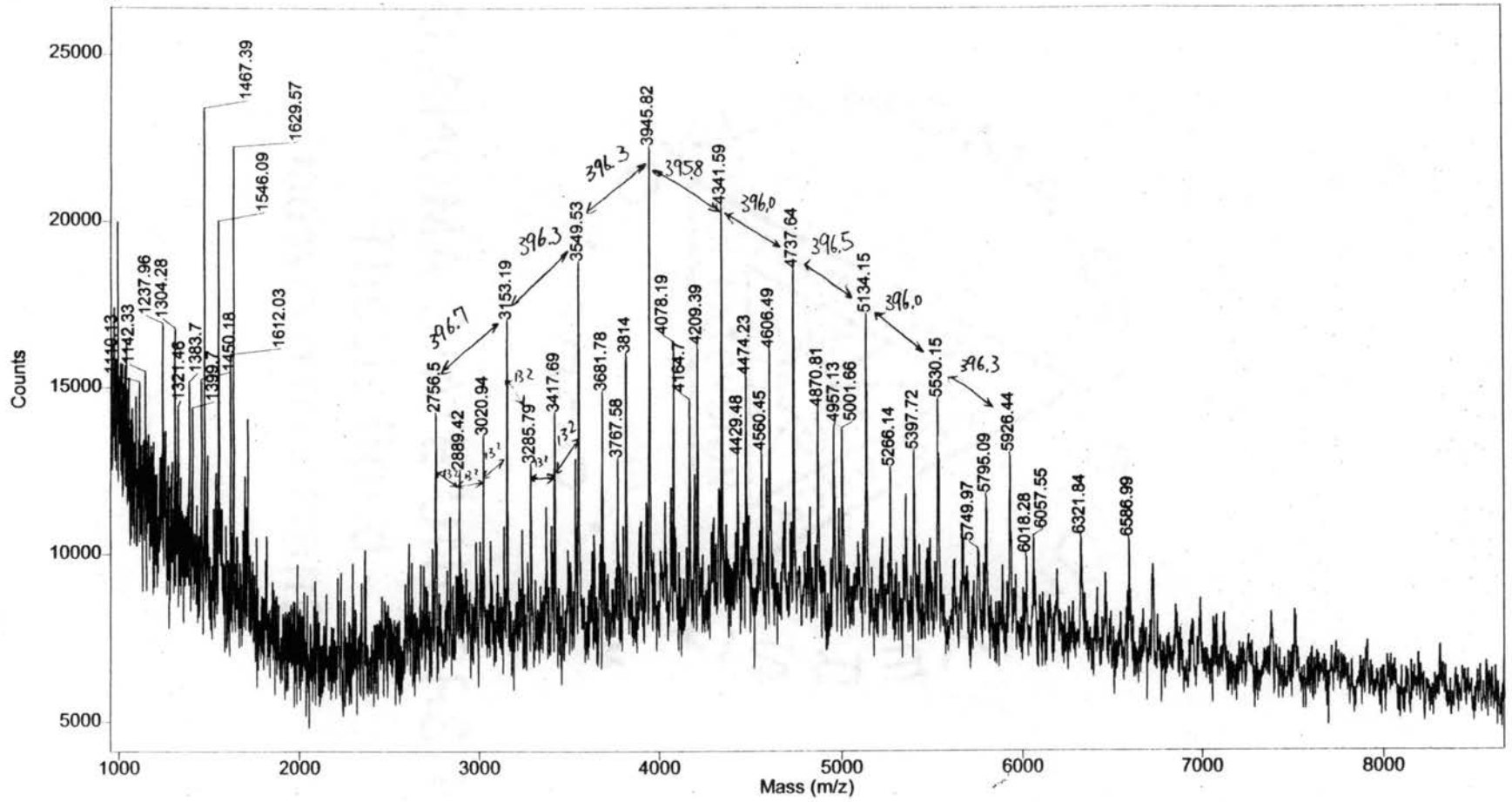

CHAPTER 7 SUMMARY AND CONCLUSION

Polysaccharides are the major components of the primary cell walls. The same six polysaccharides: cellulose, hemicellulose (xyloglucan in dicot and arabinoxylan in monocot), homogalacturonan (HG), rhamnogalacturonan I (RG I), rhamnogalacturonan II (RG II) and xylogalacturonan (XGA) are hypothesized to be present in the primary cell walls of all higher plants (1). Most current cell wall models propose that cellulose and XG form an independent network from a pectin network which is composed of HG, RG I, RG II and XGA. However, a covalent crosslink between XG and RG was indicated in cotton suspension cell walls (2). The term of RG is used instead of RG I, because the sugar composition of the isolated XG-RG crosslinked complex contains more galA than rha which indicates the presence of XGA.

The aim of this thesis was to characterize the structure of the crosslink between XG and RG. By knowing the nature of the XG-RG crosslink, we hope to understand the role of such a crosslink in the architecture of the cell wall, why it is formed and how it is formed.

Preliminary results showed that over 90% of the XG and 90% of the RG were co-extracted by 24% KOH-0.1%$NaBH_4$ from the EPG pre-treated cotton suspension cell walls (2). Further separation of the alkali extracted material on an anion exchange column revealed that half of the XG is free XG, while the other half co-eluted with RG (RG-crosslinked XG). To examine further if the XG is covalently crosslinked to the RG, the co-eluted XG-RG fraction was applied to avicel cellulose for *in vitro* binding experiments. Approximately half of the RG along with most of the XG can bind to the

avicel cellulose. This accounts for about 70% of the co-eluted material and 12% of the starting cell walls. The avicel unbound material is mostly free RG I.

The sugar weight percentage of each fraction extracted from 1.0 gram of intact walls is listed in Table 7-1. In cotton suspension cell walls, there is about 20% cellulose, 15% HG, 7% RG II, 5% free XG, 6% free RG I and 12% XG-RG crosslinked complex. The sugar weight distribution of galA, rha and fuc in each fraction is also listed in Table 7-1. GalA is present in all the pectin subregions: HG, RG II, XGA and RG I. About 60% of the galA is present in the HG, 10% in the RG II and 15% in the RG I/XGA. Rha is mainly distributed in the RG I region which is composed of alternating rha and galA residues. About 20% of rha is present in the RG II region, 30% in the XG-RG crosslinked complex and 30% in the free RG I. XG is composed of subunits (nona-, hepta-, octa- and decamer) built by glc, xyl, gal and fuc. Glc is the most abundant sugar of XG, but glc content is normally underestimated due to its cellulose like glucan backbone, which is hard to completely hydrolyze especially when it is intact. Xyl is the second most abundant sugar of XG, but it is also present in the XGA region. Gal is mainly present in the RG I region and only a small proportion is in the XG. Fuc is a minor sugar of XG, but it is only present in XG. If fuc is equally distributed in the XG polymer, then fuc distribution can be considered to represent XG distribution. About 40% of fuc is in the free XG and 40% is in the RG crosslinked XG.

To characterize the crosslink between XG and RG, we have to degrade the XG and RG polymer so as to isolate a small and intact crosslink fragment. Endoglucanase can degrade almost the entire XG polymer into the basic subunits of XXXG, XXLG, XXFG, XLFG. However, RGase could not cleave the RG polymer extensively due to the complexity of the sidechains on RG I or the junction with XGA or XG. Because XG is an "indicator" of the XG-crosslink and also used as a "selector" for isolation of the XG-crosslink from non-XG containing fragments, degradation of the XG-RG complex should start with the RG polymer.

RGase degradation of the co-eluted XG-RG complex mixture resulted in two distinct-sized fractions: a high molecular weight fraction (HMW) and a low molecular weight fraction (LMW). The LMW fraction has the size range approximately from 1,000 Da to 50,000 Da. These relatively small products are mostly generated from the free RG I and partially from the XG-RG complex. The HMW fraction is the RGase resistant XG-RG complex, the large size (100,000 Da to 200,000 Da) is mostly due to the XG polymer. The RGase resistant XG-RG complex was further degraded by endoglucanase, a putative crosslink fraction was obtained. The sugar composition of each fraction on the path towards isolation of the putative crosslink is listed in Table 7-2. The RGase resistant complex shows a high content of XG (rha: glc: xyl: gal: fuc is 1: 5.4: 10: 3.3: 1.3), but the xyl content is too high to be just present in XG (glc: xyl is 4: 3). The presence of XGA is indicated and it becomes much clearer in the putative crosslink fraction after degradation of the XG polymer. If one subtracts a 1: 1 ratio of rha: galA for RG I, the remaining xyl: galA ratio is about 1.7: 1.6. The putative crosslink fraction has been analyzed by CZE, MALDI-MS and NMR. The capillary electropherogram indicates that this fraction is a mixture of a series of fragments. The MS data obtained from MALDI illustrates that these fragments are between 2,000 Da to 10,000 Da and in a pattern of 396 mass difference. No clear information was obtained from the NMR spectrum due to the high heterogeneity of the sample. The putative crosslink fraction still could be a mixture of the real crosslink fragment and other fragments. In the future, we hope to obtain a crosslink fragment which is linked with only a few residues of XG and RG or XGA. The indication of the presence of XGA in the crosslink junction brings us closer to finding out the nature of the crosslink.

Chemical and enzymatic degradation methods have been widely used for elucidation of the cell wall structure. Polysaccharide degrading enzymes are preferred due to their high substrate specificity. Pectin is the most abundant and complicated complex in the cell walls. A wide range of pectin degrading enzymes has been found to

be present in microorganisms and plants themselves. Several key enzymes that degrade pectin are: pectin methylesterase (PME), that removes methyl-esters from galA residues of HG; endopolygalacturonase (EPG), that degrades the non-esterified HG region and RGase, that degrades the alternating rha-galA repeating region. Enzymes that degrade RG I sidechains have also been found: endoarabinase, arabinosidase, endogalactanase and galactosidase. An exo-polygalacturonase (ExoPG) from *Aspergillus aculeatus* was reported to be able to degrade the XGA region as well as the HG from the non-reducing end (3). However, no known enzyme is able to remove the substituted xyl from XGA. In addition, no endo-type enzyme is known to able to degrade the XGA or RG II. The substituion of single xyl on galA is found to be inhibitory to EPG. If the RGase resistant junction has an XGA at the non-reducing end, then the junction could be further degraded by an exo-PG. The high sidechain substitution of RG I might be an another reason for resistance to RGase. If this is the case, more specific enzymes for degradation of RG sidechains will be needed. The commercial RG sidechain degrading enzymes were found to contain contaminating endoglucanase activity, which would degrade the XG which we hope to keep it "intact" for characterization.

Degradation of the HG by EPG was reported to release much of the RG I and RG II from sycamore suspension cell walls. However, in cotton suspension cell walls, not much of the RG I can be released by EPG degradation of intact walls. RG II was found to be released along with the HG digestion products of galA mono, di, trimers. The retention of the RG I in the wall residue is because the RG I is linked either with XG or other insoluble polymers like extensin. Strong alkali, which is able to solubilize the XG from cellulose, liberates the XG crosslinked RG I and the free RG I. The alkali extracted free RG I could have been cleaved from the RG I polymer by saponification or from extensin-RG I by β-elimination. Sequential extraction of the EPG pre-treated walls by endoglucanase (no RGase activity was detected) released half of the RG I. This indicates

that at least half of the RG I is crosslinked to the XG. Extraction of the EPG pre-treated walls by RGase only solubilized arabinan-rich RG I fragments along with traces of RG I oligomers. The remaining RG I could be co-extracted with XG by alkali.

RGase degradation of apple cell walls was reported to solubilize a portion of the polymeric HG (4). However, RGase degradation of intact cotton walls only released a fraction of arabinan-rich RG I fragments. The sugar composition of the RGase solubilized fraction from intact walls and EPG-pretreated walls are similar, and the amount of the two fractions released is close, both account for about 10% of the total intact walls. To examine if any HG is released by RGase from the intact cotton walls, imidazole was used to extract the RGase treated residues. Generally, low methyl-esterified HG does not dissolve well in water solution, but it can be dissolved in imidazole which, is a calcium complexing solvent. There was about 3% weight of the material extracted by imidazole from the RGase treated residues. This fraction, from its sugar composition, is mainly HG and a trace of RG I. However, imidazole extraction of intact walls also solubilized the same amount of similar HG material. This indicates that the imidazole solubilized HG from the RGase digested residues could be originally present in the intact wall, not liberated by RGase. The RGase released arabinan-rich RG I segment could be located at the extremety of the whole pectin backbone or interspersed between smooth RG I segments. The remaining RG I could be highly substituted with sidechains or adjacent to the XGA region and thus protected from RGase degradation. Because the majority of the HG could not be liberated by RGase, we hypothesize that the HG might be connected to either the highly substituted RG I segments or the XGA where they are involved in crosslinking to the XG.

A modified cell wall model based on the results from sequential extraction of cotton suspension cell walls is illustrated in Fig. 7-1. The HG is proposed to be next to the XGA, and the XGA is closely linked to the highly substituted RG I segment, next to it is the smooth RG I segment and the arabinan-rich RG segment. The XG is proposed to

be crosslinkd to the junction region of XGA-RG I. RG II is proposed to be present within the HG region because EPG degradation could liberate it. The chemical nature of the linkages between one segment to the other and the order of the connections of these segments are unclear. Two crosslinks are proposed, one is between XG and RG and the other is between RG and extensin (5). To know the nature of the crosslink in the XG-RG complex would be of great importance to understanding of how cell wall polymers are interconnected and interacting with each other to form a dynamic wall.

REFERENCES

1. **Albersheim, P., Darvill, A. G., O'Neill, M. A., Schols, H. A., Voragen, A. G. J.** 1996. An hypothesis: the same six polysaccharides are components of the primary cell walls of all higher plants. *Pectins and Pectinases.* Elsevier Science B.V. 47-55
2. **An, J.** 1991. Isolation and cgaracterization of xyloglucan and rhamnogalacturonans from cotton cell walls of suspension culture. Disertation for the degree of the doctor of philosophy. Oklahoma State University
3. **Renard, C. M. G. C., Thilbault, J. F., Voragen, A. G. J., Van den broek L. A. M., Pilnik, W.** 1993. Studies on apple protopectin VI: extraction of pectins from apple cell walls with rhamnogalacturonase. *Carbohydr. polym.* 22: 203-210
4. **Beldman, G., van den Broek, L. A. M., Schols, H. A., Searle-van Leeuwen, M. J. F., Van Laere, K. M. J., Voragen, A. G. J.** 1996. An exogalacturonase from *Aspergillus aculeatus* able to degrade xylogalacturonan. *Biotechnol. Lett.* 18(6): 707-712
5. **Qi, X., Behrens, B., West, P. R., Mort, A. J.** 1995. Solubilization and partial characterization of extensin fragments from cell walls of cotton suspension cultures. Evidence for a covalent cross-link between extensin and pectin. *Plant Physiol.* 108(4): 1691-1701

Table 7-1 Sequentially extracted wall components by EPG and 24% KOH-0.1%$NaBH_4$ from 1.0 g of cotton suspension cell walls

Fraction	Components	Fraction weight %	GalA distribution (%)	Rha distribution (%)	Fuc distribution (%)
EPG extracts	HG	15	60		
	RG II	7	10	20	
KOH extracts	Free XG	5			40
	XG-RG I/XGA	12	7	30	40
	Free RG I/XGA	6	7	30	
KOH residue	Cellulose	20	6	8	10

Fraction weight %: total weight of each fraction per 1.0 gram of intact walls
GalA distribution (%): galA sugar weight in each fraction per total galA sugar weight in 1.0 gram of intact walls
Rha distribution (%): rha sugar weight in each fraction per total rha sugar weight in 1.0 gram of intact walls
Fuc distribution (%): fuc sugar weight in each fraction per total fuc sugar weight in 1.0 gram of intact walls

Table 7-2. Sugar composition of cotton cell walls and subsequent enzymatic and chemical treated fractions

Fraction	Sugar composition in relative molar ratio to rha							Fraction weight (mg)
	Ara	Rha	Fuc	Xyl	GalA	Gal	Glc	
Intact cotton wall	2.9	1	0.2	1.8	4.6*	1.3	0.6*	1000
EPG treated wall	3.3	1	0.2	1.9	2.5	1.4	0.7*	680
KOH solubilized fraction	2.9	1	0.3	2.4	1.4	1.6	1.4	340
Co-eluted XG-RG complex mixture	2.2	1	0.3	1.4	1.5	1.1	0.8	150
Avicel bound XG-RG complex	1.6	1	0.2	2.4	1.8	1.2	1.7	100
RGase resistant XG-RG complex	0.8	1	1.3	10	2.3	3.3	5.4	30
Putative crosslink fraction	0.1	1	0.1	1.7	2.6	0.3	0.4	~5

The number marked with an * was underestimated due to the sugar polymer's resistance to hydrolysis under the GC condition used

Figure 7-1 A modified cell wall model

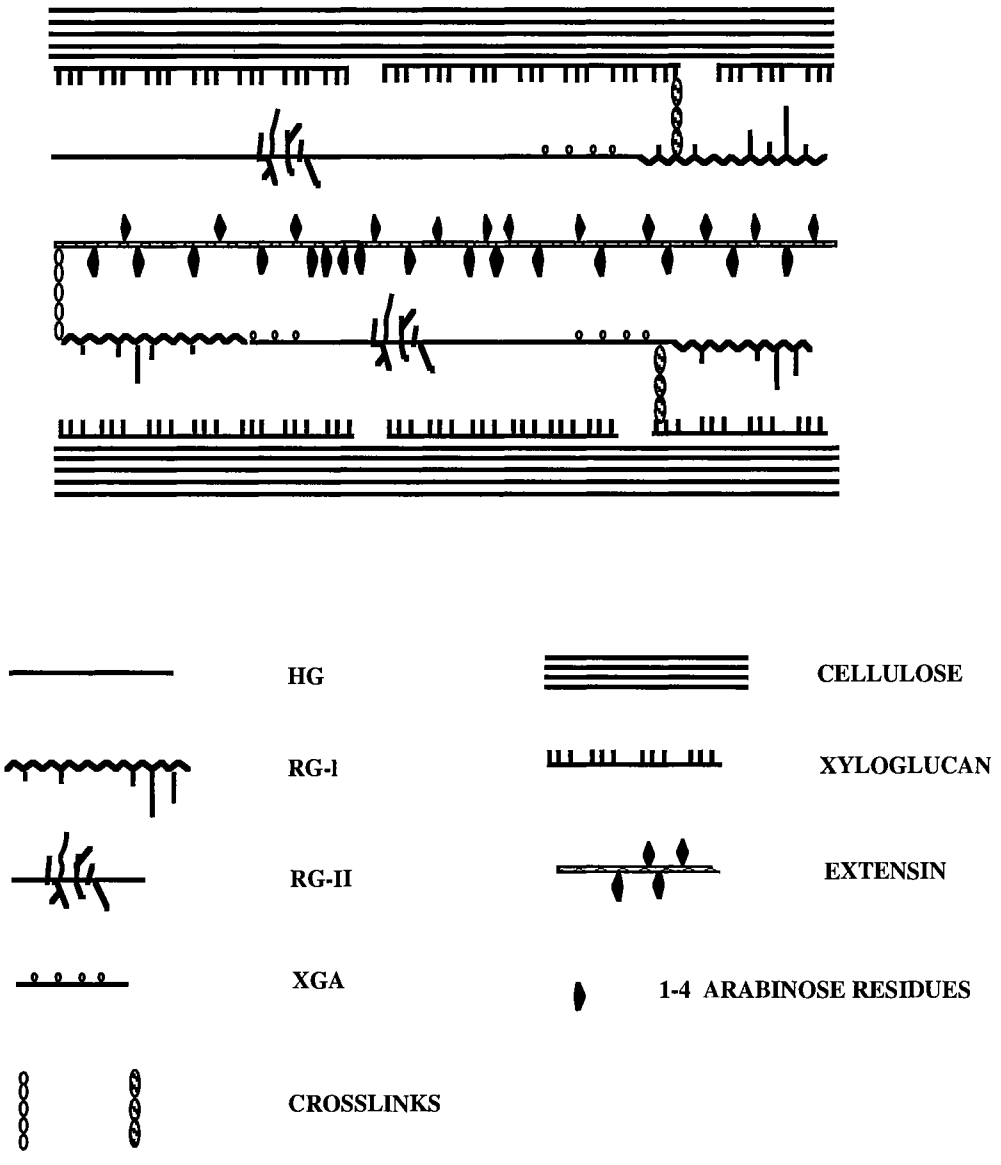

VITA

Jun Fu

Candidate for the Degree of

Doctor of Philosophy

Thesis: EXTRACTION AND CHARACTERIZATION OF XYLOGLUCAN-RHAMNOGLACTURONAN CROSSLINKED COMPLEX IN COTTON SUSPENSION CELL WALLS

Major Field: Biochemistry and Molecular Biology

Biographical:

Personal Data: Born in Huzhou, Zhejiang, China, April 13, 1970, the daughter of Yueqin Yuan and Baixian Fu.

Education: Graduated from Huzhou High School, Huzhou, Zhejiang, China, in July 1988; received Bachelor of Science Degree in Material Science from Fudan University, China, in July, 1992. Completed requirements for the Doctor of Philosophy Degree at Oklahoma State University in December, 1999.

Professional Experience: Research Assistant in the Research Center of Analysis and Measurement, Fudan University, Shanghai, China, Aug. 1992 to June. 1994; Research Assistant in the Department of Biochemistry and Molecular Biology, Oklahoma State University, Stillwater, Oklahoma, June 1994 to Present.

Honors and Organizations: Member of American Society of Plant Physiologists